IAEA TECDOC SERIES

IAEA-TECDOC-1862

Behaviour of Spent Power Reactor Fuel during Storage

Extracts from the Final Reports of Coordinated Research Projects on Behaviour of Spent Fuel Assemblies in Storage (BEFAST I–III) and Spent Fuel Performance Assessment and Research (SPAR I–III) — 1981–2014

IAEA
International Atomic Energy Agency

IAEA SAFETY STANDARDS AND RELATED PUBLICATIONS

IAEA SAFETY STANDARDS

Under the terms of Article III of its Statute, the IAEA is authorized to establish or adopt standards of safety for protection of health and minimization of danger to life and property, and to provide for the application of these standards.

The publications by means of which the IAEA establishes standards are issued in the **IAEA Safety Standards Series**. This series covers nuclear safety, radiation safety, transport safety and waste safety. The publication categories in the series are **Safety Fundamentals**, **Safety Requirements** and **Safety Guides**.

Information on the IAEA's safety standards programme is available on the IAEA Internet site

http://www-ns.iaea.org/standards/

The site provides the texts in English of published and draft safety standards. The texts of safety standards issued in Arabic, Chinese, French, Russian and Spanish, the IAEA Safety Glossary and a status report for safety standards under development are also available. For further information, please contact the IAEA at: Vienna International Centre, PO Box 100, 1400 Vienna, Austria.

All users of IAEA safety standards are invited to inform the IAEA of experience in their use (e.g. as a basis for national regulations, for safety reviews and for training courses) for the purpose of ensuring that they continue to meet users' needs. Information may be provided via the IAEA Internet site or by post, as above, or by email to Official.Mail@iaea.org.

RELATED PUBLICATIONS

The IAEA provides for the application of the standards and, under the terms of Articles III and VIII.C of its Statute, makes available and fosters the exchange of information relating to peaceful nuclear activities and serves as an intermediary among its Member States for this purpose.

Reports on safety in nuclear activities are issued as **Safety Reports**, which provide practical examples and detailed methods that can be used in support of the safety standards.

Other safety related IAEA publications are issued as **Emergency Preparedness and Response** publications, **Radiological Assessment Reports**, the International Nuclear Safety Group's **INSAG Reports**, **Technical Reports** and **TECDOCs**. The IAEA also issues reports on radiological accidents, training manuals and practical manuals, and other special safety related publications.

Security related publications are issued in the **IAEA Nuclear Security Series**.

The **IAEA Nuclear Energy Series** comprises informational publications to encourage and assist research on, and the development and practical application of, nuclear energy for peaceful purposes. It includes reports and guides on the status of and advances in technology, and on experience, good practices and practical examples in the areas of nuclear power, the nuclear fuel cycle, radioactive waste management and decommissioning.

BEHAVIOUR OF SPENT POWER REACTOR FUEL DURING STORAGE

The following States are Members of the International Atomic Energy Agency:

AFGHANISTAN
ALBANIA
ALGERIA
ANGOLA
ANTIGUA AND BARBUDA
ARGENTINA
ARMENIA
AUSTRALIA
AUSTRIA
AZERBAIJAN
BAHAMAS
BAHRAIN
BANGLADESH
BARBADOS
BELARUS
BELGIUM
BELIZE
BENIN
BOLIVIA, PLURINATIONAL STATE OF
BOSNIA AND HERZEGOVINA
BOTSWANA
BRAZIL
BRUNEI DARUSSALAM
BULGARIA
BURKINA FASO
BURUNDI
CAMBODIA
CAMEROON
CANADA
CENTRAL AFRICAN REPUBLIC
CHAD
CHILE
CHINA
COLOMBIA
CONGO
COSTA RICA
CÔTE D'IVOIRE
CROATIA
CUBA
CYPRUS
CZECH REPUBLIC
DEMOCRATIC REPUBLIC OF THE CONGO
DENMARK
DJIBOUTI
DOMINICA
DOMINICAN REPUBLIC
ECUADOR
EGYPT
EL SALVADOR
ERITREA
ESTONIA
ESWATINI
ETHIOPIA
FIJI
FINLAND
FRANCE
GABON
GEORGIA
GERMANY
GHANA
GREECE
GRENADA
GUATEMALA
GUYANA
HAITI
HOLY SEE
HONDURAS
HUNGARY
ICELAND
INDIA
INDONESIA
IRAN, ISLAMIC REPUBLIC OF
IRAQ
IRELAND
ISRAEL
ITALY
JAMAICA
JAPAN
JORDAN
KAZAKHSTAN
KENYA
KOREA, REPUBLIC OF
KUWAIT
KYRGYZSTAN
LAO PEOPLE'S DEMOCRATIC REPUBLIC
LATVIA
LEBANON
LESOTHO
LIBERIA
LIBYA
LIECHTENSTEIN
LITHUANIA
LUXEMBOURG
MADAGASCAR
MALAWI
MALAYSIA
MALI
MALTA
MARSHALL ISLANDS
MAURITANIA
MAURITIUS
MEXICO
MONACO
MONGOLIA
MONTENEGRO
MOROCCO
MOZAMBIQUE
MYANMAR
NAMIBIA
NEPAL
NETHERLANDS
NEW ZEALAND
NICARAGUA
NIGER
NIGERIA
NORWAY
OMAN
PAKISTAN
PALAU
PANAMA
PAPUA NEW GUINEA
PARAGUAY
PERU
PHILIPPINES
POLAND
PORTUGAL
QATAR
REPUBLIC OF MOLDOVA
ROMANIA
RUSSIAN FEDERATION
RWANDA
SAINT VINCENT AND THE GRENADINES
SAN MARINO
SAUDI ARABIA
SENEGAL
SERBIA
SEYCHELLES
SIERRA LEONE
SINGAPORE
SLOVAKIA
SLOVENIA
SOUTH AFRICA
SPAIN
SRI LANKA
SUDAN
SWEDEN
SWITZERLAND
SYRIAN ARAB REPUBLIC
TAJIKISTAN
THAILAND
THE FORMER YUGOSLAV REPUBLIC OF MACEDONIA
TOGO
TRINIDAD AND TOBAGO
TUNISIA
TURKEY
TURKMENISTAN
UGANDA
UKRAINE
UNITED ARAB EMIRATES
UNITED KINGDOM OF GREAT BRITAIN AND NORTHERN IRELAND
UNITED REPUBLIC OF TANZANIA
UNITED STATES OF AMERICA
URUGUAY
UZBEKISTAN
VANUATU
VENEZUELA, BOLIVARIAN REPUBLIC OF
VIET NAM
YEMEN
ZAMBIA
ZIMBABWE

The Agency's Statute was approved on 23 October 1956 by the Conference on the Statute of the IAEA held at United Nations Headquarters, New York; it entered into force on 29 July 1957. The Headquarters of the Agency are situated in Vienna. Its principal objective is "to accelerate and enlarge the contribution of atomic energy to peace, health and prosperity throughout the world''.

IAEA-TECDOC-1862

BEHAVIOUR OF SPENT POWER REACTOR FUEL DURING STORAGE

EXTRACTS FROM THE FINAL REPORTS OF COORDINATED RESEARCH PROJECTS ON BEHAVIOUR OF SPENT FUEL ASSEMBLIES IN STORAGE (BEFAST I–III) AND SPENT FUEL PERFORMANCE ASSESSMENT AND RESEARCH (SPAR I–III) — 1981–2014

INTERNATIONAL ATOMIC ENERGY AGENCY
VIENNA, 2019

COPYRIGHT NOTICE

For further information on this publication, please contact:

Nuclear Fuel Cycle and Materials Section
International Atomic Energy Agency
Vienna International Centre
PO Box 100
1400 Vienna, Austria
Email: Official.Mail@iaea.org

Printed by the IAEA in Austria
February 2019

IAEA Library Cataloguing in Publication Data

Names: International Atomic Energy Agency.
Title: Behaviour of spent power reactor fuel during storage / International Atomic Energy Agency.
Description: Vienna : International Atomic Energy Agency, 2019. | Series: IAEA TECDOC series, ISSN 1011–4289 ; no. 1862 | Includes bibliographical references.
Identifiers: IAEAL 19-01027 | ISBN 978–92–0–100319–5 (paperback : alk. paper)
Subjects: LCSH: Spent reactor fuels — Storage. | Spent reactor fuels. | Nuclear power plants..

FOREWORD

During in-reactor service, nuclear fuel is affected by phenomena such as neutron damage that can cause evolutionary changes in its structure. These changes can influence how the fuel assemblies or bundles behave during subsequent fuel cycle steps. Once the fuel is spent — meaning that it no longer supports efficient in-reactor fission — it is permanently discharged from the core and managed until its ultimate disposition, which may be either recycling or direct disposal, depending on the fuel cycle policy in place.

The original basis of the fuel cycle was reprocessing and recycling of spent fuel supported by short term storage prior to reprocessing activities. With delays in the availability of reprocessing, or decisions not to reprocess and recycle, the storage duration of spent fuel has increased steadily, leading to the need to understand how spent fuel behaves in the selected storage environment; the need for additional storage capability as reactor storage fills; and the need to understand how the fuel and the new system behave. To address these needs, the IAEA undertook coordinated research projects (CRPs) on the behaviour of spent fuel assemblies in storage (BEFAST) and Spent Fuel Performance Assessment and Research (SPAR), and reported the findings in a series of publications. Although a number of topical issues were investigated in the CRPs, the CRPs primarily provided an account of the ongoing performance, research activities and projected behaviour of spent fuel and materials in wet and dry storage.

In the present publication, the experiences reported over the past thirty years in the BEFAST and SPAR publications have been extracted, reviewed for continued relevance and consolidated into a single source. The publication is expected to be particularly valuable for those engaged in developing safety assessments.

The IAEA gratefully acknowledges the assistance of B. Hanson (United States of America), A. Hillier (United Kingdom), H. Issard (France), A. Jussofie (Germany), J. Kyffin (United Kingdom), A. Machiels (United States of America), L. McManniman (United Kingdom) and F. Takáts (Hungary) in the drafting and review of this publication. The IAEA officer responsible for this publication was P. Standring of the Division of Nuclear Fuel Cycle and Waste Technology.

EDITORIAL NOTE

This publication has been prepared from the original material as submitted by the contributors and has not been edited by the editorial staff of the IAEA. The views expressed remain the responsibility of the contributors and do not necessarily represent the views of the IAEA or its Member States.

Neither the IAEA nor its Member States assume any responsibility for consequences which may arise from the use of this publication. This publication does not address questions of responsibility, legal or otherwise, for acts or omissions on the part of any person.

The use of particular designations of countries or territories does not imply any judgement by the publisher, the IAEA, as to the legal status of such countries or territories, of their authorities and institutions or of the delimitation of their boundaries.

The mention of names of specific companies or products (whether or not indicated as registered) does not imply any intention to infringe proprietary rights, nor should it be construed as an endorsement or recommendation on the part of the IAEA.

The authors are responsible for having obtained the necessary permission for the IAEA to reproduce, translate or use material from sources already protected by copyrights.

The IAEA has no responsibility for the persistence or accuracy of URLs for external or third party Internet web sites referred to in this publication and does not guarantee that any content on such web sites is, or will remain, accurate or appropriate.

CONTENTS

1. INTRODUCTION 1

1.1. BACKGROUND: OVERVIEW OF COORDINATED RESEARCH PROJECTS ON BEHAVIOUR OF SPENT FUEL DURING LONG TERM STORAGE 1

1.1.1. Safety standards related to spent fuel storage 3

1.2. OBJECTIVE 3

1.3. SCOPE 4

2. GLOBAL SITUATION AND PUBLICATION CONTEXT 6

2.1. ELEMENTS OF THE FUEL CYCLE 6

2.2. SPENT FUEL STORAGE 8

2.3. FUEL ASSEMBLY DESIGNS 10

2.3.1. LWR 10

2.3.2. CANDU 11

2.3.3. RBMK 11

2.3.4. WWER 12

2.3.5. AGR 12

2.3.6. MAGNOX 13

3. OVERVIEW OF SPENT FUEL STORAGE TECHNOLOGIES 14

3.1. WET STORAGE TECHNOLOGY 14

3.2. DRY TECHNOLOGIES 14

3.2.1. Vaults 16

3.2.2. Silos or concrete canisters 18

3.2.3. Cask (metal and concrete) systems 19

4. SPENT FUEL DEGRADATION MECHANISMS (WET & DRY) 22

4.1. LIGHT WATER REACTORS 22

4.1.1. Wet storage 22

4.1.2. Dry storage 24

4.1.3. Impact loading on spent fuel 47

4.2. ADVANCED GAS COOLED REACTORS (AGR) FUEL 55

4.3. MAGNOX FUEL 57

4.3.1. Wet storage 57

4.3.2. Dry storage 57

4.4. CANDU FUEL 57

4.4.1. Wet storage 57

4.4.2. Dry storage 57

4.5. RBMK AND WWER-440/1000 59

4.5.1. Wet storage 59

4.5.2. Dry storage 60

5. FUEL BEHAVIOUR IN WET STORAGE 61

5.1. GENERAL PERFORMANCE 61

5.2. LWR (BWR, PWR) FUEL 61

5.3. CANDU FUEL 63

5.4. RBMK, WWER FUEL 63

5.5. AGR FUEL 64
5.6. MAGNOX FUEL 64

6. FUEL BEHAVIOUR IN DRY STORAGE 66

6.1. GENERAL PERFORMANCE 66
6.2. LWR (BWR, PWR) FUEL 67
6.3. CANDU FUEL 70
6.4. RBMK FUEL 70
6.5. WWER FUEL 71
6.6. MAGNOX FUEL 71
6.7. AGR FUEL 71

7. STRUCTURES WET AND DRY STORAGE 72

7.1. MATERIALS 72
7.1.1. Stainless steel 72
7.1.2. Aluminium alloys 72
7.1.3. Borated stainless steel or borated aluminium alloys and composites as neutron absorbers 73
7.1.4. Concrete 73
7.1.5. Cast iron 74
7.1.6. Carbon steels 74
7.1.7. Polymers 74
7.2. DEGRADATION MECHANISMS 75
7.2.1. Degradation mechanisms in metals 75
7.2.2. Concrete degradation 76
7.2.3. Polymer degradation 77
7.3. INVESTIGATIONS AND RESULTS 77
7.3.1. Stainless steel 78
7.3.2. Borated stainless steel 80
7.3.3. Borated aluminium alloys 81
7.3.4. Concrete 81
7.3.5. Polymers 83
7.3.6. Metallic seals 85

8. MONITORING (WET & DRY) 88

8.1. METHODS FOR CONFIRMING PERFORMANCE 88
8.1.1. Technologies for confirming ongoing spent fuel integrity in wet storage 90
8.1.2. Technologies for confirming spent fuel integrity in dry storage 90
8.1.3. Technologies for confirming storage system integrity 91

9. FUEL INTEGRITY (LEAKING/DAMAGED FUEL) 93

9.1. FUEL INTEGRITY DEFINITION AND CRITERIA 93
9.2. EXAMPLES OF DAMAGED FUEL 93
9.2.1. Damaged fuel rods 93
9.2.2. Damaged structural parts 93
9.2.3. Reconstitution of damaged fuel 95
9.3. DETERMINATION OF SPENT FUEL INTEGRITY 95
9.4. EXPERIENCE OF STORING DAMAGED FUEL 96

9.4.1. Wet storage 96
9.4.2. Dry storage 97

10. CONCLUSIONS 99

10.1. SPENT FUEL PERFORMANCE IN WET AND DRY STORAGE 99
10.2. SPENT FUEL DEGRADATION MECHANISMS (WET AND DRY) 99
10.3. STRUCTURES WET AND DRY STORAGE 100
10.4. MONITORING (WET AND DRY) 100
10.5. FUEL INTEGRITY (LEAKING/DAMAGED FUEL) 100

REFERENCES 103

LIST OF ABBREVIATIONS 109

CONTRIBUTORS TO DRAFTING AND REVIEW 113

1. INTRODUCTION

In 1979, the International Atomic Energy Agency (IAEA) initiated a survey of world experience of water reactor spent fuel in wet storage. The results of this survey were later published in a Technical Reports Series publication [1]. The main findings from the survey were:

- Experience exists with wet storage of light water reactor (LWR) and pressurized heavy water reactor (PHWR) fuel for periods up to 20 years with low burnup fuel;
- No significant difficulties were expected in projecting spent fuel behaviour in wet storage for longer times and higher burnups;
- Nevertheless, observation and investigation should be continued to evaluate the behaviour of high burnup spent fuel assemblies during prolonged storage periods and to confirm the present and positive experience.

These findings became the basis for the initiation of the IAEA's first coordinated research project (CRP) on the behaviour of spent fuel during long term storage.

At the initiation of the CRP, the only licensed power reactor dry storage facilities in operation were those at the Wylfa nuclear power plant (NPP) in the United Kingdom (UK). The dry storage facilities, for magnesium non-oxidizing (MAGNOX) fuel, comprised three carbon dioxide cooled vaults (1971) and two air cooled vaults (1979). The storage facilities are currently being decommissioned following the shutdown of the Wylfa NPP on 30 December 2015.

In addition, there was significant interest in the dry storage of zirconium alloy clad fuels, as shown by several active demonstrations and laboratory based research programmes that were ongoing in Austria, Canada, Germany, Japan and the United States of America (USA) [2].

The efforts at the start of the project were therefore primarily aimed at maintaining a technology watch on the continued performance of spent fuel in wet storage (with a trend to higher burnup fuels), gaining a better understanding of how spent fuel would behave in dry storage and on dry storage system development [2]. The technical questions being asked in the first CRP [3] in relation to dry storage were:

- What are suitable storage media?
- What is the maximum cladding temperature below which a significant amount of cladding failures will not occur?
- How well can the cladding temperature be predicted to ensure that the temperature limit will not be exceeded?

1.1. BACKGROUND: OVERVIEW OF COORDINATED RESEARCH PROJECTS ON BEHAVIOUR OF SPENT FUEL DURING LONG TERM STORAGE

The information in the section has been sourced from Refs [2,4]. Other references are cited within the text as appropriate.

Since 1981, the IAEA has been organizing CRPs on the behaviour of power reactor spent fuel during long term (or extended) storage. The programmes were initially called BEFAST-I to III (BEhaviour of spent Fuel Assemblies in STorage), and later SPAR-I to III (Spent fuel

Performance Assessment and Research), respectively. Upon completion of each CRP, a summary of the results was published in an IAEA technical publication (TECDOC) [2–7].

The overall objectives of the CRPs were to develop a technical knowledge base on long term storage of power reactor spent fuel through evaluation of operating experience and research by participating Member States, and to extrapolate predictions of spent fuel behaviour over long periods of time. Specific research objectives included:

- Performing timely survey of the accumulated experience with spent fuel storage in participating Member States;
- Investigating potential fuel and storage component degradation mechanisms under wet and dry storage conditions;
- Assessing the potential impact of interim storage on subsequent spent fuel management activities (such as handling and transport);
- Developing a capability to assess the impact of potential deterioration mechanisms on spent fuel and storage components over extended periods of time;
- Exchanging results from surveillance and monitoring programmes of spent fuel storage facilities;
- Creating a synergy among research projects of the participating Member States;
- Facilitating technology transfer by documenting technical bases for spent fuel storage.

The first phase of the BEFAST, 'Behaviour of Spent Fuel and Storage Facility Components during Long-term Storage', project (1981–1986) involved 12 organizations from 11 countries: Austria, Canada, Czechoslovakia (CSSR), Finland, Federal Republic of Germany (FRG), German Democratic Republic (GDR), Hungary, Japan, Sweden, United States of America (USA) and Union of Soviet Socialist Republics (USSR).

A subsequent programme BEFAST-II, implemented during the years 1986–1991, involved 16 organizations from 13 countries: Argentina, Canada (2), FRG, Finland, GDR, Hungary, Italy, Japan, Republic of Korea, Sweden, UK (2), USA and USSR (2).

BEFAST-III, implemented during the years 1991–1996 involved 15 organizations from 12 countries: Canada (2), Finland, France, Germany, Hungary, Japan, Republic of Korea, Russian Federation (2), Slovakia, Spain, UK (2) and USA. There was also an observer from Sweden.

During the three BEFAST CRPs, the participating countries contributed their R&D results on fundamental questions of spent fuel storage.

Towards the end of the BEFAST-III project, it became apparent that the R&D component of the project was decreasing steadily; more emphasis was being placed on the operation and implementation of storage technology. The storage technology (particularly dry storage) was undergoing a rapid evolution: new fuel and material design changes were coming on stream and target discharge burnup were steadily increasing; in addition, predicted storage times were increasing steadily. With the increased burnup came higher fission gas and fission product inventories, increased sheath (cladding) strains and increased cladding oxidation and hydriding. Because of the changes that surfaced during the course of BEFAST-III, a subsequent project was proposed to address the impacts of these new parameters on long term storage and to determine their consequences on subsequent operations, especially handling and transportation.

The first phase of the IAEA spent fuel performance assessment and research (SPAR) CRP (1997–2002) involved 11 organizations from 10 countries: Canada (2), France, Germany, Hungary, Japan, Republic of Korea, Russian Federation, Spain, UK and USA. Sweden participated in the project as an observer.

The second phase of the IAEA SPAR-II CRP (2004–2008) involved the European Commission as well as 11 other organizations from 10 countries: Argentina (joined later), Canada, France, Germany, Hungary, Japan (2), Republic of Korea (for a limited period), Slovakia, Spain and USA. Sweden and the UK participated in the project as active observers.

The third phase of the IAEA SPAR-III CRP (2009–2014) involved the European Commission and 11 other organizations from 9 countries: Argentina, France, Germany, Hungary, Japan (2), Republic of Korea, Slovakia, Spain and USA (2). Switzerland and the UK participated in the programme as active observers.

Overall, 21 countries and 1 international organization participated in one or more of the CRPs.

The major topics for both wet and dry storage during all six CRPs are summarized in Table 1. It provides a record of the shift in emphasis between the various phases of the project between 1981 and 2014.

1.1.1. Safety standards related to spent fuel storage

Following the safety standards categorization, the hierarchy of safety standards related to spent fuel storage starts with the all-encompassing fundamental safety principles [8], cascades through the general safety requirements applicable to all nuclear fuel cycle facilities and activities, given in the publications on predisposal management of radioactive waste [9] and the specific safety requirements on safety of fuel cycle facilities [10], and ends with the specific safety guides. Relevant specific safety guides include: Predisposal management of radioactive waste from nuclear fuel cycle facilities [11]; Safety of nuclear fuel cycle research and development facilities [12]; Design of fuel handling and storage systems for nuclear power plants [13]; and Spent nuclear fuel storage [14].

In addition, there are safety standards associated with management systems and radiation protection. These include: Management system for the processing, handling and storage of radioactive waste [15]; and Radiation protection and radioactive waste management in the operation of nuclear power plants [16].

1.2. OBJECTIVE

In 2013 the technical working group on nuclear fuel cycle options and spent fuel management (TWG-NFCO) recommended that the experience reported in the BEFAST and SPAR CRPs should be consolidated into a single publication.

This publication fulfils that recommendation and also includes the experiences from the third phase of SPAR, which were in the process of being finalized at the time that the recommendation was made.

The information contained in the BEFAST and SPAR TECDOCs [2–7] has been reviewed and only information that is most relevant in the context of today's implementation of the technology has been included. When appropriate, reference is made to the individual

TECDOCs that contain more detailed descriptions of the research projects; which may be of interest to the reader.

The BEFAST and SPAR TECDOCs addressed only the storage periods in at reactor (AR) and away from reactor (AFR) facilities. The fuel cycle also includes some transportation components. The behaviour of fuel under transport conditions is not reported here, however, some spent fuel related aspects of transport have been looked at in the projects; for example, impact of fuel [7] and transport of damaged fuel [2].

1.3. SCOPE

This publication focuses on the storage of spent nuclear fuel from power reactors.

Spent fuels from some 'exotic' single reactors, which operate or operated in Member States, spent fuel from research reactors, the interim storage of separated plutonium, reprocessed uranium and vitrified wastes are not covered.

TABLE 1. RESEARCH SUBJECTS IN THE CRPs

Long term behaviour	B-I	B-II	B-III	SPAR-I	SPAR-II	SPAR-III	Surveillance	B-I	B-II	B-III	SPAR-I	SPAR-II	SPAR-III	Facilities & Operation	B-I	B-II	B-III	SPAR-I	SPAR-II	SPAR-III
Material aspect (cladding and components)	X			X	X	X	Monitoring; Wet + Dry - Environment - Components - Fuel assemblies - Workers' dose rate			X	X	X	X	Capacity enhancement - High density racks - Re-racking - Double tiering - Doped coolant - Rod consolidation		X				
Degradation mechanisms and models	X	X		X	X	X	Fuel conditions - Operational - Fabrication - Technology - Defected fuel rods and assemblies		X	X	X	X	X	Changing modes Wet – Dry		X	X	X	X	
Validation - experiment - experience		X	X	X	X	X	Different reactor types		X	X	X	X	X	Handling of heavily damaged fuel		X	X		X	
														System performance	X	X	X	X	X	

2. GLOBAL SITUATION AND PUBLICATION CONTEXT

2.1. ELEMENTS OF THE FUEL CYCLE

A conceptual model has been developed to represent existing, anticipated and potential (future) nuclear fuel cycle elements. The four main elements consist of (1) Thermal reactor power block; (2) Spent fuel management block; (3) Geological disposal pathway; and (4) Advanced reactor power block [17]. Various options of the first two blocks (thermal reactor power and spent fuel management) are globally or regionally deployed at a commercial scale. There is presently no operating geological disposal repository for spent fuel or reprocessed high level wastes, but progress is apparent in a few countries, such as Finland[1], France and Sweden. Similarly, there is no significant commercial power generation by advanced reactors at this time, although the Russian Federation has successfully operated a BN-600 sodium cooled fast reactor at Beloyarsk (Unit 3) since 1980 and more recently started-up a BN-800 fast reactor also at Beloyarsk (Unit 4).

The four elements are illustrated in Fig. 1 for the LWR technology, given that more than 85% of the installed nuclear capacity presently consists of pressurized and boiling water reactors.

Light water reactor power block

The front-end infrastructure (uranium mining and milling, conversion, enrichment and fuel fabrication) is well established for LWR technology. Substitution of LWR reactor/fuel by other reactor technologies such as advanced gas reactor (AGR), Reaktor Bolshoy Moshchnosti Kanalniy (RBMK), and Wodo-Wodyanoi Energeticheskiy Reaktor (WWER) reactors/fuels can be readily fitted in. Similarly, by deleting the enrichment process, Canada Deuterium Uranium reactor (CANDU) and MAGNOX technology could be adequately represented.

[1] Finland issued a construction licence in November 2015.

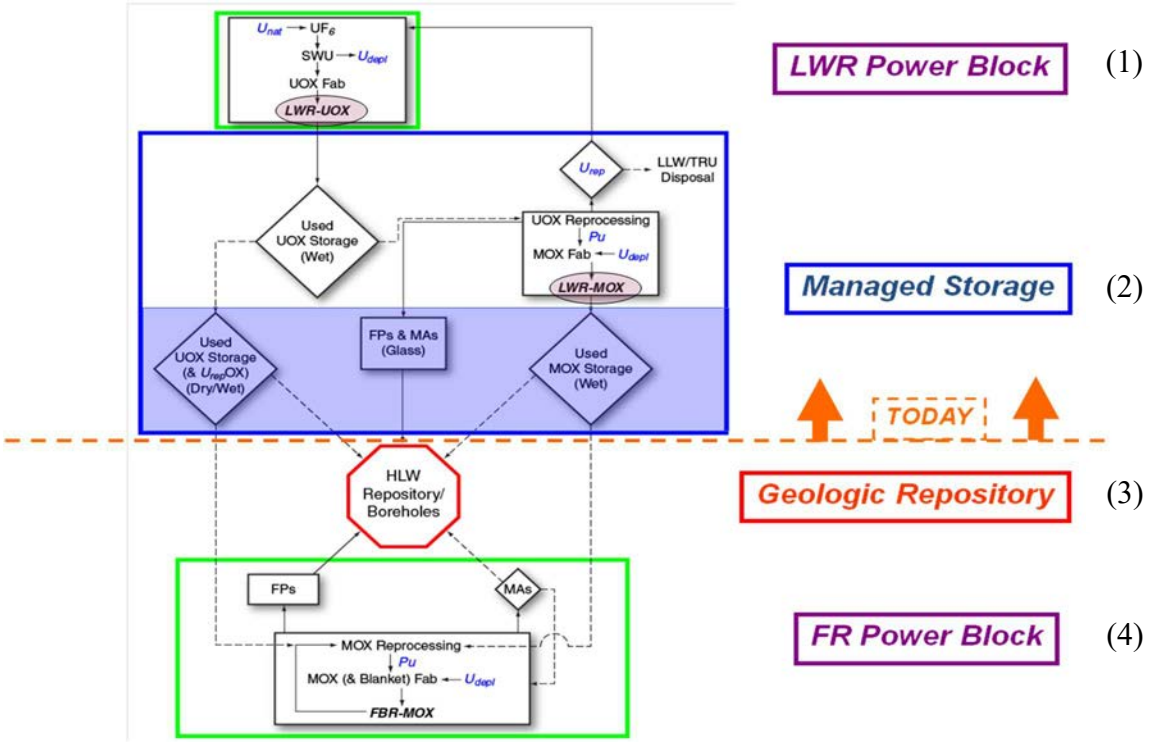

FIG. 1. Today's (LWR power block and managed storage), anticipated (geological repository), and potential (FR power block) nuclear fuel cycle elements (diagram courtesy of EPRI [17]).

Spent fuel and high level waste (HLW) management (managed storage)

Managed storage is generic to all fuel cycles. It does not preclude any end point for fuel discharged from power reactors. Discharged uranium oxide fuel ('used' or 'spent' UOX) is either placed in interim storage or reprocessed. Interim storage of spent UOX fuel has been implemented in centralized facilities or at reactor sites.

Reprocessing of spent UOX fuel yields reprocessed uranium (U_{rep} or RepU), reactor grade plutonium (Pu), and HLW. Reprocessed uranium and plutonium have been recycled in existing LWRs, resulting in combined natural uranium savings of up to 25%. Discharged fuel containing reprocessed uranium, (spent $U_{rep}OX$) or plutonium (spent MOX) is placed in interim storage. Among the different waste streams resulting from reprocessing operations, vitrified HLW, containing the fission products and minor actinides, is also placed in interim storage.

The end result for both the no reprocessing and reprocessing options is thus interim storage, although the radiotoxicity distributions in the different systems are different. The technology and facilities to implement interim storage, reprocessing and fuel re-fabrication have all been deployed at commercial scale.

Modifications of this diagram to accommodate other thermal reactor technologies (AGR, MAGNOX, CANDU, RBMK and WWER) can be readily implemented.

Geological repository

All options require a geological repository. There is broad agreement among the technical community that deep geological disposal constitutes a safe option for the relatively small

volumes of spent fuel and HLW generated by nuclear power plants. Political will and societal acceptance are the limiting factors for implementation in most countries.

Advanced reactor power block

The leading design is the sodium cooled fast reactor operating in the near breeder or breeder mode. Depending on the reprocessing scheme, separation and transmutation of some long lived fission products and minor actinides can be contemplated. Significant commercial deployment of these technologies is not likely for several decades.

2.2. SPENT FUEL STORAGE

Storage of spent fuel is an interim step. The duration of this interim step is very much related to the back end of the fuel cycle policy that has been adopted by the Member State [1]. For Member States opting for a once through fuel cycle policy, the reality is there are no spent fuel disposal facilities currently available. The first geological disposal facility is expected to be operational before 2025, but it will be several decades before geological repositories become available in all the major nuclear countries.

Delays in the implementation of the fuel reprocessing option in some countries, abandonment at some time of this option in other countries, and delays in the availability of final spent fuel disposal in all countries have led to steadily increasing periods of interim spent fuel storage. While the latter is undesirable in terms of not burdening future generations, it has become less of a burden, from a technical stance, as a result of greater efficiencies being achieved in the front end of the cycle. Such developments have reduced the amount of spent nuclear fuel (SNF) being produced, but are putting a greater burden on the SNF storage system; as a result, innovative approaches are necessary to meet this challenge, either through dry or wet storage. Higher burnup fuel is usually the result of longer irradiation time in-reactor. This may result in increased cladding corrosion but, leads to greater decay heat, higher fission gas release and leads to increased duty on the cladding (defects, stress, etc.). Higher fuel decay heat also impacts reprocessing operations and geological disposal acceptance criteria. Before geological disposal, the fuel may have to be stored for long periods of time to ensure that thermal loading on the materials in the engineered and natural barrier systems remain below design limits. Under several plausible scenarios, fuel cooled for 100 years or more may be required.

In terms of zirconium alloy clad fuels, higher fuel burnup leads to increased hydrogen pick-up in some cladding alloys. Due to the higher residual heat in these fuels, there is a potential for the circumferentially aligned zirconium hydride platelets to reorientate in the radial direction during dry storage (including accompanying operations, such as drying) and transportation (including re-wetting after transportation). Cladding mechanical property changes induced by hydride reorientation could lead, especially in the lower temperature range, to a decrease or loss of ductility when the fuel rods are subjected to pinch loading forces. The investigation of hydrogen behaviour in spent zirconium alloy clad fuels and its impact on cladding mechanical properties are just two of the areas of research, which have been ongoing in Member States to improve understanding of the processes that can impact long term spent fuel performance under dry storage conditions.

Data on wet and dry storage experience in the CRP Member States are presented in Tables 2 and 3. The information is based on contributions at the time, when the Member State participated in the CRPs. The data has been adjusted using general fuel cycle information to achieve a common baseline.

TABLE 2. REPORTED WET STORAGE EXPERIENCE IN THE CRP COUNTRIES

Country	Reactor type	Cladding type	Comment/contributions reported in the publication
Argentina	CANDU	Zry-4	1, 5 and 6.
Canada	CANDU	Zry-4	1, 2, 3, 4 and 5.
Finland	PWR	Zry-4	1, 2 and 3.
	WWER	Zr-1%Nb	1, 2 and 3.
France	LWR	Zry-4, M5™	1, 2, 3, 4, 5 and 6.
			1, 2, 3, 4, 5 and 6.
Germany	PWR	Zry-4, M5™	1, 2, 3, 4, 5 and 6.
	WWER	Zr-1%Nb	1, 2, 3, 4, 5 and 6.
	BWR	Zry-2	1, 2, 3, 4, 5 and 6.
Hungary	WWER	Zr-1%Nb	1, 2, 3, 4, 5 and 6.
Japan	BWR	Zry-2	1, 2, 3, 4, 5 and 6.
	PWR	Zry-4, MDA™, ZIRLO™	1, 2, 3, 4, 5 and 6.
	GCR	MagnoxAL80	1, 2, 3?
Korea, Republic of	PWR	Zry-4	2, 3, 4, 5 and 6.
	CANDU	Zry-4	2, 3, 4, 5 and 6.
Russian Federation	WWER440	Zr-1%Nb	1[b], 2[b], 3 and 4.
	WWER1000	Zr-1%Nb	1[b] 2[b], 3 and 4.
	RBMK1000	Zr-1%Nb	1[b], 2[b], 3 and 4.
Slovakia	WWER440	Zr-1%Nb	1[c], 2[c], 3, 5 and 6.
Spain	PWR	Zry-4, ZIRLO™	3, 4, 5 and 6.
	BWR	Zry-2	3, 4, 5 and 6.
Sweden	LWR/PHWR	Zry-2	1, 2, 3, 4 and 5.
Switzerland	LWR	Zry-2, 4	6.
UK	MAGNOX	MagnoxAl80	2, 3, 4, 5 and 6.
	AGR	20Cr:25Ni:Nb SS	
	LWR	Zry-2, 4	
	SGHWR	Zry-4	
USA	PWR	Zry-4, ZIRLO™, M5™	1, 2, 3, 4, 5 and 6.
	PWR	SS	1, 2, 3, 4, 5 and 6.
	BWR	Zry-2	1, 2, 3, 4, 5 and 6.
	HTGR	n/a	1, 2, 3, 4, 5 and 6?.

[a] The CRPs are numbered consecutively, e.g. BEFAST-II is 2, and SPAR-I is 4.
[b] Soviet Union
[c] Czechoslovakia

TABLE 3. REPORTED DRY STORAGE EXPERIENCE IN THE CRP COUNTRIES

Country	Reactor type	Storage type	First system deployed	Comment/contributions reported in the publications[1]
Argentina	CANDU	Vertical silos	1993	5 and 6.
Canada	CANDU	Vertical silos	1985	1, 2, 3, 4 and 5.
		Concrete Casks	1995	1, 2, 3, 4 and 5.
Germany	PWR	Metal casks	1995	1, 2, 3, 4, 5 and 6.
	WWER	Metal casks	1999	1, 2, 3, 4, 5 and 6.
	BWR	Metal casks	2002	1, 2, 3, 4, 5 and 6.
Hungary	WWER	Vault	1997	3, 4, 5 and 6.
Japan	BWR	Metal casks	1995	1, 3, 4, 5 and 6.
Korea, Republic of	CANDU	Vertical silos	1992	2, 3, 4, 5 and 6.
Spain	PWR	Metal casks	2002	3, 4, 5 and 6.
	PWR	Concrete casks	2009	3, 4, 5 and 6.
Switzerland	PWR	Metal casks	1983	6.
	BWR	Metal casks	2005	6.
UK	MAGNOX	Vault	1972	2, 3, 4, 5 and 6
USA	PWR	Metal casks	1986	1, 2, 3, 4, 5 and 6.
	PWR	Horizontal silos	1986	1, 2, 3, 4, 5 and 6.
	PWR	Concrete casks	1994	1, 2, 3, 4, 5 and 6.
	BWR	Horizontal silos	1999	1, 2, 3, 4, 5 and 6.
	BWR	Concrete casks	2000	1, 2, 3, 4, 5 and 6.
	BWR	Metal casks	2000	1, 2, 3, 4, 5 and 6.

[a] The CRPs are numbered consecutively, e.g. BEFAST-II is 2, and SPAR-I is 4.

2.3. FUEL ASSEMBLY DESIGNS

The following section provides an overview of commercial fuel designs that have been the subject of reporting in the BEFAST and SPAR projects:

- LWR fuels made up of pressurized water reactor (PWR) and boiling water reactor (BWR) fuels;
- Russian origin RBMK and WWER fuels;
- CANDU PHWR fuel; and
- Gas reactor MAGNOX and AGR fuels.

2.3.1. LWR [2, 4]

LWR fuel assemblies comprise fuel rods and numerous structural components.

All PWR and BWR fuel assemblies/bundles contain fuel rods equally spaced from each other. Cylindrical uranium oxide pellets are inserted in zirconium based alloy tubing. PWR and BWR fuel designs differ in terms of: Fuel rod diameter and number of fuel rods; BWR fuel assemblies have an outer Zircaloy sheath which channels the coolant water through the fuel assembly; BWR fuel assemblies have multiple fuel enrichments. Modern PWR fuel assembly designs consist of fuel rods bundled in the range 14 × 14 to 18 × 18 in a square array. BWR designs consist of fuel rods bundled in 7 × 7 to 10 × 10; for example, Fig. 2. The different structural components of the fuel assembly, such as spacers, guide tubes, top and bottom end nozzles, tie plates, debris screens, water tubes and water or fuel channels are manufactured mainly from zirconium based alloys, stainless steel and Inconel.

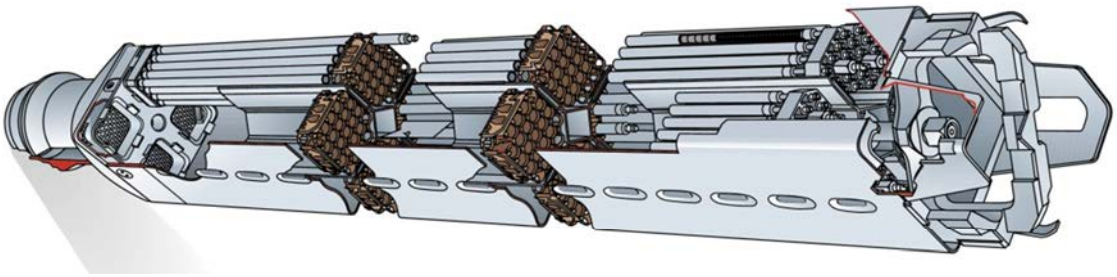

FIG. 2. Schematic of a BWR fuel assembly (figure courtesy of SKB).

2.3.2. CANDU [2, 4]

The fuel bundles used in modern CANDU reactors are composed of either 28 or 37 fuel rods, held together in a cylindrical array by welds that attach the end caps of each fuel rod to two Zircaloy endplates (Fig. 3). Each fuel rod consists of a Zry-4 tube containing a stack of UO_2 pellets. The overall length of the fuel bundles is approximately 50 cm. Dependent upon the location of the fuel rods within the bundle assembly, either spacers or bearing pads are brazed to the outside surface of the cladding. The spacers are designed to maintain coolant flow around the rods while the bearing pads protect the cladding from wear due to friction with the pressure tube during reactor operation. Zr-5Be brazements are used for attaching the Zircaloy spacers and bearing pads to the Zircaloy fuel sheath.

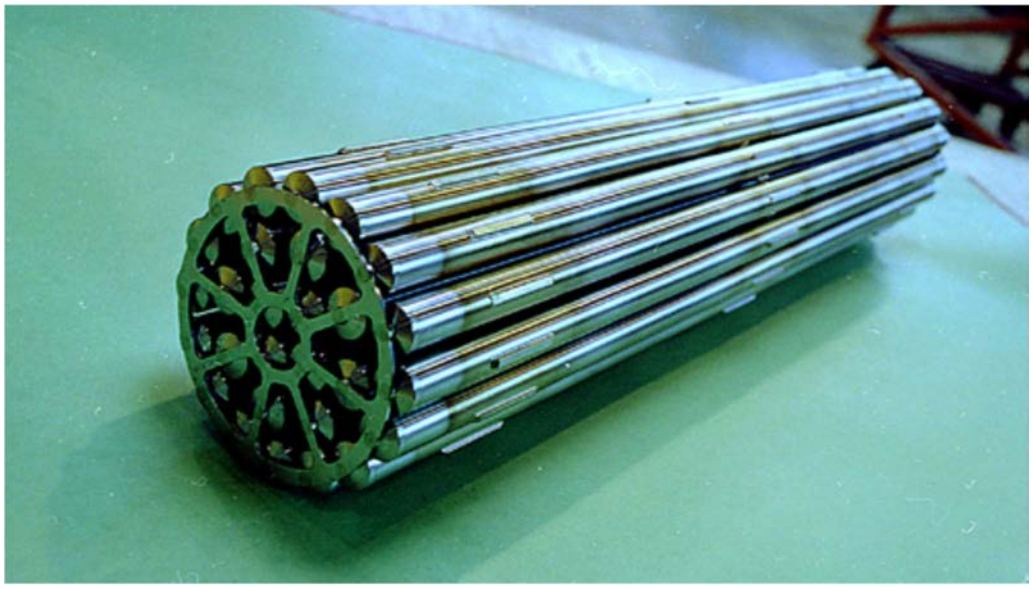

FIG. 3. CANDU fuel bundle; ~50 cm in length (photograph courtesy of Ontario Power Generation (OPG)).

2.3.3. RBMK

RBMKs are Russian designed channel type graphite moderated BWRs. RBMKs are now operated exclusively in the Russian Federation at three NPP sites. There are eleven 1000 MW(e) capacity units in operation.

The fuel assembly is around 10 m in length and comprises a central guide tube, two fuel bundles (which are spaced to allow for thermal expansion of the rods between the bundles during irradiation) and an extension rod. Each bundle comprises 18 fuel rods held in a

skeleton structure by nine spacer grids and a central tube. The fuel is uranium dioxide with an enrichment of up to 2.8% ^{235}U and all fuel rods contain the neutron absorber erbium with a content of about 0.6% [2].

The main characteristics of the fuel assemblies are summarized in Table 4. Upon reactor discharge, the fuel assemblies are initially cooled before being size-reduced into individual fuel bundles; with the extension rod being consigned as waste.

2.3.4. WWER

WWER reactors are Russian designed pressurized water type reactors. Fuel assemblies are hexagonal either with or without an outer metal shroud to channel the water flow. Modern WWER fuel assemblies are designed with removable top nozzles to facilitate fuel rod replacement. The main differences between WWER-1000 and WWER-400 fuel designs are:

- WWER-1000 FAs have 312 fuel rods compared to 126 in the WWER-440 design;
- WWER-1000 FAs are much larger than the WWER-440 counterparts being both longer and wider; and
- WWER-440 FAs have an outer hexagonal shroud or water channel made of Zr-2.5%Nb while almost all WWER-1000 FAs have none.

The main characteristics are summarized in Table 4.

TABLE 4. MAIN CHARACTERISTICS OF RUSSIAN ORIGIN FUEL ASSEMBLIES

Characteristic	Reactor		
	WWER-440	WWER-1000	RBMK-1000
Outer diameter of fuel rod, mm	9.1	9.1	13.6
Fuel rod cladding thickness, mm	0.65	0.67	0.90
Material of cladding	Zr-1%Nb	Zr-1%Nb	Zr-1%Nb
Overall Fuel Assembly length, mm	3200	4570	10 014
Fuel Assembly diameter, mm	145	235	80
Material of spacer grid[a]	Zr-1%Nb	Zr-1%Nb	Zr-2.5%Nb
Structural material (tubes at FA centre or corner)	Zr-1%Nb	Zr-1%Nb	Zr-2.5%Nb
Burnup			
– Present	40–43	45–49	24
– Planned	45–50	55	35

[a] Spacer grids were originally made of stainless steel.

2.3.5. AGR

AGR fuel assemblies (see Fig. 4) comprise: Graphite sleeve; Bottom grid plate; Guide tube; Two braces; 36 fuel pins. The fuel pins and guide tube are fixed to the bottom grid. Except for the outer graphite sleeve, all other components are made from highly alloyed stainless steel. In-reactor, up to eight AGR fuel assemblies are joined together by a stainless steel tie bar passed through the central guide tube of each fuel assembly to form a fuel stringer [2, 4]. The

stringer comprises a ~8 m fuelled section and a tie bar which is ~15 m long (except Dungeness B where the fuelled section is 7 m).

Upon discharge from the reactor AGR stringers are initially cooled in carbon dioxide before being dismantled in the reactor unit hot cell into individual fuel assemblies, which are then stored wet.

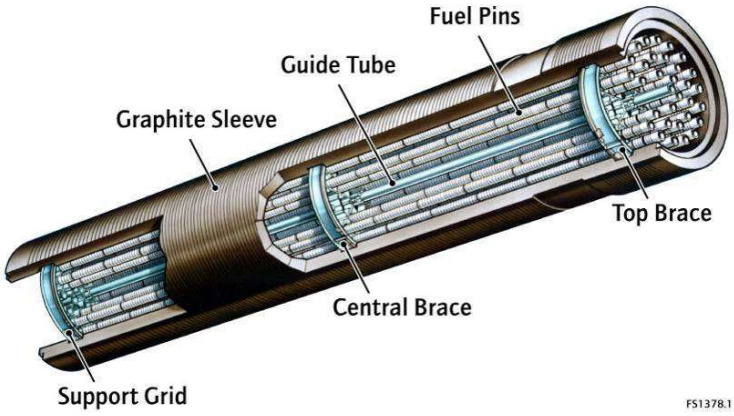

FIG. 4. AGR fuel assembly (figure courtesy of Sellafield Ltd.).

2.3.6. MAGNOX [2, 4]

The manufacture of commercial MAGNOX fuel was completed in 2008. The designs of MAGNOX fuel elements, although similar, were tailored for each reactor. Each element basically comprised an inner natural uranium rod machined with groves to reflect its core position, and one of either two types of outer hollow extruded and machined magnesium alloy can (polygonal or 'herringbone'); a cone end fitting, ceramic insulating discs and machined end cap complete the element (as shown in Fig. 5). The interspace is charged with a small amount of helium prior to the application of external pressure to lock the outer can into grooves in the uranium rod. In the reactor, the elements are placed on top of one another forming stringers within the graphite channel. The purpose of machining groves into the natural uranium rods and locking the external cans into them is to minimize localized stressing of the cladding during irradiation. The end cap is the only structural component of MAGNOX fuel.

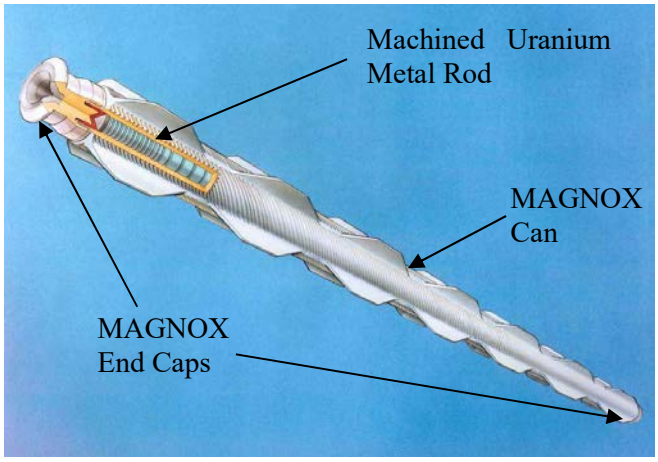

FIG. 5. MAGNOX fuel assembly (figure courtesy of Sellafield Ltd.).

3. OVERVIEW OF SPENT FUEL STORAGE TECHNOLOGIES

There are two basic spent fuel storage technologies; wet and dry. The design objectives for both technologies are the same and are summarized below [1]:

- Subcriticality of the spent fuel is to be maintained under normal and accidental conditions;
- Residual heat of the spent fuel should be removed effectively;
- Radiological shielding of the spent fuel should protect plant operators, the public and the environment from receiving radiation doses in excess of regulatory limits;
- Fuel cladding integrity should be maintained during handling and exposure to corrosion effects of the storage environment;
- Fuel degradation during storage should be prevented through providing adequate cooling in order not to exceed fuel temperature limits;
- Environmental protection should be assured by minimizing the release of radioisotopes; and
- Fuel retrievability should always be available.

Further guidance is provided in the specific safety guide on spent fuel storage [14].

3.1. WET STORAGE TECHNOLOGY

Wet storage is the most common technology and is typically associated with AR storages and large buffer storage for reprocessing facilities. Water provides efficient cooling and shielding after discharge. In the context of this publication AR refers to spent fuel storage that is physically connected to the power reactor or is in the same building.

At the outset of the project, wet storage was already considered a relatively mature technology with around 20 years of operating experience. Over the past 30+ years there have been some technological improvements in terms of instrumentation, remote handling, improvements in storage densities etc., but the basic technology has mostly remained the same. It is not intended to discuss wet storage technology further in this publication. To give an indication of the wet storage experience in participating countries a summary of the AFR wet storage, either on the reactor site (RS) or at an off-site location (OS), is provided in Table 5. This is presented as number of facilities, total design capacities, first operations and approximate inventory in 2013.

Further information on wet storage technology and lessons learned can be found in the following TECDOCs:

- Spent fuel storage options [18];
- Spent fuel storage – Lessons learned [19].

3.2. DRY TECHNOLOGIES

Unlike wet storage, dry storage technologies were in their infancy 30+ years ago with use being limited to the storage of some research reactor fuels and some gas cooled power reactor fuel. Over the period there has been both a growth in the use of dry storage (see Fig. 6) and the development of dry storage technologies. For example, in 1985 wet storage was the only licensed technology in the USA, and by 2014 there were 66 operational independent dry spent fuel storage installations, accommodating ~28% of the total USA spent fuel inventory.

TABLE 5. SUMMARY OF AFR WET SPENT FUEL STORAGE IN THE PARTICIPATING COUNTRIES

Member State	AFR pools in operation			
	Number of facilities	Total design capacity, t(HM)	Approximated inventory in 2013, t(HM)	First Operations (2nd AFR, 3rd AFR...)
Argentina	1	2000	1850	1988
Finland	2	1890	1673	1980 (1987)
France	4	17 600	9799	1981 (1984, 1986, 1988)
Germany	1	286	100	1999
Japan	2	4300	3951	1997 (1999)
Russian Federation	6	22 500	17 300	1977 (1984, 1985, 1986, 1986, 1996)
Slovakia	1	1694	1631	1987
Sweden	1	8000	5740	1985
Switzerland	1	425	195[a]	2008
UK	4	10 200	4608	1964 (1981, 1986, 1988)
USA	1	675	675	1984

[a] Reported includes both AR and AFR(RS) stored inventory at Gösgen NPP.

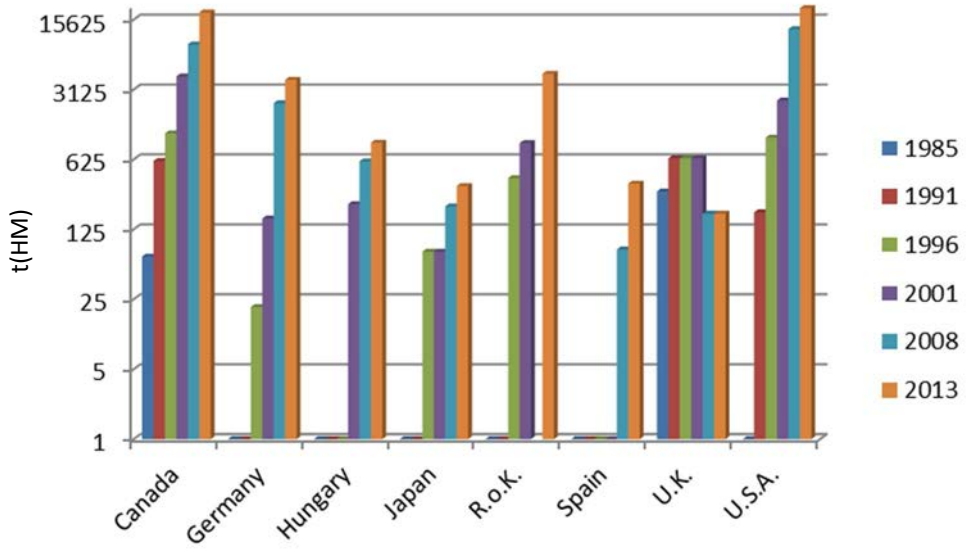

FIG. 6. Growth of dry spent fuel storage in the participating countries.

Initially dry storage technologies were single purpose systems. They only provided AFR (RS) storage (with one exception) without the capability or authorization for eventual transport off-site (without re-handling and reloading the fuel into transport casks) [4]. Examples of single purpose systems are: vaults; silos; and non-transportable casks.

With continuing development of dry storage technology, it was recognized that casks and containers for encapsulating the fuel could perform multiple functions. Dual purpose casks were developed (e.g. CASTOR® cask in Germany, or the NAC-STC in the USA), which allowed storage and transport to and from a storage facility without re-handling the fuel assemblies. The fuel containers of some storage systems may be used for transport and/or final disposal. These are often referred to as dual or multipurpose systems, respectively [1].

Table 6 provides an overview of the number of deployed facilities, total design storage capacity and an indication of the inventory in 2013 for participating countries.

TABLE 6. STATUS OF POWER REACTOR SPENT FUEL DRY STORAGE IN THE PARTICIPATING COUNTRIES

Member State	Dry storage systems in operation			
	Number of facilities	Date of first operations	Design capacity, in 2013 t(HM)	Approximate inventory t(HM) in 2013
Argentina	1	1993	2460	1950
Canada	7[a]	1984[b]	27 700	18 427
Germany	15	1992	22 370	3924
Hungary	1	1997	1080	837
Japan	2	1995	760	340
RoK	1	1992	6237	4903
Russian Federation	3	2012	9 500	1000
Spain	3	2002	1236	360
Switzerland	2	2001	3800	410
UK	1	1971	258	180
USA	60	1986	43 000	20 200

[a] Excludes the facilities at the research centres Chalk River and Whiteshell.
[b] Date given is for prototype CANDU power reactor fuel storage. The first dry storage systems were deployed at CRL in 1977 for early power development/research reactor fuels.

The following sections provide an overview of dry storage technologies which have been deployed in participating countries and reported during the CRPs.

3.2.1. Vaults

Vaults were the first dry storage systems to be used for commercial power reactor spent fuel. The technology was initially used for AR gas cooled reactor fuel storage and is the only dry storage technology that has ever been used for this purpose.

The design basis is the storage of spent fuel assemblies in an array of storage channels held within a reinforced concrete building. Shielding is provided by the exterior structure and heat removal is accomplished by natural convection of air on the outside of each storage channel. The decay heat is either exhausted directly to the outside atmosphere or dissipated via a secondary heat removal system [1]. Cooling provision can also be provided by forced air cooling. The spent fuel is stored either as single or multiple units. Although the original technology stored the fuel un-containerized in each storage channel, newer designs are based on the storage of containerized fuel. The modern systems have channels which use bolted metal 'O' ring sealed enclosures and are charged with an inert atmosphere. Containers use weld enclosures also with an inert atmosphere. Unlike other dry storage technologies, the atmosphere inside the storage channels can be monitored.

Vault facilities have been constructed in France, Hungary, the UK and the USA. Although not available at the time when the Russian Federation participated in the CRPs, they have since constructed a vault complex at the Mining Chemical Combine at Zheleznogorsk for RBMK and WWER-1000 spent fuel[2]. Spain is also proposing to construct a centralized dry storage facility based on vault technology in the future.

[2] Plans to build this facility were reported [2]. The facility was originally planned to be operational in 2007 with a total storage capacity of 33 000 t(HM).

Figure 7 provides views of the modular vault dry store (MVDS) at Paks NPP (Hungary); the first system to be constructed for the storage of commercial water reactor fuel. Table 7. provides a summary of vault facilities in participating countries. Further information on vault stores is provided in Ref. [18].

FIG. 7. Paks MVDS, operator PURAM, Hungary. Views of the top of the storage tubes and the charge hall (photographs courtesy of PURAM).

TABLE 7. SUMMARY OF DRY STORAGE IN VAULT FACILITIES IN PARTICIPATING COUNTRIES

Country/ Facility	Number of facilities	Design capacity t(HM) in 2013	Approximate inventory t(HM) in 2013	First operations
France[a]	1	180	180	1990
Hungary	1	1080	837	1997
Russian Federation	1	8200	330	2012
UK	1	3 × 86	180	1971
USA[a]	1	14.7	14.7	1991

[a] The vaults in France and USA store fuels from unique types of power reactors.

3.2.2. Silos or concrete canisters

The technology for dry storing spent fuel in silos or concrete canisters was first developed by Atomic Energy Canada Limited (AECL) at their Whiteshell Laboratories in the 1970s with a prototype system being deployed in 1975. The original design relies upon natural convection from the concrete shielding and therefore leads to restricted heat loading limit with the need to load long stored fuel. The later silo systems (NUHOMS and MACSTOR) incorporate vents to aid thermal dissipation as shown in Fig. 8.

The technology comprises a fixed monolithic or modular concrete reinforced structure. The concrete provides shielding while containment is provided by either an integral inner metal liner, which can be sealed after fuel loading, and fuel being sealed into a basket, or by a separate sealed metal canister. Silos are either vertical (CANDU) or horizontal orientation (LWR). Fuel loading into silos always takes place at the storage site using a metal transfer cask [1].

More information on silos is provided in [18]. Table 8 summarizes the use of silos and concrete canister facilities in participating countries.

FIG. 8. NUHOMS® system at Calvert Cliffs (photograph courtesy of US NRC File Photo).

TABLE 8. SUMMARY OF SILOS AND CONCRETE CANISTER FACILITIES IN THE PARTICIPATING COUNTRIES

Country	Number of facilities	Total design capacity, in 2013 t(HM)	Inventory t(HM) in 2013	First operations
Argentina	1	2210	1950	1993
Canada[a]	4	5047	3924	1984
Republic of Korea	1	6250	4900	2012
United States[b]	26	8500	7800	1986

[1] Excludes the research facilities at Whiteshell and Chalk River
[2] Some sites contain a mixture of cask and silo systems, therefore there is some double counting in terms of design capacity. Design capacities taken from IAEA nuclear fuel cycle information system where available.

Storage in silos or concrete canisters was reported during the CRPs by Argentina, Canada, Republic of Korea and the USA.

3.2.3. Cask (metal and concrete) systems

Metal and concrete casks are variations of containers. A container is a receptacle to hold spent fuel to facilitate movement and storage or eventual disposal, according to the IAEA glossary of spent fuel terms [1, 20]. They are either thick walled containers, or a thin walled container which uses a separate overpack for shielding purposes. The structural materials of metal casks may be forged steel, ductile cast iron, steel/lead or a forged steel/resin/steel shell sandwich structure [1]. Concrete casks are steel/concrete/steel sandwich structures or a thin walled steel canister which is then placed inside an overpack (usually reinforced concrete).

Large varieties of container systems have been designed and are described in Ref. [18].

Dry cask storage facilities have been constructed in Canada, Germany, Japan, the Russian Federation, Switzerland and the USA; Table 9 summarizes the use of dry cask storage in participating countries.

TABLE 9. SUMMARY OF DRY STORAGE IN CASKS IN THE PARTICIPATING COUNTRIES

Country	Number of facilities	Design Capacity, in 2013, t(HM)	Inventory in 2013, t(HM)	First Operations
Canada	3	22 645	14 503	1996
Germany	15	22 370	3924	1992
Japan	2	900	250	1995
Russian Federation	2	1300	656	2012
Spain	3	1236	360	2002
Switzerland	2	3800	438	2001
United States[1]	42	33 750	15 149	1986

[1] Three sites contain a mixture of casks and silos, therefore the figures are subject to some double counting

3.2.3.1. Metal casks

The feasibility of using a metal cask for both the storage and subsequent transportation of spent fuel was first investigated in Germany in 1977. After a period of proofing the concept and conducting demonstration trials, the first commercial systems were deployed at Surry NPP in the USA in 1986.

Metal casks are usually transferred directly from the fuel loading area to the storage site. Some metal casks are licensed for both storage and off-site transportation on public roads. Fuel is loaded vertically into the casks, which are usually stored in a vertical position [1].

Metal cask storage was reported by a number of countries such as Germany, Japan, Spain, Switzerland and the USA in various stages of the CRPs [1]. Some examples are shown in Figs 9 and 10.

FIG. 9. TN-32 storage casks at Surrey NPP in the USA (photograph courtesy of US NRC File Photo).

FIG. 10. CASTOR casks in Ahaus and Gorleben in Germany (photographs courtesy of GNS).

3.2.3.1. Concrete casks

The concept of using a concrete cask for the transport, storage and possible disposal of spent fuel was first investigated by Ontario Hydro (Canada). A demonstration programme was set-up in 1988, and the first commercial system using this technology, the dry storage cask (DSC) as shown in Fig. 11, was later deployed in 1996.

FIG. 11. CANDU DSCs (photograph courtesy of OPG).

Around about the same time an alternative concrete cask system was being investigated in the USA by a consortium using what later became known as the Sierra Nuclear ventilated storage cask (VSC). This differed from the Ontario Hydro system in that the fuel was loaded into a metal canister which was then transferred to a concrete storage cask (only metal lined on the inside) using a metal transfer cask. The main advantage of this system over the DSC was that it could accommodate shorter cooled/high burnup fuel. The thermal loading limits of the DSC have since been improved by the use of high performance concrete systems.

Further vertical concrete casks, such as HOLTEC's HI-STORM ventilated modules, NAC's UMS, GNB's CONSTOR casks were developed later. More information on concrete casks is provided in Ref. [18].

Storage in concrete casks during the CRPs has been reported by Canada, Spain and the USA.

4. SPENT FUEL DEGRADATION MECHANISMS (WET & DRY)

The information in the chapter has been sourced from Refs [2,4]; it will be noted for sections where this is not the case. Other references are cited within the text as appropriate.

Maintaining structural assembly and fuel cladding integrity is important. Intact cladding acts as the primary containment barrier for both fuel pellets and fission products over the storage period and during subsequent fuel handling operations. This is valid for all the types of spent power reactor fuels considered: LWR and WWER, RBMK, AGR, MAGNOX and CANDU. For CANDU and some BWR fuel designs, cladding integrity may also be important for fuel assembly (bundle) integrity, because some of the fuel rods (pins) also act as structural elements.

4.1. LIGHT WATER REACTORS

Apart from a limited number of early fuel designs, all current LWR fuel rod claddings are made of zirconium based alloys. In BWRs, Zry-2 is used, whereas in PWRs, Zry-4 and Zr-Nb alloys are the preferred materials.

4.1.1. Wet storage

The degradation mechanisms that may affect cladding integrity during wet storage are as follows:

1) Uniform (aqueous) corrosion;
2) Localized corrosion (Pitting, galvanic and microbial induced corrosion (MIC)); and
3) Hydriding.

Degradation mechanisms that may impact fuel clad integrity during wet storage are illustrated in Fig. 12.

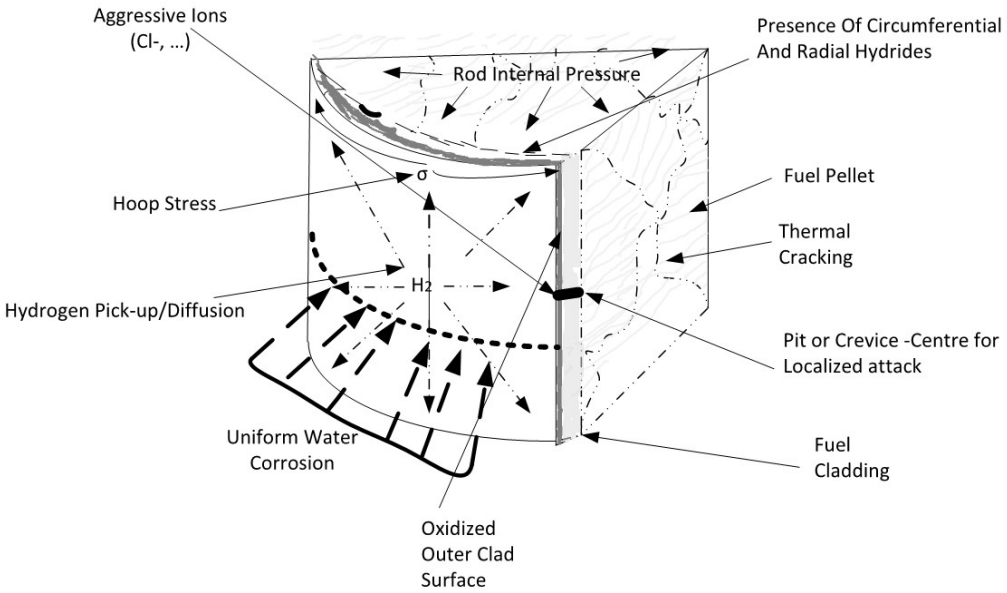

FIG. 12. Schematic illustration of the phenomena which may affect spent fuel cladding performance during wet storage.

4.1.1.1. Uniform corrosion

The corrosion behaviour of zirconium alloys in pressurized water and water vapour is well known for temperatures above 200°C. Because the corrosion rate follows the Arrhenius law in the linear, post transition corrosion regime, corrosion rates in pool water at 30°C to 45°C are a factor of ~10^{10} lower[3] than those under operational reactor conditions. Therefore, zirconium based alloys are virtually immune to uniform corrosion during wet storage, at least under controlled chemistry water conditions.

In 2012 immersion tests on irradiated Zry-4 clad specimens at 50°C in a variety of potential storage chemistries were reported to SPAR-III [7]. Polished and oxide layer intact specimens were immersed in sodium hydroxide (pH 11.4), sodium nitrate (up to 50 ppm) and demineralized water. Sodium hydroxide and sodium nitrate solutions were made up with demineralized water. The duration of the tests was up to one year. Samples were removed at selected time intervals based on the previous results and analysed by weight loss and metallography using scanning electron microscopy (SEM).

The results of the study were:

- Corrosion rates were below the limit of detection. The default resolution limit of the SEM at 50 nm was therefore taken as the worst case rate of corrosion for all chemistries; i.e. 50 $nm \cdot y^{-1}$;
- No spallation of the original ZrO_2 layer or localized corrosion was observed; and
- No effects on the adherence thickness or morphology of the oxide layer by any of the chemistries could be concluded.

Apart from zirconium based materials, other materials used in fuel assembly structures/bundles include stainless steel (304L) and Inconel (625, 718 and X-750). While their uniform corrosion rates are higher than zirconium based materials in water, both materials still show excellent durability in wet storage environments (<1 $\mu m \cdot y^{-1}$).

4.1.1.2. Localized corrosion (galvanic, pitting and MIC)

In wet storage, where the pool water acts as an electrolyte, galvanic corrosion is the preferential attack of one of two electrically dissimilar metals which are in electrical contact. Galvanic corrosion is an area of potential concern for fuel assembly materials in contact with storage racks, containers etc.

Stainless steel finds common use in storage racks and containers because, like zirconium alloys, it is at the near noble end of the galvanic series and therefore no electrochemical attack occurs. The evidence to date supports that this is the case. The other material that has found use in storage is aluminium. Aluminium alloys, which are near the active end of the series, if in electrochemical contact with zirconium alloys, would generate enough potential to oxidize the aluminium and hydride the zirconium. In reality this does not happen because both materials readily form passivating oxide layers which act as a barrier preventing the materials coming into direct electrical contact with one another.

[3] Putting this in context, the corrosion resulting from one full power day is equivalent to the corrosion that would occur over a period of several millions years in wet storage.

Zirconium based alloys and stainless steel based materials are not susceptible to pitting corrosion under normal water chemistry conditions existing in spent fuel pools. MIC is the result of metabolic activity by some bacteria species; particularly sulphate reducing bacteria in stagnant water. While there has been some evidence for MIC in cooling structures, the MIC of zirconium based alloys and pool storage equipment has not been observed. Periodic sampling to detect for the presence of harmful species can be implemented as a precautionary measure; especially for out-door storage facilities.

4.1.1.3. Hydriding

Maximum cross-section averaged hydrogen concentrations in zirconium alloy claddings at the end of in-reactor operation are typically between 50 and 600 ppm; depending on material, fuel rod elevation and in-reactor fuel cycle duty. When the fuel is cooled to the storage pool temperature, hydrogen in solid solution in the alloy precipitates in the form of hydride platelets, except possibly for the hydrogen that is associated with (or trapped in) irradiation defects, such as vacancy dislocation loops. Due to the heat transfer characteristics of water, hydrogen redistribution by thermal diffusion and formation of so called pits by an Ostwald ripening can be ruled out during long term wet storage at the pool temperatures of practical interest.

4.1.2. Dry storage

Potential degradation mechanisms that may affect cladding integrity of LWR fuels during dry storage and subsequent handling and transportation operations are:

1) Air oxidation;
2) Thermal creep;
3) Stress corrosion cracking (SCC);
4) Delayed hydride cracking (DHC);
5) Hydride reorientation; and
6) Hydrogen migration and redistribution.

The first mechanism is of specific interest when considering loss of inerting conditions when inert gas (typically helium) is replaced with air. The next three mechanisms have the potential to result in through wall cladding defects during storage. The last two are unlikely to result in fuel rod failure during storage; rather, they have the potential to impair the ability of the cladding to effectively withstand potentially adverse mechanical challenges resulting from handling or transportation accidents.

The end of irradiation conditions existing in a LWR fuel pin section which can impact fuel clad (zirconium based) integrity in dry storage are shown in Fig. 13.

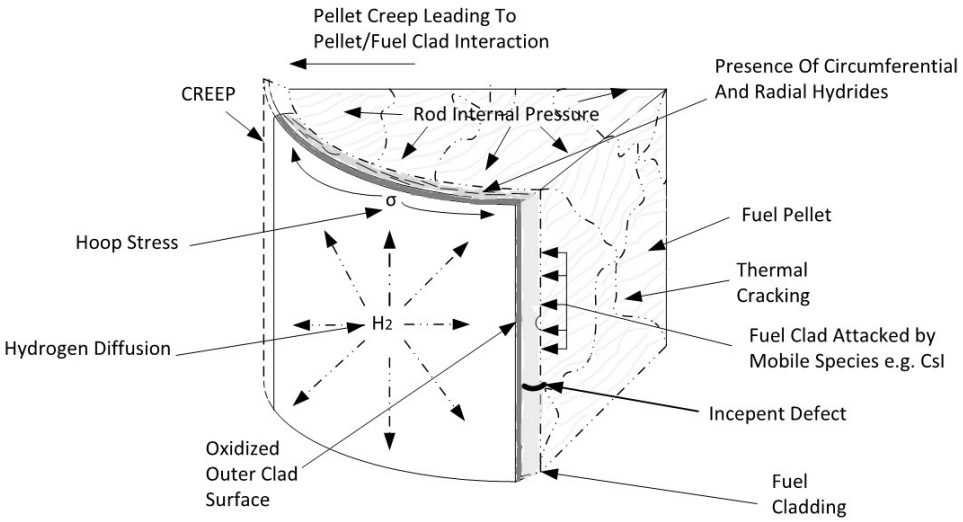

FIG. 13. Imparted properties which can affect spent fuel cladding (zirconium based) performance during dry storage.

Potential systemic conditions leading to loss of cladding integrity are either prohibited by regulations, or considered undesirable complications, especially those resulting from gross cladding ruptures. Stress corrosion cracking and DHC are generally not considered to be active mechanisms for fuel elements with thin walled cladding, given that stress intensity factor values are well below threshold values for crack initiation and/or propagation. However, DHC is considered to be a limiting degradation mechanism for CANDU bundles. Much experimental work has been performed to get a better understanding of the conditions under which hydride reorientation can occur, in order to obtain a better understanding of the potential degradation in cladding mechanical properties and its potential impact on spent fuel handling and transportation operations. Hydrogen migration due to axial temperature profiles has been found to be of limited consequence.

4.1.2.1. Air oxidation

Inert atmosphere conditions during dry storage, preceded by appropriate drying and inerting operations, rule out the presence of significant amounts of air in contact with stored spent fuel. Normal conditions do not result in oxidation beyond that incurred during reactor duty. Therefore, oxidation is not an active degradation mechanism under normal inert storage conditions. Air oxidation is possible for off normal or accident conditions that would result in the failure of the storage system seals. Two scenarios can be considered: (1) fuel rods with no through wall defects; and (2) fuel rods with through wall defects.

Cladding oxidation

Because oxidation rates of zirconium based cladding by air are relatively low at temperatures typical of dry storage conditions[4], losses in cladding wall thickness are limited to a few

[4] Using the equation developed in *The Corrosion of Zircaloy Clad Fuel Assemblies in a Geological Repository Environment* [Hillner E., Franklin, D.G., and Smee, J.D., WAPD-T3173 (1998)], it is predicted that only 20 μm of additional cladding would be lost for fuel held at 400°C for 100 days. The Hillner et al.'s equation was developed for steam corrosion, but the corrosion rates in steam and air are similar.

percent, even for prolonged air exposure. Therefore, cladding remains an effective containment barrier protecting the fuel pellets from exposure to air for fuel rods that do not contain through wall defects.

Fuel oxidation

For cladding with through wall defects, air will come in contact with the fuel inside the rod. UO_2 oxidation rates remain very low below ~250°C. If the temperature exceeds 250°C, UO_2 conversion to U_3O_8 becomes possible. Oxidation of spent fuel in air is a two step process of the form (Eq. (1)):

$$UO_2 \rightarrow U_4O_9 \rightarrow U_3O_8 \quad (1)$$

In spent fuel oxidation experiments [21], the oxygen-to-metal (O/M) ratios first approach a plateau near 2.4 (rather than 2.25 corresponding to U_4O_9). The oxidation process according to the reaction in Eq. (2) does not result in appreciable fuel pellet density changes.

$$UO_2 \rightarrow UO_{2.4} \quad (2)$$

Once the spent fuel oxidizes to $UO_{2.4}$, the fuel appears to 'resist' further oxidation to higher oxides. Following this plateau, oxidation may resume and continue until the U_3O_8 phase is reached (Eq. (3)).

$$UO_{2.4} \rightarrow U_3O_8 \quad (3)$$

This reaction, Eq. (3), is strongly dependent on both fuel temperature and fuel burnup and the transition results in a volume expansion of greater than 36%. The increase in volume as fuel oxidizes to U_3O_8 results in high stress levels on the cladding; gross cladding rupture, or 'unzipping', may result.

The investigations of the effect of high burnup on oxidation behaviour were carried out on irradiated UO_2 fuels with burnups of 50 GW·d·t(HM)$^{-1}$ and 65 GW·d·t(HM)$^{-1}$ [22]. Fuel samples were exposed to dry air at temperatures between 300 and 400°C. Figure 14 shows the weight gain curves at 300°C (left graphic) and 350°C (right graphic); a weight gain of 4% corresponds to 100% formation of U_3O_8 from UO_2. At 300°C, there is no significant burnup difference in the oxidation behaviour between 50 and 65 GW·d·t(HM)$^{-1}$. On the other hand, at 350°C, the oxidation rate of the sample with a burnup of 65 GW·d·t(HM)$^{-1}$ is higher than the oxidation rate of the sample with a burnup of 50 GW·d·t(HM)$^{-1}$ beyond the O/M of 2.4. It has been speculated that the microstructure of the pellet affected its oxidation behaviour at 350°C.

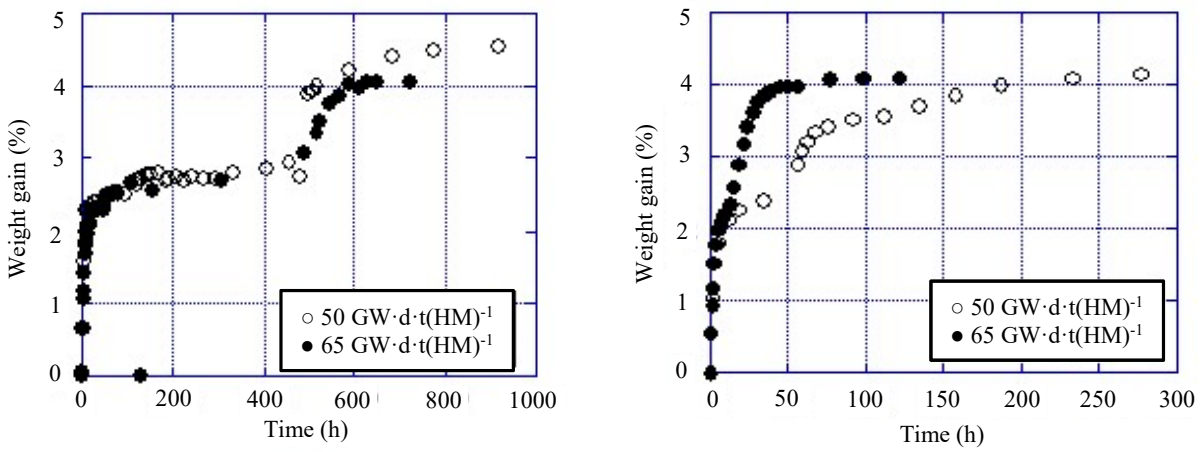

FIG. 14. Oxidation behaviour dependence on burnup and temperature (figures courtesy of CRIEPI [4]).

4.1.2.2. Thermal creep

Cladding rupture resulting from excessive creep deformation would most likely result in a 'pinhole' (or tight crack) type of rupture, given the loss of the driving force (i.e., rod internal pressure) upon depressurization coupled with the very low mechanical energy (the 'pV' term) stored in a fuel rod. Highly conservative criteria were initially established for the amount of creep strain that could develop over the licensed storage period to protect against the possibility of creep rupture during dry storage. A 1% end-of-storage creep strain was first proposed by Spilker et al. [23] as a sufficiently conservative limit that would be acceptable to German regulatory authorities. Significant progress in the state of the art of spent fuel behaviour evolution has been reported during the past twenty years. As a result, there presently exists a wide variation in regulatory guidance related to thermal creep. The latter covers the field from an adherence to the 1% creep strain limit, as proposed by Spilker, to no imposition of an explicit creep strain limit, as presently exists in the U.S. regulatory regime.

Early implementation of a creep limited approach in Germany led to a methodology that relies on the following considerations:

Conservative application of correlations obtained on unirradiated claddings to conservatively predict post irradiation thermal creep behaviour of irradiated claddings. The degree of conservatism can be obtained by comparing creep data of unirradiated and irradiated alloys (Fig. 15);

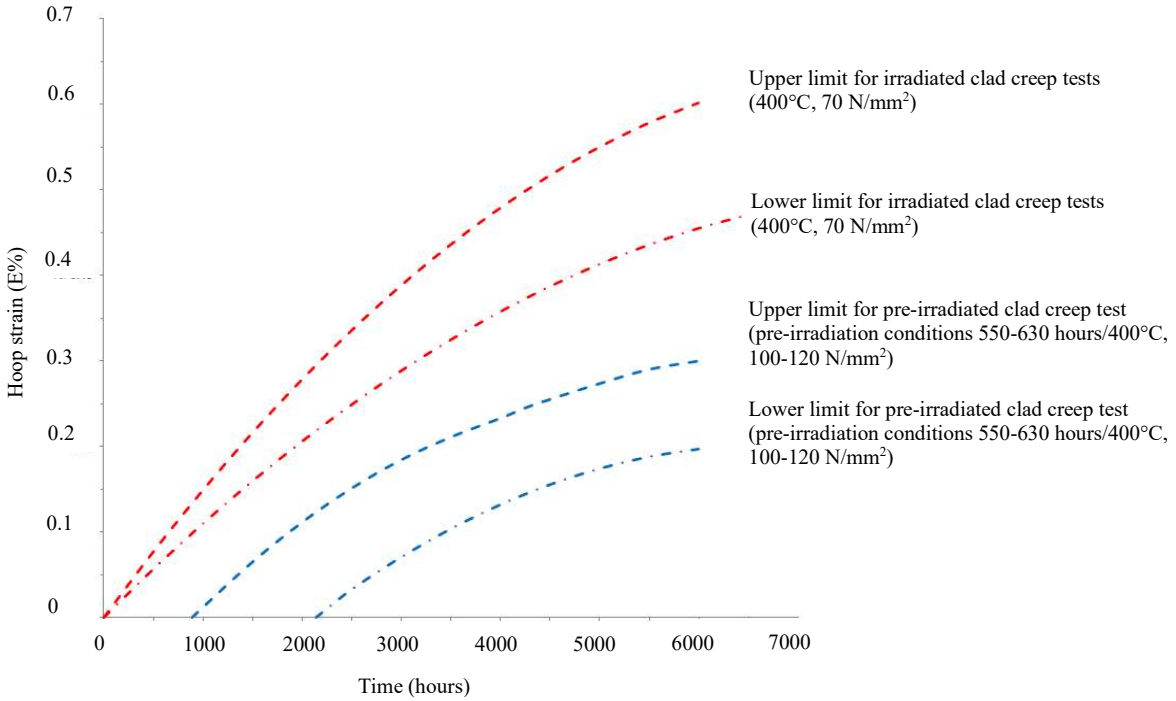

FIG. 15. Comparison of creep strain of irradiated and unirradiated Zry-4 cladding adapted from [4].

Collection of a database of the total creep strain capability of fuel rod cladding under simulated dry storage conditions. For a burnup less than 40 $GW \cdot d \cdot t(HM)^{-1}$, data from post-pile burst testing indicate that cladding will reach a 1% uniform strain before rupture. Because the rupture strain capability of the cladding tube decreases with fluence, the conservative approach of using burst testing with its very high strain rates is replaced by accelerated creep testing with lower strain rates. Such a test programme was conducted with spent fuel with burnup up to 64 $GW \cdot d \cdot t(HM)^{-1}$ [23]. The programme provided the basis for the present

German licence to store spent UO_2 and mixed oxide fuel assemblies with average batch burnup up to ~55 GW·d·t(HM)$^{-1}$.

Although dry storage of commercial spent nuclear fuel is not an option presently envisioned in the French programme, much work has been performed, both experimentally and analytically, in the context of the PRECCI ('Programme de Recherches sur l'Evolution à long-terme des Colis de Combustibles Irradiés') project in order to better understand the long term evolution of spent fuel under environmental conditions relevant to dry storage and geological disposal. In particular, experimental data, derivation of creep rupture criteria and constitutive equations for cladding creep have been established. The work was pursued in the framework of the French laws for the management of nuclear wastes [24].

In Japan, creep behaviour of fuel cladding is regarded as one of the most important issues for fuel integrity during long term dry storage of spent fuel. Creep properties have been investigated under various hoop stress, temperature and irradiation conditions in two different controlling creep deformation regimes, respectively identified as grain boundary sliding and dislocation climb. The transition from dislocation climb (at higher values of the σ/E ratio, where σ is the hoop stress and E is Young's modulus) to grain boundary sliding (at lower values of the σ/E ratio) is illustrated in Fig. 16.

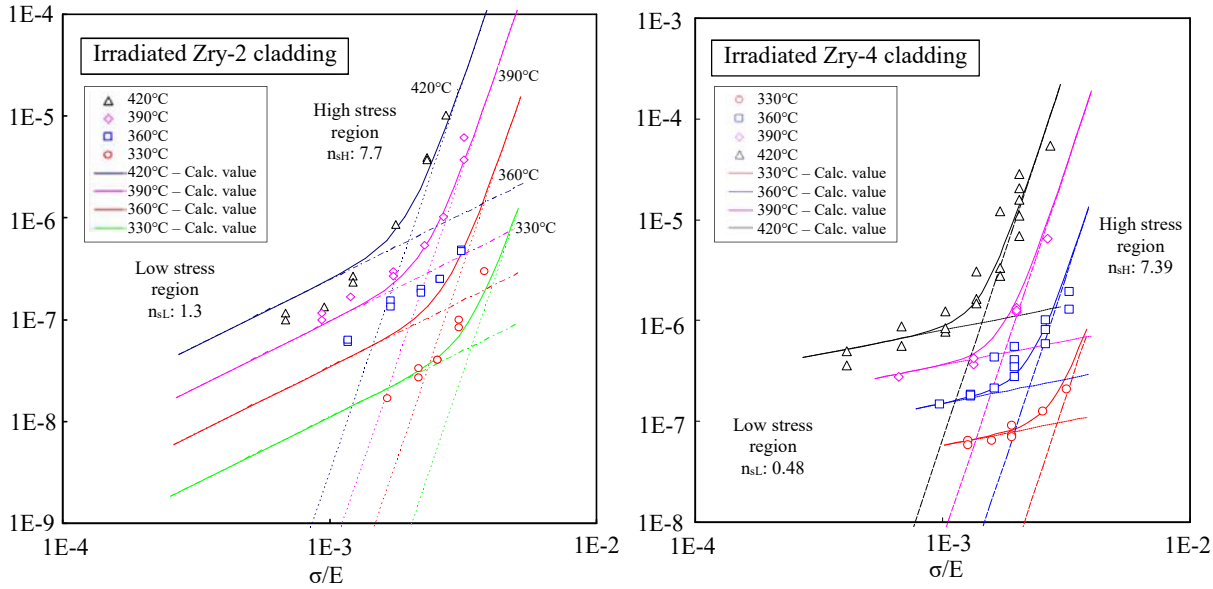

FIG. 16. Stress dependency of secondary creep rate (figures courtesy of JNES [4]).

Creep strain equations expressed as the sum of conventional primary creep and secondary creep strains have been derived for unirradiated and irradiated BWR (Zry-2 irradiated up to 50 GW·d·t(HM)$^{-1}$) and PWR (Zry-4 irradiated up to 48 GW·d·t(HM)$^{-1}$) claddings. Equations are documented in Ref. [4].

The secondary creep rate and creep strain of irradiated cladding were, for all temperature conditions and stress regions, smaller than those of unirradiated cladding. These results confirm, within the range of testing conditions, the lower creep strains due to neutron irradiation. The effect was smaller at lower temperature and lower stress. Assuming the creep mechanisms to be dislocation climb and grain boundary sliding in the high and low stress regions, respectively, irradiation defects such as point defect clusters, interstitial and

dislocation loops, etc. hamper dislocation movement. As a result, creep suppression becomes more apparent in the high stress regions where creep by dislocation climb is predominant. On the other hand, because irradiation defects are not considered to be very effective in suppressing creep due to grain boundary sliding, the suppressive effects in the low stress regions are relatively small.
For the tests conducted on unirradiated cladding, the effects of hydrogen on cladding creep behaviour in the investigated range of temperature and hoop stress were as follows:

- Hydrogen content below solubility limit: For BWR Zry-2 cladding, creep showed a slight acceleration by charged hydrogen, while no significant tendencies were observed for PWR Zry-4 cladding;
- Hydrogen content above solubility limit: Creep suppressive effects increased with increased hydrogen content in PWR cladding, while, for BWR cladding, a slight accelerating effect was observed in low stress region, and suppressive effects were observed in the high stress region; and
- No effects on creep rate due to hydrides reoriented in the radial direction were observed.

The Spanish organizations CSN, ENRESA and ENUSA have successfully carried out a programme to generate thermal creep data on high burnup ZIRLO™ (68 $GW \cdot d \cdot t(HM)^{-1}$) irradiated in the Spanish Vandellos nuclear power plant [25]. The creep results were consistent with the expected creep behaviour of CWSR Zry-4 material used as reference. During one test, a specimen leaked at an engineering strain of the tube section of 17%; remarkably, the crack closed due to de-pressurization, indicating that the material retained significant ductility.

In support of interactions between the U.S. utility industry and the U.S. Nuclear Regulatory Commission (NRC), EPRI developed a creep based methodology for high burnup fuel placed in dry storage [26–27]. Behavioural regimes considered included the effects of irradiation damage recovery and hydrogen content on cladding creep rates. The effects of outer surface corrosion, including oxide spallation, on cladding stress localization and its consequent effect on creep deformations as well as the dependence of stress on temperature, due to progressive cooling during dry storage, were also considered. Creep rupture tests showed that creep rupture is a stress induced plastic instability as a terminal state of tertiary creep, which is highly unlikely to occur during dry storage of spent LWR fuel. This is because cladding creep deformations under dry storage conditions are self-limiting, characterized by a continuously decreasing strain rate due to a continuously decreasing cladding stress in proportion to the creep induced volume expansion and decreasing temperature. As a result, it was shown that, during dry storage, the creep strain is unlikely to exceed the critical strain domain leading to plastic instability.

Concurrently, experiments carried by Argonne National Laboratories (ANL) demonstrated the creep capacity of Zry-4 claddings from spent Surry (~35 $GW \cdot d \cdot t(HM)^{-1}$) and H.B. Robinson (HBR) (~68 $GW \cdot d \cdot t(HM)^{-1}$) fuels. Diametral creep strains as high as 8.5% (Surry) and 5.5% (HBR) were measured with no indication of local reductions in cladding thickness.

An example of analytical simulation of dry storage for a high burnup fuel rod with oxide thickness of 120 μm, and a hydride lens of depth equal to 50% of the original wall thickness is shown in Fig. 17. Initial temperature and internal pressure of 400°C and 19.1 MPa were selected. In addition, a temperature of 440°C was assumed during a 24-hour drying cycle, including heat-up and cool down period of 8 hours each. Figure 17 shows the hoop strain in the hydride lens ligament (thin section) and away from the lens (thick section) with the oxide

thickness treated as an equivalent metal loss. This figure shows the self-limiting behaviour of cladding creep (even in the local hydride lens region).

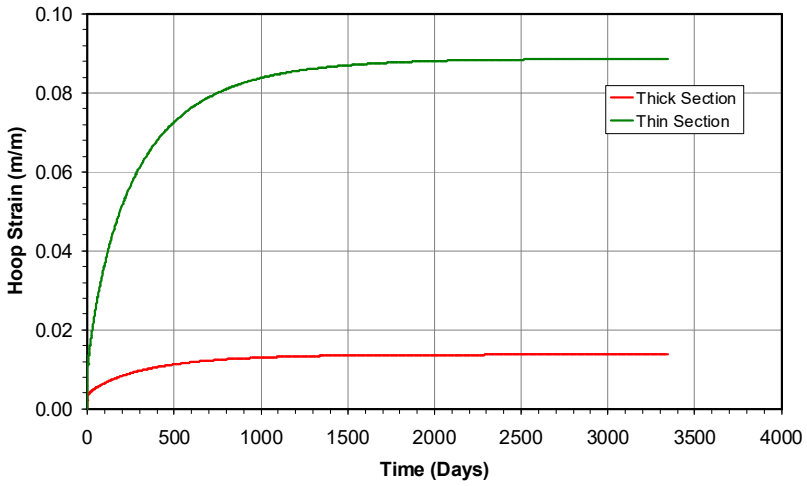

FIG. 17. Strain history for a fuel rod in a dry cask subjected to a 24-hour drying cycle with a peak temperature of 440°C (figure courtesy of EPRI [4]).

An important behaviour characteristic that is not simulated in pressurized tube creep tests is the effect of fuel pellets on constraining the creep deformations of high burnup fuel rods containing localized hydrides. Figure 18 shows the deformation resulting from creep in a fuelled rod cladding segment (left side) compared to a defueled cladding segment (right side) in the presence of a hydride lens decreasing the cladding effective wall thickness by a factor two. As a result, the creep deformations are not uniform. For the defueled specimen, the deformations tend to be localized in the hydride lens ligament. This causes the cladding to be pulled inward at a position 90 degrees away from the lens region, further increasing the deformations in the thinned ligament. The fuel pellets prevent this behaviour from developing and constrain the deformations in the hydride lens region. The difference between the two creep deformation behaviour modes is quite significant.

The result of these investigations resulted in a determination by the US NRC summarized as follows:

> *"In general, these data and analyses support the conclusions that: (1) deformation caused by creep will proceed slowly over time and will decrease the rod pressure; (2) the decreasing cladding temperature also decreases the hoop stress, and this too will slow the creep rate so that during later stages of dry storage, further creep deformation will become exceedingly small; and (3) in the unlikely event that a breach of the cladding due to creep occurs, it is believed that this will not result in gross rupture. Based on these conclusions, the NRC staff has reasonable assurance that creep under normal conditions of storage will not cause gross rupture of the cladding and that the geometric configuration of the spent fuel will be preserved, provided that the maximum cladding temperature does not exceed 400°C (752°F)"* [28].

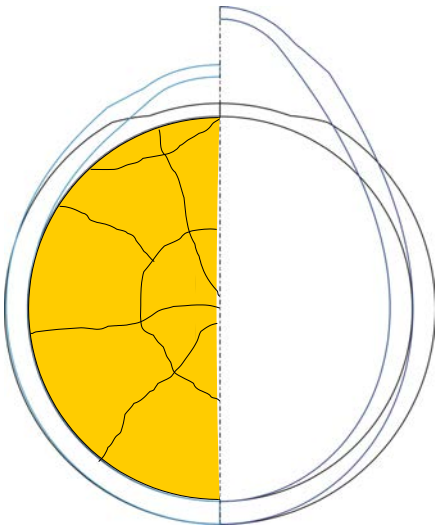

FIG. 18. Comparison of the creep response of a fuelled rod (left side) with the empty tube creep test simulation (right side), illustrating the constraining effect of fuel pellets on the local creep deformations (figure courtesy of EPRI [4]).

4.1.2.3. Stress corrosion cracking

Iodine induced stress corrosion cracking (SCC) occurs only within a specific high temperature range, in the presence of chemically active iodine and adequate stresses. Fission product behaviour can be characterized by a high stability against release. UO_2 fuel crystallizes in a CaF_2 type lattice and contains a plurality of vacancies, which aid in the retention of fission products generated by reactor operation. Also, each fissioned U-atom leaves an additional vacancy in the lattice. As a result, even in high burnup fuels, not all vacancies are occupied, and the UO_2 crystal has sufficient capability to retain fission products. A complete discussion of this topic is available in Peehs et al. [29]. The fission products generated in the UO_2 fuel under in-service conditions are practically immobile in the UO_2 fuel lattice in the temperature ranges typical of dry storage, and iodine is not present in a form that could trigger SCC.

As the combination of SCC agent and stress conditions required for crack propagation are normally absent, it can, therefore, be concluded that cladding failure via this mechanism is not expected to occur. Consequently, all fission product driven defect mechanisms such as stress corrosion cracking, uniform fuel rod internal fission product corrosion of the cladding, and localized fuel rod internal fission product corrosion of the cladding are not active.

4.1.2.4. Delayed hydride cracking

There are many ways in which hydrogen induced cracking of zirconium based alloys can occur. DHC is a very specific mechanistic process requiring triaxial stressing of the zirconium to dilate the crystal lattice. Triaxial stresses dilate the zirconium lattice tetrahedral sites that are the ones occupied by hydrogen atoms in solution. This allows the hydrogen atoms to diffuse up the stress gradient and precipitate in the peak stress region. Although DHC has been observed in Zircaloy specimens that are sufficiently thick, DHC is not expected to be an active degradation mechanism in cladding tubes, given that the latter do not appear to have enough wall thickness to generate much triaxial stress.

Laboratory tests of notched and pre-cracked specimens show that the DHC process evolves in two stages. Stage I is comprised of crack initiation followed by a rapid increase in crack velocity until it transitions into a stable crack growth regime, i.e., Stage II. During Stage II,

under isothermal conditions, the hydrogen in solution diffuses to the high stress zone surrounding the crack tip. With the continuous hydrogen diffusion to the crack tip region, the local hydrogen concentration rises until it exceeds the solubility limit and hydrides begin to precipitate ahead of the crack tip in the form of platelets oriented perpendicular to the direction of the stress. When the hydride reaches a critical size, it may fracture, allowing the crack to advance until it is arrested in the tougher Zircaloy material past the hydride, where a new highly stressed crack tip is formed, and the process is repeated. The crack continues to propagate in this intermittent manner until failure by plastic instability of the remaining ligament. This process is illustrated in Fig. 19 in which the crack velocity is plotted as a function of the stress intensity factor, K_I (Eq. 4):

$$K_I = f\sigma\sqrt{\pi a} \tag{4}$$

Where;
σ is hoop stress
a is length of cladding defect (crack)
f is numerical factor depending on cladding defect shape (= 1.04 to 1.26)

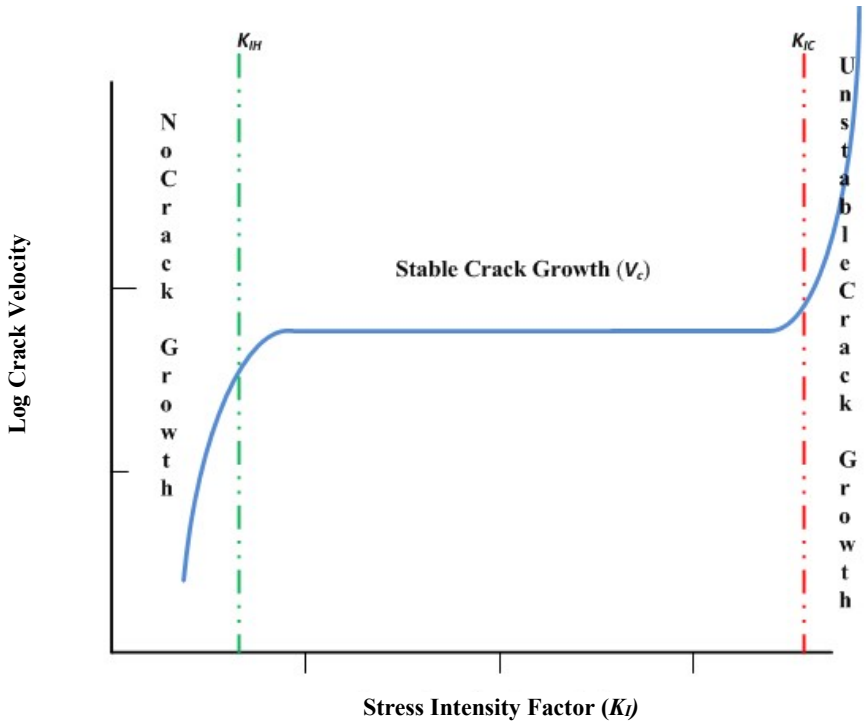

FIG. 19. Schematic representation of the dependence of the crack velocity as a function of the stress intensity factor, K_I. K_{IH} is the value of K_I at the transition between Stage I and Stage II. K_{IC} is the value of K_I at the end of Stage II, which is associated with unstable crack growth

Rashid et al. [30] present an analysis defining five conditions that should exist for DHC to be an active mechanism in LWR fuel during dry storage. The analysis concludes that DHC is not an operative mechanism in dry storage. It shows that stress intensity factors (K_I) in LWR fuel cladding are typically well below the critical stress intensity factors (K_{IH}) for either crack initiation or sustaining crack growth. However, DHC is considered to be the most critical mechanism that could affect the CANDU bundle integrity during dry storage (see later section).

4.1.2.5. Hydride reorientation

This subsection uses only the references cited.

An important issue in the safety evaluation of spent fuel during storage and transportation is the effect of hydrides on cladding resistance to failure [4]. At issue are safety and operational consequences of impact loadings that may incur during handling and transportation of spent fuel. The degree to which spent fuel cladding, after a number of years in dry storage, can retain sufficient strength and ductility depends, among several factors, on the spatial distribution and orientation of the hydrides. At the end of the active fuel cycle in PWRs, the total hydrogen content in Zry-4 cladding can be as high as 500–600 ppm. The cladding tube manufacturing process generates a texture in the cladding that causes hydrides to precipitate in the form of platelets in a predominantly tangential (or circumferential) orientation. This hydride morphology evolves very slowly during reactor operation as a consequence of hydrogen uptake during the slow waterside corrosion process, causing significant, but operationally tolerable, changes in the cladding mechanical properties [2, 4]. Additional circumferentially oriented hydrides precipitate during reactor shutdown due to the decrease in hydrogen solubility with temperature.

Hydride reorientation can occur as a result of the following sequence of events. Following wet storage in pools at prevailing temperatures of ~30–40°C, spent fuel is moved to dry storage, or transported to a centralized storage or reprocessing facility. Dry storage and/or transport operations may cause significant increases in cladding temperature: peak cladding temperatures of up to 400°C (dry storage) or up to 420°C (transport) are generally considered. The temperature increase from pool conditions to dry storage/transport conditions results in hydride dissolution and in a corresponding increase of the hydrogen in solid solution in the zirconium alloy matrix up to the hydrogen solubility limit. The temperature increase also leads to an increase in the rod internal pressure. Subsequent cooling during dry storage or re-wetting after transportation causes hydrogen in solid solution in the cladding materials to re-precipitate, but possibly aligned in the radial and axial directions (or simply ‘radial’) due to the influence of the tensile hoop stress in the cladding caused by the internal rod pressure that is no longer compensated by external means such as the coolant pressure in the reactor. This can result in a mixed, circumferential and radial hydride structure, depending on temperature and cladding hoop stress histories. Such a hydride structure can have a significant effect on cladding mechanical properties and failure limits, especially in the lower range of temperatures (<200°C) [4].

The two main factors driving hydride reorientation are cladding temperature and hoop stress [4]. Results obtained in several investigations pursued in France on Zry-4 are illustrated in Fig. 20, which shows the boundary between the domain where hydride reorientation has not been observed (left side) and the domain when hydride reorientation has been observed (right side). The extent of hydride reorientation on the right of the boundary increases as the temperature-hoop stress conditions are more severe, i.e., as temperature and stress increase.

An alternative approach was used by JNES to determine the temperature and hoop stress conditions for which no impact on mechanical properties due to hydride orientation would be observed [31]. In this case, the boundary was derived by ring compression testing of the ductility of the cladding after imposing a radial heat treatment (RHT[5]) defined by its initial cladding temperature and hoop stress. The latter approach, however, yields results that can be

[5] Also referred to as HRT.

strongly dependent on other parameters of the RHT, most notably the cooling rate, especially for zirconium lined BWR Zry-2 cladding, as will be covered in a later section. The results of the JNES investigation, shown in Tables 10 (PWR claddings) and 11 (BWR claddings), provide maximum temperature and hoop stress values of the RHT treatments, for which no deterioration in ductility was observed by ring compression testing at room temperature.

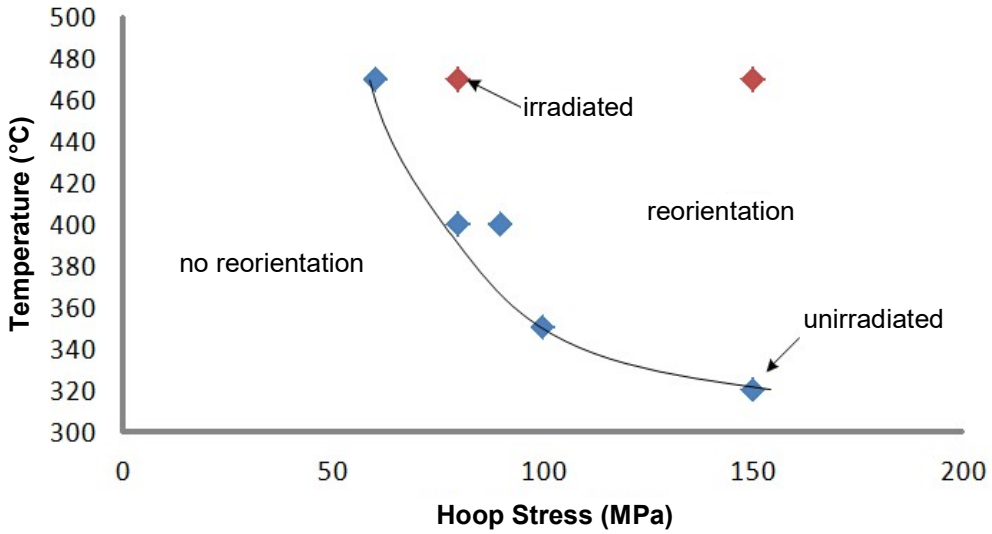

FIG. 20. Hydride reorientation domains vs. stress/temperature, adapted from Ref. [24].

TABLE 10. SUMMARY OF PWR CLADDING RHT THRESHOLDS OF NO DUCTILITY DEGRADATION AFFECTED BY HYDRIDE REORIENTATION [7]

	Cladding Type	Threshold of No Ductility Degradation That Would Be Due to Hydride Reorientation	
		Temperature (°C)	Hoop Stress (MPa)
PWR	39 GW·d·t(HM)$^{-1}$ Zry-4 (CWSR)	≤275	≤100
	48 GW·d·t(HM)$^{-1}$ Zry-4 (CWSR)	≤275	≤100
	55 GW·d·t(HM)$^{-1}$ MDA™	≤250	≤90
	55 GW·d·t(HM)$^{-1}$ ZIRLO™	≤250	≤90

TABLE 11. SUMMARY OF BWR CLAD RHT THRESHOLDS OF NO DUCTILITY DEGRADATION AFFECTED BY HYDRIDE REORIENTATION [7]

Cladding Type		Threshold of No Ductility Degradation That Would Be Due to Hydride Reorientation	
		Temperature (°C)	Hoop Stress (MPa)
BWR Zry-2 (RXA)	40 GW·d·t(HM)$^{-1}$ no liner	≤200	≤70
	50 GW·d·t(HM)$^{-1}$ with liner	≤300	≤70
	55 GW·d·t(HM)$^{-1}$ with liner	≤300	≤70

Effect of temperature on hydride reorientation

Only circumferential hydrides that dissolve due to the increase in cladding temperature upon transfer from a wet to a dry environment and then subsequently re-precipitate during cooling can potentially reorient [4]. Therefore, the maximum cladding temperature determines how much hydrogen goes back into solid solution in the zirconium based alloy matrix.

Hydrides typically show a significant hysteresis between precipitation and dissolution characterized by temperature gaps between the two solvi. This means that during cooling hydrides start to precipitate at a certain temperature, TTSSP (temperature of terminal solid solubility in precipitation), and during heating hydride dissolution ends at a quite different temperature, TTSSD (temperature of terminal solid solubility in dissolution) [4]. McMinn et al. [32] and Kammenzind et al. [33] observed hysteresis temperature gaps in Zry-2 and Zry-4 for dilute hydrogen contents (≤80 ppm) and for high hydrogen contents (<500 ppm) in Zry-4, respectively. The materials tested in both of these studies were in the stress free condition. For stress free zirconium alloys, the hysteresis gap is about 55±10°C between dissolution and initiation of precipitation of circumferential hydrides.

For illustration purpose, the solubility curves (TSSD and TSSP) established for non-irradiated alpha annealed Zry-4 are shown in Fig. 21. Heating from pool temperature to 400°C results in up to ~210 ppm of hydrogen going into solution in the alloy matrix. Heating to 300°C only dissolves up to ~77 ppm. Upon cooling from 400°C, re-precipitation of hydrogen in the form of hydrides is initiated at ~335°C, based on the curves shown in Fig. 21. This is the expected behaviour when the material contains hydrogen at or near the solubility limit of 210 ppm.

When the alloy contains 500 ppm of hydrogen, ~210 ppm of hydrogen is in solid solution upon heating to 400°C as stated in the previous example, with the balance of H (~290 ppm) being unaffected and remaining as hydrides. Upon cooling, K. Colas [34] found, using in situ XRD, for unirradiated cold worked stress relieved annealed Zry-4 cladding, that some hydride re-precipitation may occur with no or little hysteresis when there is residual hydride present when cooling begins. Under these conditions, the threshold hoop stress for hydride reorientation was between 150 and 200 MPa, which is substantially higher than the threshold stress observed for samples with no hydride present at 400°C.

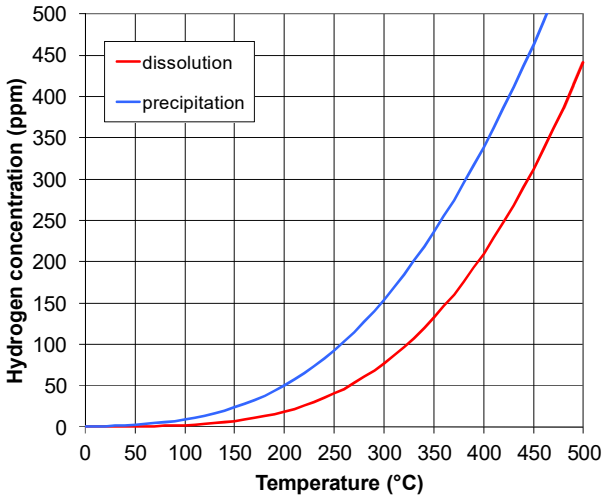

FIG. 21. Solubility curves for alpha annealed Zry-4 (adapted from Ref. [33]).

Comisión Nacional de Energía Atómica (CNEA), Argentina, is engaged in a research project to experimentally investigate hydride dissolution–precipitation phenomena. Hydride size distributions are determined from optical and transmission electron microscopy (TEM) field images. Histograms are shown in Fig. 22. In this analysis, 1 μm was taken as the border between the optical and TEM fields. Summarizing the results of the statistical analysis, it can be stated that a non-negligible amount of sub-microscopic hydrides, higher than 13%, exists but is not visible in the optical range. Considering that in the optical range 25% of hydrides are shorter than 5 μm, a wide hydride size distribution exists, extending over four orders of magnitude, from 10 nm to 100 μm, biased to sizes shorter than 5 μm. Additional details are provided in Ref. [7].

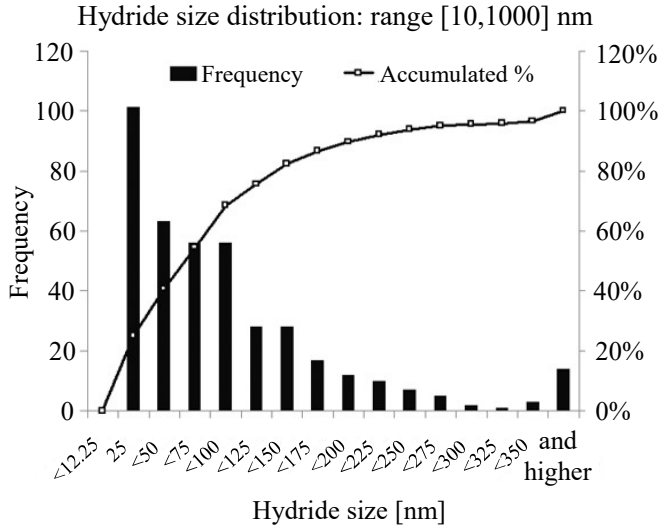

FIG. 22. TEM range histogram showing a hydride size distribution biased to small sizes. The maximum frequency is observed at 20-30 nm (courtesy of CNEA [7]).

Effect of stress on hydride reorientation

As shown in Fig. 20, both cladding stress and temperature affect the degree of reorientation. The end-of-life (EOL) rod internal pressure (RIP) is the primary protagonist for evolutionary changes during long term dry storage. At the maximum temperature attained either during

vacuum drying or dry storage, EOL rod internal pressures determine the maximum stress state in the fuel rod cladding, which in turn sets the initial conditions for several time dependent changes in the cladding as the latter undergoes slow cooling in the inert environment of the storage cask. Eventually, local cladding temperatures reach levels where the hydrogen in solid solution begins to re-precipitate, as discussed in the previous section, which is when the state of cladding stress is most relevant for assessing the potential for hydride reorientation.

End-of-life rod internal pressure values must be computed taking into account the temperature profile and the void volume distribution, which exist in the fuel rod during vacuum drying and dry storage operations. During the very slow cooling process, the rod internal pressure is slowly reduced (temperature effect). In addition, the rod internal pressure may also be reduced due to cladding creep, which causes the fuel rod void volume to increase (volume effect). When calculating cladding stresses, there is an additional uncertainty due to the existence of interaction layers between cladding and fuel (i.e., fuel cladding bonding) when dealing with spent high burnup fuel. Fuel cladding bonding may be sufficiently strong to impede thermal creep, but may transfer part of the load from the cladding to the fuel as the result of forming a composite structure consisting of interlocking pellet fragments attached to the cladding wall. In such a situation, cladding stresses are likely to be significantly lower than the stresses that are calculated when it is assumed that a gap exists between fuel and cladding.

Using the pressurized tube method and allowing the stress to decrease with temperature, ANL evaluated the effects of the initial stress at maximum temperature on the degree of hydride reorientation using the radial hydride continuity factor (RHCF) as a measure of the reorientation [35]. As can be seen in Table 12 the higher the initial applied stress the higher the reorientation.

TABLE 12. RADIAL HEAT TREATMENT CONDITIONS AND POST-RHT CHARACTERIZATION RESULTS FOR 70 GW·d·t(HM)$^{-1}$ ZIRLO™ AND FOR 67 GW·d·t(HM)$^{-1}$ ZRY-4.

Material	σ_θ at 400°C MPa	C_H ppm	RHCF %	RHCF Data Points
ZIRLO™	140	650±190	65±17	16
	110	425±63	27±10	8
	110	350±80	33±14	33
Zry-4	140	615±82	16±4	12
	110	520±90	9±5	11

The effect of stress is further illustrated in Figs. 23–25. In Fig. 23, $F_n(40)$[6] and $F_l(45)$[7] are plotted versus hoop stress for BWR Zry-2 claddings with zirconium liner. For 300°C RHT specimens, a slight increase in $F_n(40)$ and $F_l(45)$ is observed at hoop stresses of 40 and 70 MPa, and a certain degree of hydride reorientation is readily visible at a hoop stress of 100 MPa; both factors, $F_n(40)$ and $F_l(45)$, appear to be increasing linearly with stress at 300°C; at 100 MPa, the degree of reorientation is still less than 40%. In 400°C RHT specimens, both $F_n(40)$ and $F_l(45)$ increase with hoop stress within the tested hoop stress range.

[6] $F_n(40)$ is (Sum of the number of hydrides in radial direction ±40°) / (Sum of the number of all hydrides)
[7] $F_l(45)$ is (Sum of the lengths of hydrides in radial direction ±45°) / (Sum of the lengths of all hydrides)

F_n can be normalized by considering the hydrogen content in solid solution at the HRT temperature, as shown in Eq.(5):

$$F_{ne}(40) = \frac{C_{H\_t} \cdot F_n(40) - (C_{H\_t} - C_{H\_d}) \cdot F_n(40)_0}{C_{H\_d}} \quad (5)$$

Where:

C_{H_t} is total hydrogen content of the specimen;
C_{H_d} is dissolved hydrogen content at RHT temperature;
C_{H_d} is equal to *TSSD* of the cladding, if C_{H_t} is more than C_{H_d};
C_{H_d} is equal to C_{H_t} and $F_{ne}(40)$ is equal to $F_n(40)$, if C_{H_t} is less than C_{H_d};
$F_n(40)_0$ is equal to $F_n(40)$ of the as-irradiated specimen.

The normalized value, F_{ne}, calculated using the data given in Fig. 23(a), is shown in Fig. 24, for irradiated BWR Zry-2 cladding with zirconium inner liner.

The results from the hydride reorientation tests on irradiated PWR 48 GW·d·t(U)$^{-1}$ Zry-4 cladding were evaluated in the same way as for BWR cladding; the results are shown in Fig. 25. The radial hydride ratio increased for the specimens after a 115 MPa, 300°C, 30°C·h^{-1} HRT compared to the as-irradiated specimens, as shown in Fig. 27 [4].

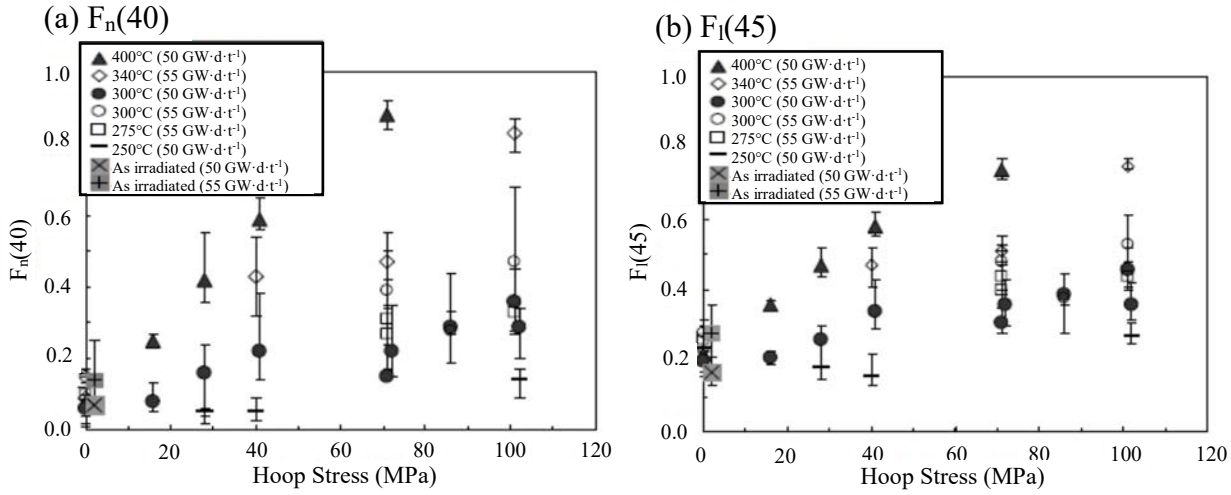

FIG. 23. Correlation between the degree of reorientation, $F_n(40)$ and $F_l(45)$, and the RHT conditions for irradiated BWR Zry-2 cladding with zirconium liner (cooling rate: 30°C·h^{-1}) (figure reproduced with permission from Ref. [31], copyright ASTM International, 100 Barr Harbor Drive, West Conshohocken, PA 19428).

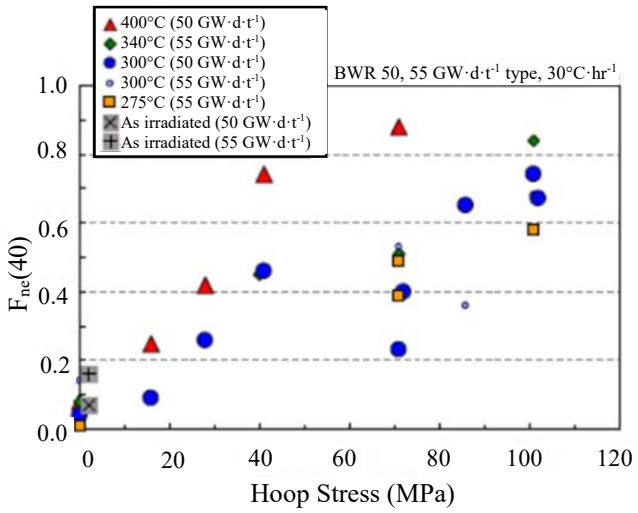

FIG. 24. Correlation between the normalized degree of reorientation, $F_{ne}(40)$ and the RHT conditions for irradiated BWR Zry-2 cladding with a zirconium liner (cooling rate: 30°C·h^{-1}) (figure reproduced with permission from Ref. [31], copyright ASTM International, 100 Barr Harbor Drive, West Conshohocken, PA 19428).

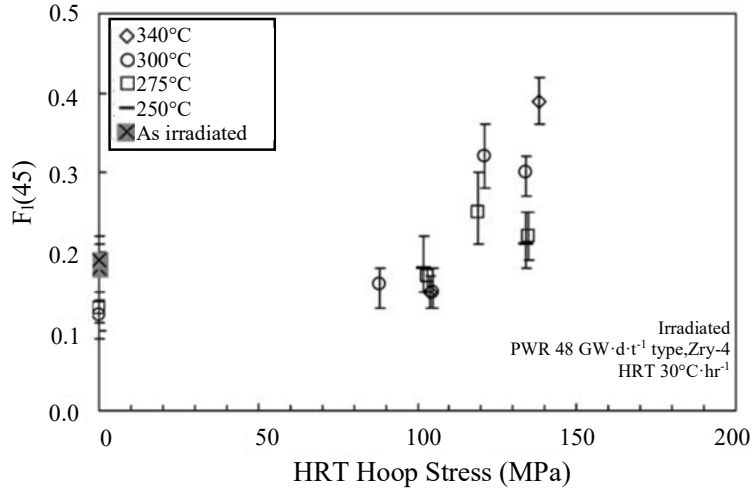

FIG. 25. Correlation between the degree of reorientation and the RHT conditions for irradiated PWR Zry-4 cladding (figure reproduced with permission from Ref. [31], copyright ASTM International, 100 Barr Harbor Drive, West Conshohocken, PA 19428).

Effect of radial heat treatment conditions on cladding ductility

ANL and several other investigators have used the offset displacement measured in a ring compression test (RCT) to determine the degree of cladding ductility after hydride reorientation treatments.

The results of RCTs conducted at ANL indicate a significant difference in the extent of radial hydride formation (in the form of the radial hydride continuity factor or RHCF[8]) and in ductile-to-brittle transition temperature (DBTT) for high burnup ZIRLO™ rodlets compared to high burnup Zry-4 rodlets. The rodlets were tested following the same temperature and stress histories, which were chosen to simulating drying–storage conditions [35]. Several factors were considered in evaluating these results:

- Pre-test radial distribution of hydrides;
- Texture;
- Residual stresses; and
- Alloy composition.

Based on metallographic examination of sibling pre-test samples, the hydride rim was denser and more localized for high burnup ZIRLO™ cladding as compared to high burnup Zry-4 cladding. Significantly, the average hydrogen content below the hydride rim appeared to be higher for Zry-4 than for ZIRLO™. Based on optical microscopy images, it was estimated that the average hydrogen content in the inner two thirds of the Zry-4 segments was >200 ppm, while the average hydrogen content in the inner two thirds of ZIRLO™ segments was <150 ppm. Differences in pre-test hydrogen content can have a significant effect on RHCF [35]. The absence of pre- and post-RHT hydrides at the Zry-4 inner surface suggests that the primary difference between results for high burnup ZIRLO™ and Zry-4 was not due to differences in the pre-test radial distribution of hydrides. The results suggest that high burnup ZIRLO™ may be more susceptible than high burnup Zry-4 to radial hydride precipitation at the inner surface of the cladding during reactor shutdown; as well as during simulated drying–storage conditions.

Texture has been shown to have a significant impact on the susceptibility of cladding materials to radial hydride precipitation during cooling under tensile hoop stress. The ZIRLO™ and Zry-4 used in the ANL test programme are both CW-SRA materials. Zry-4 fabrication details were provided to ANL for this cladding manufactured in 1977 and used to fabricate HBR fuel rods. No such details, however, were provided for the ZIRLO™ cladding used to fabricate the North Anna rods, for which irradiation was initiated in 1987. It is possible, but unlikely, that there were texture differences between these two cladding materials that may have contributed to differences in results.

In terms of alloy composition, ZIRLO™ differs from HBR Zry-4 in Sn content (about 1 wt.% vs. 1.4 wt.%) and Nb content (about 1 wt.% vs. 0 wt.%). Other Nb bearing zirconium alloys used as cladding are RXA M5™ (Zr-1%Nb). In Japan, MDA™ and ZIRLO™ claddings prepared from PWR spent fuel rods were also tested [31]. As shown in Fig. 26, at a burnup of 55 GW·d·t(HM)$^{-1}$, the $F_l(45)$ for ZIRLO™ cladding was relatively large compared to other PWR cladding materials tested in this study [2]. MDA™ cladding, which contains 0.5% Nb, showed the same level of $F_l(45)$ as 48 GW·d·t(HM)$^{-1}$ Zry-4 cladding. Therefore, it is unlikely that the presence of Nb in ZIRLO™ is the main cause for higher susceptibility to radial

[8] The radial hydride continuity factor (RHCF) is similar to the hydride continuity factor (HCC) defined by Canadian researchers. The latter is determined by projecting the radial hydrides within a 0.11 mm circumferential band onto the radius across the metal wall. The net length of these projected hydrides is normalized to the metal wall thickness to determine HCC. The RHCF follows a similar procedure over a 150 μm cladding wall band.

hydride precipitation, which was observed in high burnup ZIRLO™ tested in the ANL and JNES investigations.

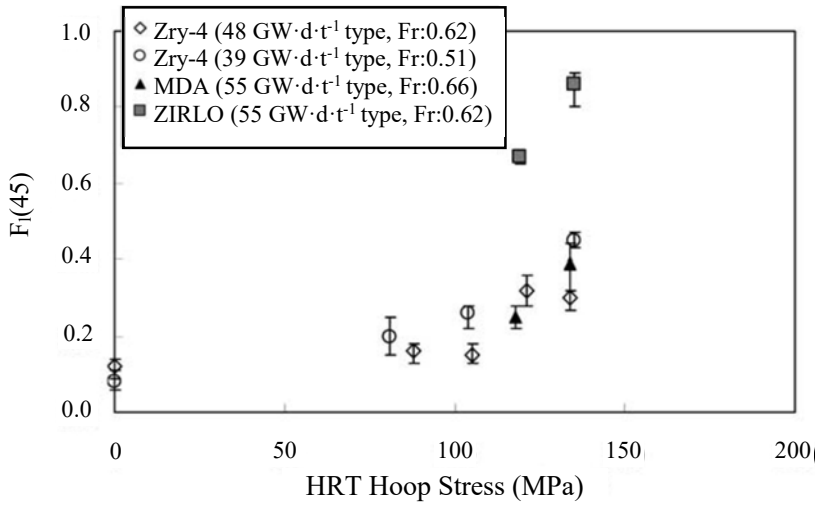

FIG. 26. Comparison of reorientation behaviour among irradiated PWR cladding materials (HRT 300°C, 30°C·h^{-1}) (figure reproduced with permission from Ref. [31], copyright ASTM International, 100 Barr Harbor Drive, West Conshohocken, PA 19428).

The JNES investigation also revealed the different reorientation behaviour between cladding materials. The difference in reorientation behaviour between Zry-2 (RXA) and PWR cladding materials (CW-SRA), such as Zry-4 and ZIRLO™, is attributed to the effect of heat treatment; which affects material properties such as grain structure including grain size, grain boundary orientation, internal stress/strain, and so on. As for the difference in reorientation behaviour among PWR cladding materials (CW-SRA), it is proposed that the factor which caused the larger reorientation for ZIRLO™ cladding was not texture, because the Kearns factor (Fr) values for ZIRLO™ was the same as that for the 48 GW·d·t(HM)$^{-1}$ Zry-4. The effect of the alloying element seemed not to be the dominant factor because Zry-4 and MDA™ showed relatively similar behaviour. The annealing temperature in the tube production process for ZIRLO™ cladding was lower than that for Zry-4 cladding [36]. Hence, properties which are affected by annealing temperature, grain size for example, might be possible factors.

Effect of power reactor irradiation on ductility

The high costs associated with working with irradiated materials (specimens cut from spent fuel assembly components) beg the question whether non-irradiated hydrogen-charged samples are a good surrogate for irradiated samples when studying the potential for hydride reorientation and the effects of that orientation.

Results of RCTs for pre-hydrided and RHT non-irradiated cladding samples were initially evaluated on a pass–fail basis at ANL in the sense that the success criterion was survival of 1.7 mm RCT displacement with wall cracks that penetrated into ≤50% of the wall thickness. Figure 27 shows results of the pass–fail RCTs conducted at 150°C, where open symbols represent rings that survived 1.7 mm displacement with ≤50% wall cracks. Solid symbols represent samples with cracks >50% of the wall thickness. Pass–fail embrittlement was observed as the hydrogen content dropped below a critical level: 275±25 ppm for 150 MPa hoop stress at 400°C; 200±20 ppm for 135 MPa hoop stress at 400°C; and <100 ppm for 120 MPa hoop stress at 400°C.

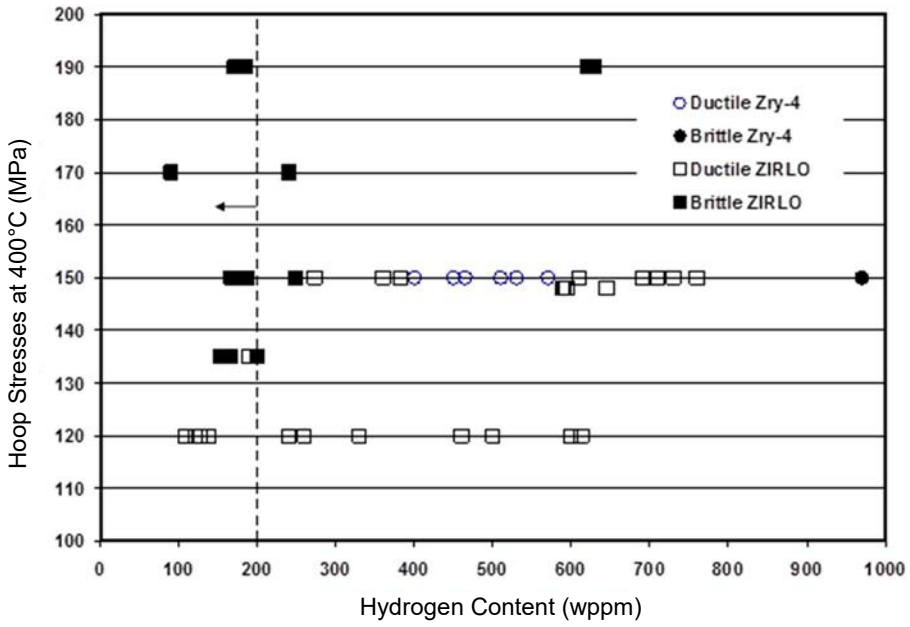

FIG. 27. RCT data at 150°C for pre-hydrided Zry-4 and ZIRLO™ following RHT (figure courtesy of U.S. NRC [7]).

RCT on rings of pre-hydrided rodlets with hydrogen contents (350–650 ppm), representative of high burnup cladding material, were tested with 150 MPa hoop stress at 400°C. The rings exhibited high ductility (>10% offset) at 150°C where all, but one, of the rings survived the RCT with no indication of cracking. The high ductility matrix samples, with uniform distributions of hydrogen across the radius, however, proved to be very poor surrogates for high burnup cladding. The high burnup ZIRLO™ rodlet (650 ppm hydrogen) subjected to the same thermal cycle at a slightly lower stress (140 MPa at 400°C) behaved in a highly brittle manner at 150°C RCT temperature. The primary difference between the test materials was the pre-test radial distribution of hydrogen; uniform for pre-hydrided cladding and highly non-uniform for high burnup cladding.

Although it appears that pre-hydrided non-irradiated cladding may not be a good surrogate for high burnup cladding, the experience gained from conducting tests with pre-hydrided cladding has proved to be useful in determining a metric to define the extent of radial hydride formation, in visualizing the discontinuity of cracks along the axial direction (indicative of discontinuity of radial hydride platelets), and in determining the effects of low hydrogen content on radial hydride precipitation and radial-hydride-induced embrittlement. Pre-hydrided, non-irradiated samples may prove more useful when the morphology of the hydrides can be made more like that of irradiated cladding with the same hydrogen content.

Effect of cooling rate

There can be a distinct difference between the effects of varying the cooling rate on BWR Zry-2 cladding with inner liner compared to those on PWR Zry-4 cladding. Given the lower hydrogen solubility in pure or weakly alloyed zirconium compared to standard Zry-2, a zirconium liner acts as a hydrogen sink. As a result of maintaining higher cladding

temperatures for longer periods of time by lowering the cooling rate, there is less hydrogen left in the Zry-2, which is available for reorientation.

In the top three pictures of Fig. 28, the increased size of the hydrogen-denuded zone adjacent to the liner is observed as a function of the cooling rate in a BWR Zry-2 cladding specimen cut from a 50 $GW \cdot d \cdot t^{-1}$ rod. As a result, no ductility loss is experienced in zirconium lined Zry-2 cladding at sufficiently low cooling rate.

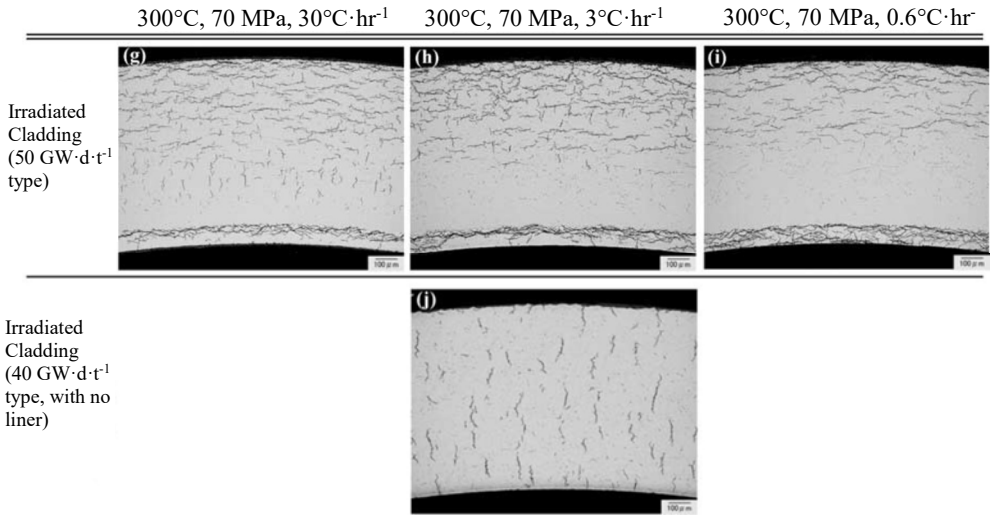

FIG. 28. Metallographic sections of BWR Zry-2 cladding specimens in hydride reorientation tests (photographs courtesy of JNES [4]).

The bottom picture in Fig. 28 presents the same Zry-2 cladding with no zirconium liner. A relatively large degree of hydride reorientation markedly different from the behaviour exhibited by the zirconium lined cladding is observed [4].

For PWR cladding, the effect of cooling rate on hydride morphology is shown in Fig. 29. $F_l(45)$ in $3°C \cdot h^{-1}$ cooled specimens seemed to be larger than that in $30°C \cdot h^{-1}$ cooled specimens; while it was almost the same in $0.6°C \cdot h^{-1}$ cooled specimens (Fig. 29(a)). Radial hydride length increased when the rate of cooling was decreased from $30°C \cdot h^{-1}$ to $3°C \cdot h^{-1}$; the effect was less noticeable for the decrease from $3°C \cdot h^{-1}$ to $0.6°C \cdot h^{-1}$.

The effect of RHT cooling rate on ductility in ring compression deformation is shown in Fig. 30. The crosshead displacement ratio in $0.6°C \cdot h^{-1}$ cooled specimens are similar to those cooled at $3°C \cdot h^{-1}$; in comparison there was a decrease between $3°C \cdot h^{-1}$ cooled specimens with those cooled at $30°C \cdot h^{-1}$. As shown in Fig. 29, an increase in both the degree of reorientation ($F_l(45)$) and the length of hydride was observed in $3°C \cdot h^{-1}$ cooled specimens compared to those cooled at $30°C \cdot h^{-1}$, while those cooled at $0.6°C \cdot h^{-1}$ gave similar results to $3°C \cdot h^{-1}$ cooled specimens. It is deduced that the effect of cooling rate on ductility is in agreement with the change in hydride morphology as illustrated in Fig. 29 [4].

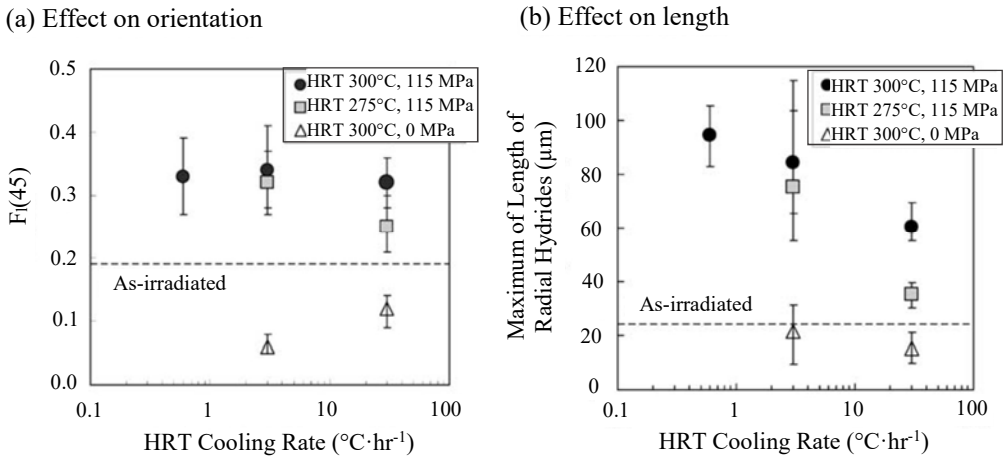

FIG. 29. Effect of RHT cooling on hydride morphology for irradiated PWR 48 GW·d·t(HM)$^{-1}$ Zry-4 cladding (the definition of vertical axis in (b) is "the maximum value among the length of hydride in radial direction ±45°" (figure reproduced with permission from Ref. [31], copyright ASTM International, 100 Barr Harbor Drive, West Conshohocken, PA 19428).

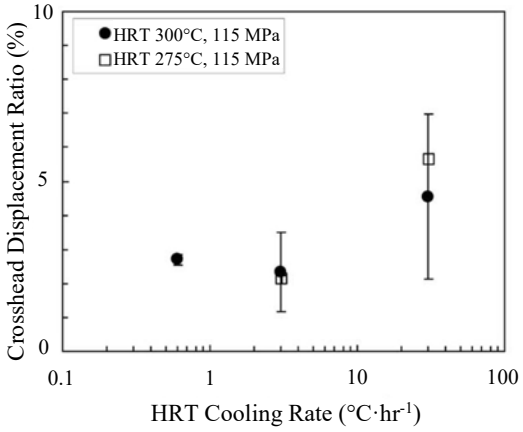

FIG. 30. Effect of RHT cooling rate on ring compression deformation for irradiated PWR Zry-4 cladding (figure reproduced with permission from Ref. [31], copyright ASTM International, 100 Barr Harbor Drive, West Conshohocken, PA 19428).

Ductile-to-brittle transition temperature

Ring compression tests were performed at ANL at increasing temperature to detect shifts between brittle and ductile behaviour. The temperature at which a change is observed is referred to the ductile-to-brittle transition temperature observed by RCT, or simply DBTT. The DBTT is a function of the cladding material, stress at maximum drying storage temperature, and pre-drying radial distribution of hydrogen.

The DBTT values for high burnup Zry-4 after radial heat treatment at 110 MPa and 140 MPa, following simulated drying at 400°C, were <20°C and about 55°C, respectively [7]. Most radial hydrides were relatively short and close to the cladding mid-wall where the RCT hoop bending stresses were very low. They participated in crack propagation, but not in crack initiation.

For high burnup ZIRLO™, radial hydrides were found to be relatively long and to extend from the inner cladding surface, which is subjected to the maximum RCT hoop bending stress under the applied load and above the support plate. DBTT values were about 120°C and 190°C at 110 MPa and 140 MPa.

For comparison, Aomi et al. [31] tested high burnup Zry-4 at only room temperature (RT). Aomi's RHT differed from the ANL study in that pressure and stress were held constant during cooling. Most of Aomi's data was generated for the faster cooling rate of $30°C \cdot h^{-1}$. For high burnup Zry-4 tested by Aomi et al., the hydrogen contents appear to be low relative to the samples used in the ANL study and the maximum annealing temperature was lower (250°C–340°C vs. 400°C).

The only Zry-4 data point that indicated brittle behaviour (<2% offset strain) at room temperature was for the sample annealed at 340°C and about 140 MPa hoop stress prior to cooling. The result is consistent with the ANL RT data point for high burnup Zry-4 subjected to a 400°C anneal with a 140 MPa hoop stress prior to cooling. The Aomi et al. data points for Zry-4 subjected to a 340°C anneal with about 100 MPa indicated ductile behaviour at RT. Again, this result may be consistent with the ANL data point for Zry-4 subjected to an RHT at 400°C and having 110 MPa hoop stress prior to cooling. For other data in Ref. [31], RHT conditions (250°C–300°C) were too low to allow for a one-to-one comparison.

4.1.2.6. Hydrogen migration and redistribution

Hydrogen in solid solution can migrate from the high temperature to the low temperature region of the cladding as a result of the existence of axial temperature profiles in the storage system [37–39]. Hydrogen will precipitate in the colder regions in the form of hydrides, if and only if, a high enough supersaturation is realized. When this is the case, precipitation of hydrides leads to increased embrittlement, which may affect fuel integrity.

Hydrogen redistribution experiments in the axial direction of cladding tube were carried out and the data related to hydrogen migration such as heat of transport, hydrogen diffusion coefficient, and solubility limit were obtained [40]. Samples from twenty year dry stored spent PWR UO_2 fuel rods, whose burnups were 58 $GW \cdot d \cdot t(U)^{-1}$ and 31 $GW \cdot d \cdot t(U)^{-1}$, were investigated. Unirradiated claddings were also used as reference materials. Samples of 30 mm length was mounted between heaters, and surrounded with thermal insulators. The temperature at one end of the sample was kept at 380°C and that at the other end was kept at 260°C. The atmosphere during the experiment was air in order to keep an oxide layer on the cladding surface to prevent hydrogen from escaping out of the sample (Fig. 31).

Figure 32 shows the hydrogen concentration analysed on each specimen after heating for ten days. Hydrogen migrated from the high temperature to the low temperature region in the samples. Before the test, the difference in hydrogen concentration of adjacent specimens was less than 2.2 ppm and hydrogen profiles in the samples were regarded as almost flat. From these results, the heat of transport, diffusion coefficient and solubility limit of hydrogen were calculated by best fitting using a time dependent hydrogen diffusion equation [40].

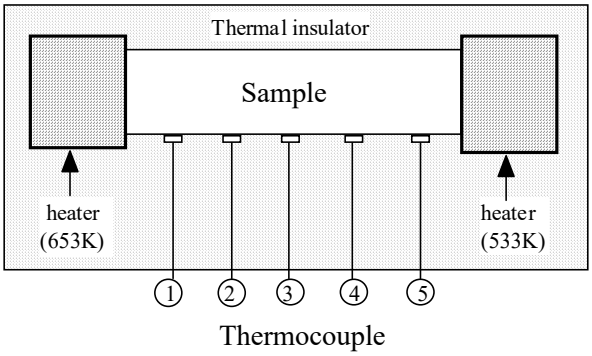

FIG. 31. Apparatus used for the hydrogen redistribution experiment (figure courtesy of CRIEPI [4]).

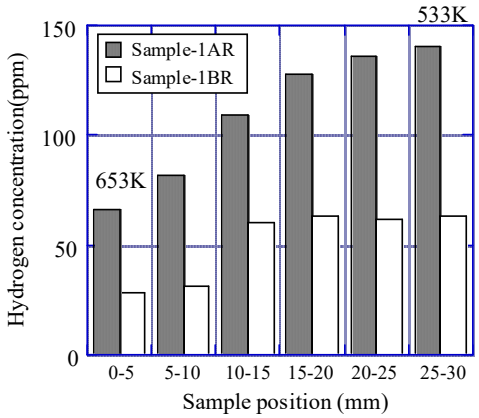

FIG. 32. Hydrogen distribution in samples after the 10-day redistribution experiment (figure courtesy of CRIEPI [4]).

The hydrogen redistribution in the PWR UO_2 rod after forty years of storage was then estimated by a one-dimensional hydrogen diffusion calculation using the heat of transport, the diffusion coefficient and the solubility limit obtained in the study [40]. Figure 33 shows the calculated hydrogen redistribution in a fuel rod after forty years of storage. The axial hydrogen migration is not significant after forty years of storage under helium atmosphere, due to the low value of the hydrogen diffusion coefficient, except at fuel rod ends. Hence, the hydrogen profile was not significantly different from the initial one. It was, therefore, concluded that hydrogen migration has no significant effects on fuel cladding integrity during dry storage.

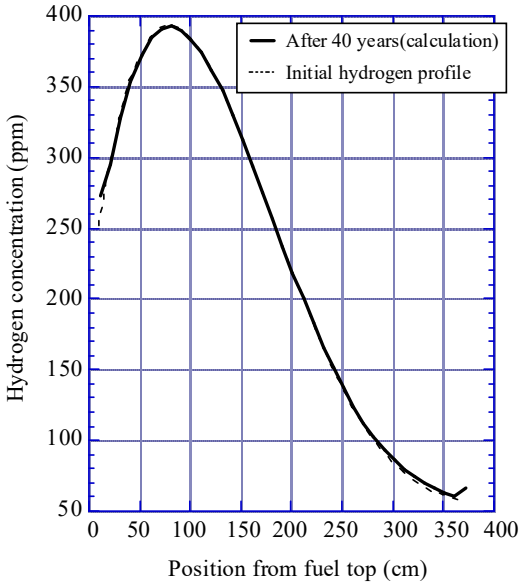

FIG. 33. Calculation of Axial hydrogen redistribution after 40 years of storage (figure courtesy of CRIEPI [4]).

4.1.3. Impact loading on spent fuel

This subsection uses only the references cited.

Data has been acquired from 9 m drop tests of casks loaded with depleted UO_2 FAs or on fuel rods [7]; for example, Figs 34 and 35. The tests provided information on fuel pin deformation modes, grid and nozzle yielding, fuel pin array deformation and sliding, and the maximum allowable loads for unirradiated cladding.

Some elementary tests, dynamic and quasi-static, were carried out on unirradiated PWR and BWR fuel rods to determine the maximum load which can be supported by the cladding material. In the case of an axial 9 m cask drop test, the rods showed only minor lateral deformations and did not result in any cracking or rupture of the cladding material.

Lateral bending tests on PWR and BWR rodlets and quasi-static inter-grid bending tests resulted in 35 mm rod elongation at rupture (at 25°C) and 60 mm deflection at rupture (at 500°C); 2.60 g of fuel material was released per rupture.

Quasi-static bending tests on BWR irradiated fuel rod ends resulted in a 10 mm deflection at rupture, the angle of rupture ranged from 25–30°, and 7.65 g fuel material was released. Crush tests on empty irradiated BWR fuel pin cladding demonstrated that for a longitudinal loading, the empty cladding material retained significant strength before it crushed and subsequently rupture.

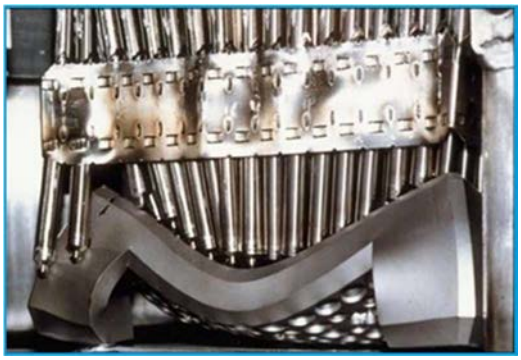

FIG. 34. Fresh PWR FA after 9 m drop test (picture courtesy of TN International and INS Ltd. [7]).

FIG. 35. Fresh BWR FA after 9 m drop test (picture courtesy of TN International and INS Ltd. [7]).

For a lateral drop (Fig. 36), moderate g-load, there is a slight packing down of the end grids and complete collapse of the central grids; the risk of fuel rod rupture has been concluded to be limited. In contrast, for high g-loads, complete packing down of the fuel pin array in the FA central part results and there is an uncontrollable risk of fuel rod rupture.

For an axial drop (Fig. 37), moderate g-loads, general bending or elastic buckling of the fuel rods occurs. At higher loads local plastic buckling, unacceptable deformations and rupture of the fuel rods results.

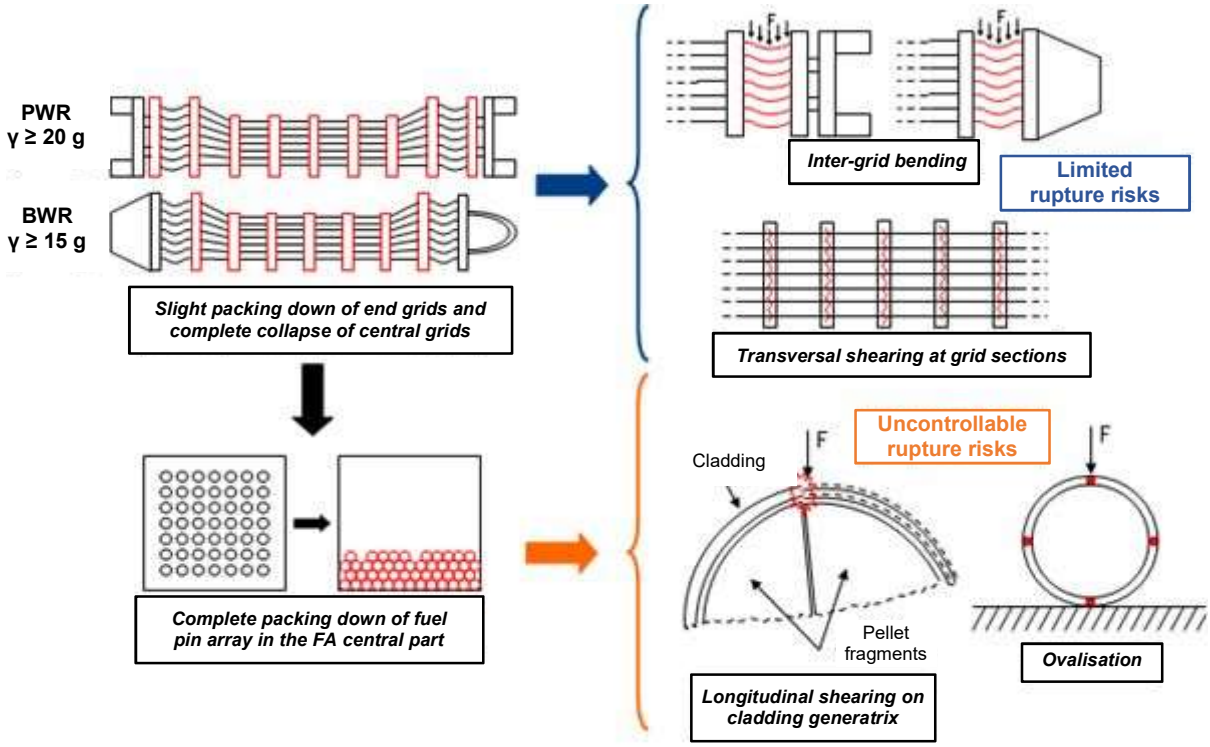

FIG. 36. Cladding rupture risks evaluation in lateral drop (figure courtesy of TN International and INS Ltd. [7]).

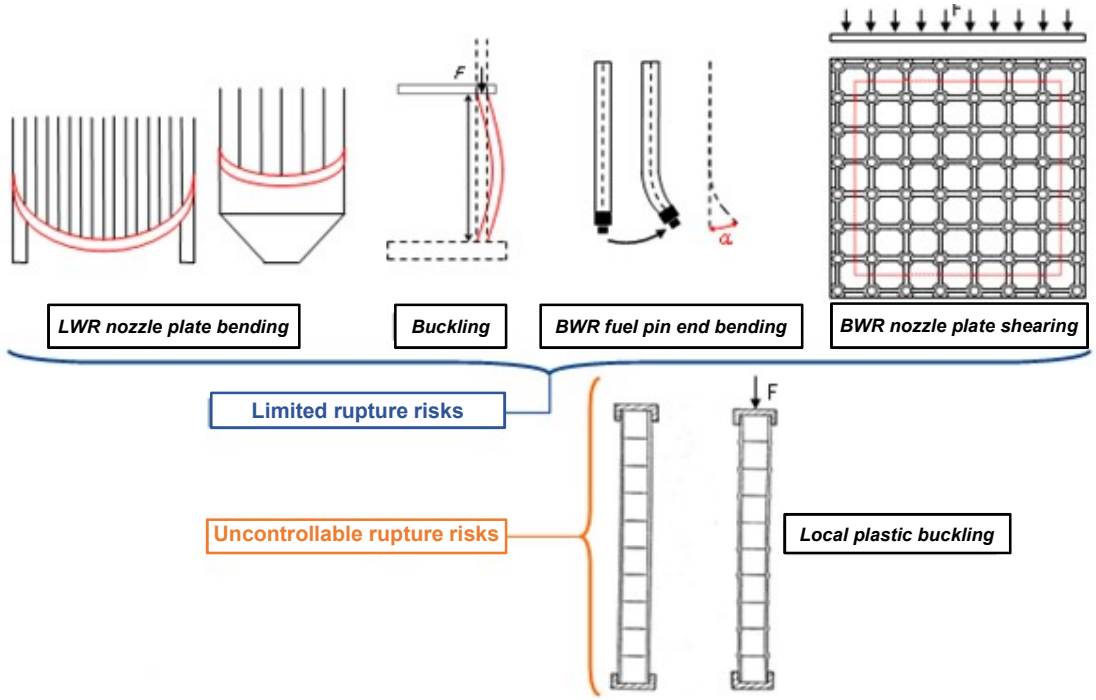

FIG. 37. Cladding rupture risks evaluation in axial drop (figure courtesy of TN International and INS Ltd. [7]).

The rupture locations for a lateral and axial drop are given in Fig. 38. The amount of fuel released per rupture is estimated to be 1 or 3.5 pellets per section of broken fuel pin.

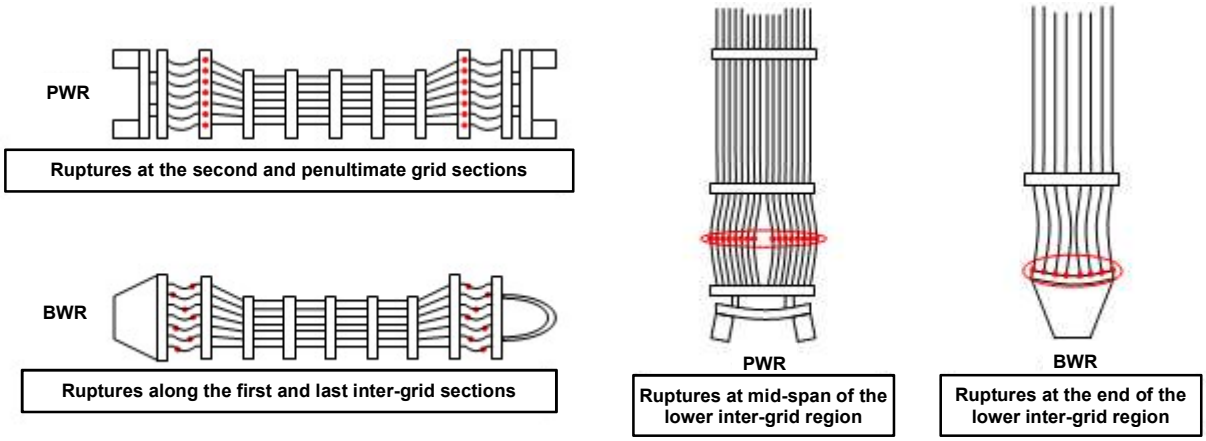

FIG. 38. Rupture locations in relation to drop direction; lateral and axial drop (figure courtesy of TN International and INS Ltd. [7]).

Array deformation for a lateral drop is a function of grids collapse pattern. As grids collapse in the central part of the FA there is a reduction in FA fissile cross-section and generally a reduction in reactivity in the case of LWR FAs. The conservative approach is to retain the initial fissile cross-section as the base data set for criticality analysis.

For PWR fuel rods Euler buckling occurs which leads to an expansion of the PWR fuel array. In comparison, BWR fuel rod ends bend and the BWR fuel array contracts at the bottom inter-grid region. For BWR FAs, similarly to the lateral drop, the conservative approach is to apply the initial non-deformed geometry in the bottom inter-grid, while an expansion could be introduced in the next inter-grid because of the continuity of deformation. For PWR FAs, the pessimistic approach is to consider a uniform expansion of the array in the deformed bottom inter-grid (Fig. 39).

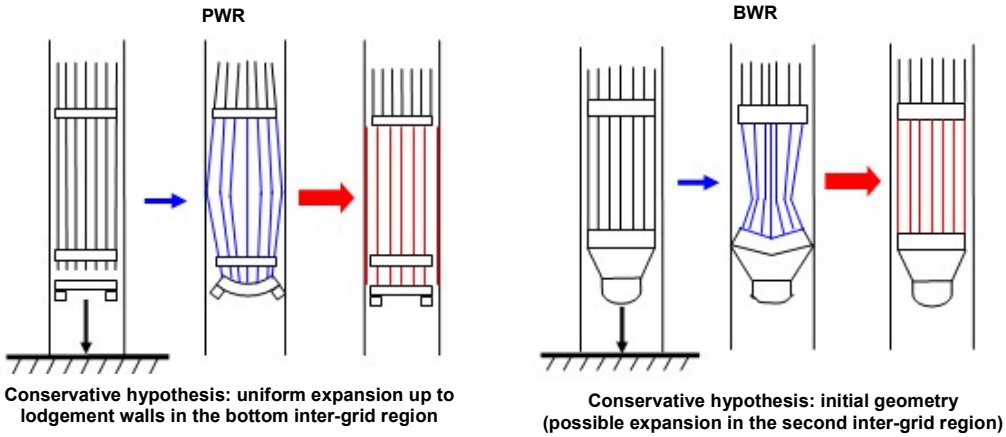

FIG. 39. Array deformation in axial drop (figure courtesy of TN International and INS Ltd. [7]).

4.1.3.1. Potential for rod sliding

For a lateral drop, there is no load to induce either fuel rods sliding through the grids or nozzle deformation; in consequence, no array displacement is considered so that the active zone of fuel rods (active zone: with fissile content) remains in its initial position.

For an axial drop, except for extremely low g-loads, PWR fuel rods move uniformly to close the gap between their ends and the bottom nozzle plate. There is no such gap in BWR FA as BWR fuel rods are fixed to nozzles (Fig. 40).

4.1.3.2. Fuel rod fracture behaviour studies

Studies have also been carried out [7] to assess the fracture behaviour of spent fuel rods under transversal impact load conditions and the amount of fuel material released in the event of rod fracture. The procedure consisted of releasing a free-falling hammer through a vertical guiding column. Figure 41 shows some photographs, captured by high speed camera, before and during the impact on a 74 GW·d·t(HM)$^{-1}$ PWR rodlet.

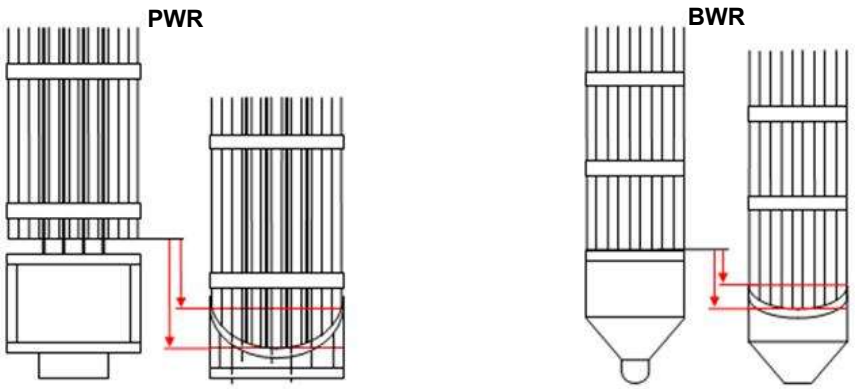

FIG. 40. Assumptions used for fuel array displacement for an axial drop (figure courtesy of TN International and INS Ltd. [7]).

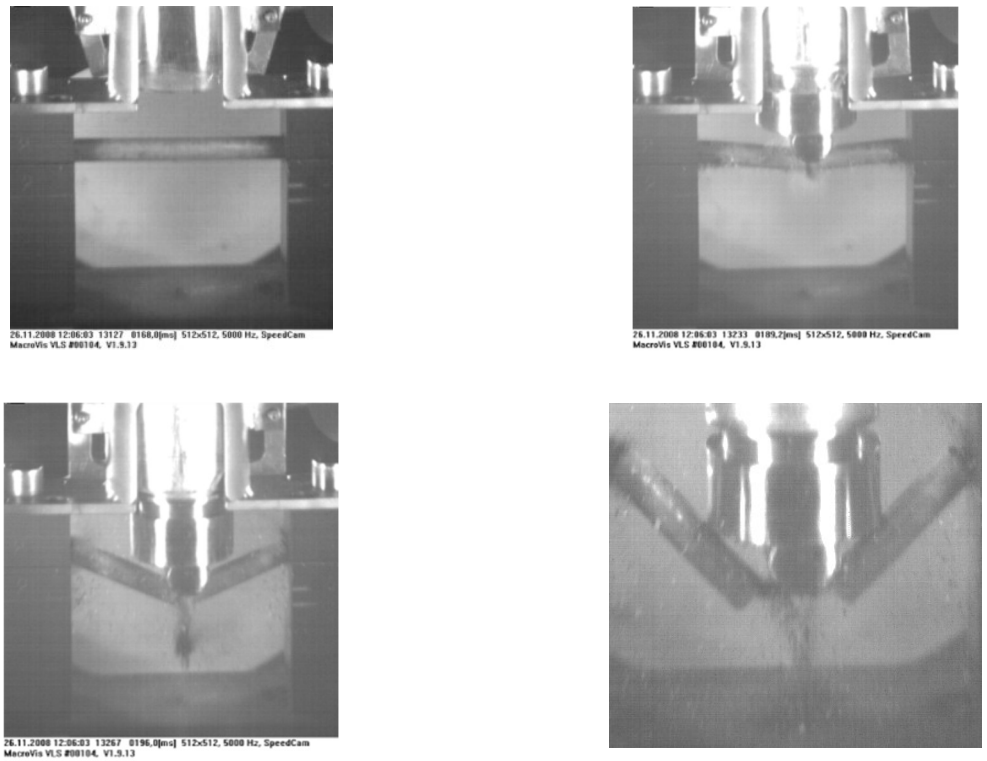

FIG. 41. Impact tests: High speed camera photographs showing the impact fracture of a ~74 GW·d·t(HM)$^{-1}$ PWR fuel rodlet (pictures courtesy of GNS).

Table 13 reports the amount of fuel particles collected after each test. The amount of fuel released per fracture is comparable for all the samples. In all the tests the released fuel collected at the bottom of the device corresponded to < 2 g per fracture.

As can be seen from Table 13 no clear relationship can be drawn between the amount of fuel that is released versus fuel burnup [4].

TABLE 13. MASS OF FUEL RELEASED DURING THE IMPACT TESTS

Fuel type	Burnup ($GW \cdot d \cdot t(HM)^{-1}$)	Number of fracture positions	Amount of fuel released (g)
PWR	19.0	3[a]	3.9
	42.6	3	4.8
BWR	73.6	3	5.6
	53.0	3	4.7

[a] No full severing of the sample.

Other dynamic impact tests have been carried out on high burnup spent fuel rods irradiated in commercial BWR and PWR reactors in Japan [7]; the test matrix is provided in Table 14. Axial and lateral loading of fuel rods were studied to establish fuel rod failure loads, failure strain and the amount of fuel material released on impact.

Elemental mechanical tests consisted of tensile and ring compression tests. Axial tensile yield strength, failure strain, ring compressive strength and failure fattening ratio were acquired.

The results of dynamic tensile tests on BWR and PWR fuel claddings have been plotted in terms of ultimate tensile strength vs. strain rate and total elongation vs. strain rate; as shown in Fig. 42. With an increase in strain rate, ultimate tensile strength increased and total elongation decreased.

TABLE 14. JAPANESE TEST MATRIX FOR DYNAMIC IMPACT TESTING OF IRRADIATED FUEL RODS AND CLADDING

Fuel type/burnup			BWR 55 $GW \cdot d \cdot t(HM)^{-1}$	PWR 55 $GW \cdot d \cdot t(HM)^{-1}$
Cladding type			Zircaloy-2	MDA™
Elemental mechanical test of cladding	Dynamic tensile test (up to $10^2\ s^{-1}$)		6	12
Dynamic impact test of fuel rod	Dynamic ring compression test (up to 4000 $mm \cdot s^{-1}$)	As irradiated	4	3
		Hydride reoriented	4	6
Dynamic load impact test of fuel rod	Axial load		5	5
	Lateral load	As irradiated	5	6
		Hydride reoriented	1[a]	2[b]

[a] Zirconium liner.
[b] Contains dummy pellets made from forsterite 2 mg/pellet

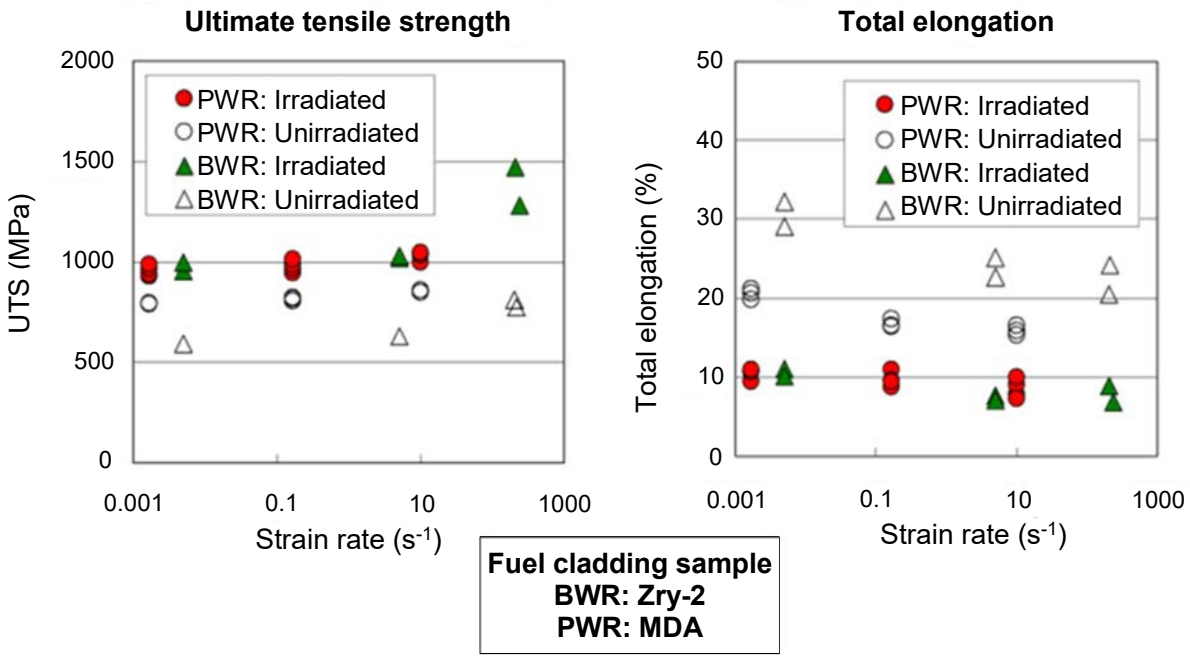

FIG. 42. Results of tensile tests (figure courtesy of JNES [7])

The results in Fig. 43 from dynamic ring compression tests on BWR and PWR fuel claddings presented as crosshead displacement ratio vs. compression speed show that the ductility decreases as the compression speed increases.

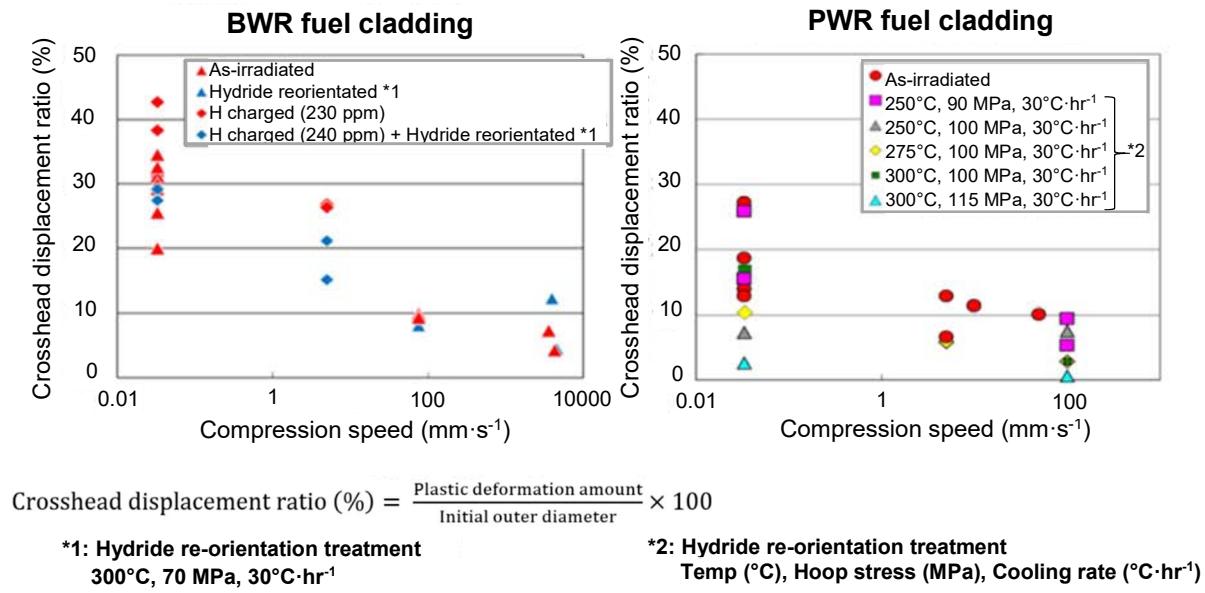

$$\text{Crosshead displacement ratio (\%)} = \frac{\text{Plastic deformation amount}}{\text{Initial outer diameter}} \times 100$$

***1: Hydride re-orientation treatment**
300°C, 70 MPa, 30°C·hr^{-1}

***2: Hydride re-orientation treatment**
Temp (°C), Hoop stress (MPa), Cooling rate (°C·hr^{-1})

FIG. 43. Results of dynamic ring compression tests (figure courtesy of JNES [7]).

The hydride reorientation treatment was 300°C for material with an initial 70 MPa hoop stress. The cool down rate was 30°C·h^{-1}. At a given compression speed, the hydride reorientation treatment applied to BWR cladding specimens had no effect on the value of the ductility index of BWR cladding. In the case of PWR cladding the effect of the hydride reorientation treatment on cladding ductility index can be clearly seen. Collision speed was varied between 3.7–12 m·s^{-1}. Cladding rupture and release of fuel material only occurred in the 12 m·s^{-1} test (Table 15).

TABLE 15. IMPACT TEST RESULTS ON BWR RODS – AXIAL DIRECTION

	(a)	(b)	(c)	(d)	(e)
Weight mass			3.5 kg		
Collision Speed	12 $m \cdot s^{-1}$	9 $m \cdot s^{-1}$	6 $m \cdot s^{-1}$	3.7 $m \cdot s^{-1}$	6 $m \cdot s^{-1}$
Specimen Type		Fuel section (hard bonding material)			Upper plenum
Pellet Dispersion	Yes	No	No	No	No
Deformation	Spiral breakage	Bowing at lower part	None	None	Jack knifing at plenum part

Where BWR fuel rods ruptured, the amount of fuel material released, axial impact testing, was equivalent to approximately two pellets and about 60% of the material was very fine powder. In case of lateral impact testing, the amount was equivalent to approximately three pellets and about 40% was very fine powder.

For the PWR cases, the amount of fuel material released was less; around 1.4 g.

Another study investigated fuel cladding response under impact conditions. To this end, a comparison between results obtained in both dynamic (i.e. drop weight tests) and static RCTs was made. The material employed was unirradiated ZIRLO™ cladding in stress relieved condition.

Samples cut into rings 10 mm length with 150, 250 and 500 ppm of hydrogen were prepared. The resulting (heat treatment) hydride distribution was homogeneous through the cross-section, with hydrides oriented along the hoop direction of the samples.

The impact experiments were performed in a drop tower test machine. The applied impact velocity was 3 $m \cdot s^{-1}$. Samples were tested at 25, 135 and 300°C. Quasi-static tests were carried out at three displacement rates: 0.5, 100 and 1000 $mm \cdot min^{-1}$.

The shape of the drop weight tests (3 $m \cdot s^{-1}$) curves were similar to the ones produced from static testing (Fig. 44).

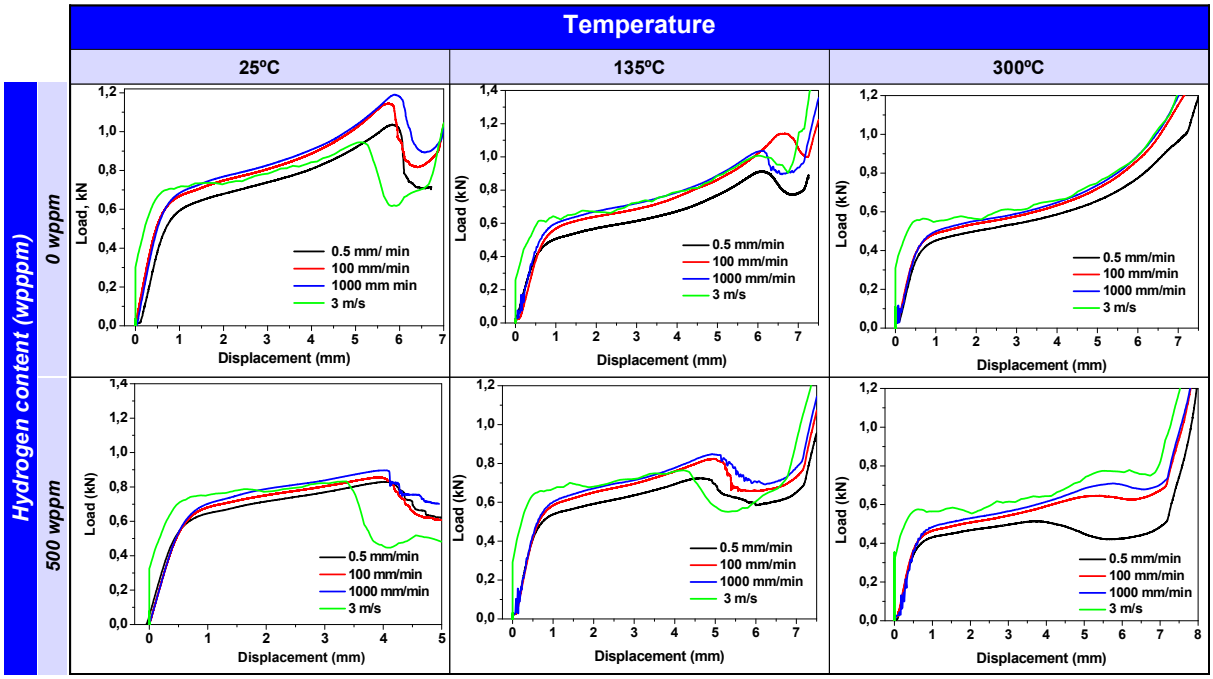

FIG. 44. Load versus displacement curves - static and dynamic RCT tests (figure courtesy of ENRESA [7]).

The slope of the RCT curves, after the initial displacement, increases with an increase in strain rate. This means that the cladding stiffness, Young's modulus, is increased. There was no significant difference between samples with and without hydrogen. Only a variation in the maximum load reached, and the displacement value at this point, can be observed.

In quasi-static loading conditions, a typical ductile fracture surface aspect was developed (micrography), with large micro voids oriented in the direction of crack growth. Test temperature does not seem to influence the fracture mechanism. Similar results were obtained for both, hydrided and as received samples.

Table 16 summarizes the observations for different test conditions on hydrided specimens.

TABLE 16. CHARACTERISTICS OF FRACTURE SURFACE OF HYDRIDED SPECIMENS (500 PPM) TESTED UNDER QUASI-STATIC AND DYNAMIC LOADING

	Temperature		
	25°C	135°C	300°C
Quasi-static tests (conventional RCTs)	Ductile	Ductile	Ductile
Dynamic tests (drop weight conditions)	Brittle	Brittle + ductile	Ductile

In the fracture surface of specimens tested at room temperature, there is a predominance of brittle areas. Ductile fracture also occurs, but is limited to ZIRLO™ matrix. At 135°C, ductile and brittle characteristics coexist in the fracture surface. At 300°C, fracture is totally ductile. From these results, it could be inferred that temperature has a beneficial effect on cladding resistance.

In conclusion, cladding stiffness and strength increased at increasing displacement rates. This fact is in good agreement with the generally accepted assumption that during an accident the higher load application rate would lead to better cladding strength.

The effect of temperature and hydrogen concentration on load versus displacement curves is similar in both the dynamic and quasi-static ring compression tests.

4.2. ADVANCED GAS COOLED REACTORS (AGR) FUEL

The cladding material used in the manufacture of AGR fuel pins is 20Cr:25Ni:Nb stabilized stainless steel. During reactor operation, stainless steel components in the 340–520°C temperature range (peak at 420°C) become sensitized, primarily as a result of radiation induced segregation. Sensitization, coupled with stress induced at the anti-stacking grooves of the fuel pin, can result in cladding failures for pins stored in moist air conditions or in pond storage environments (with high chloride ion concentrations) through the failure mechanism known as irradiation-induced intergranular stress corrosion cracking (IGA). This has implications for potential air ingress at reactor shutdowns, initial cooling/storage at reactor in dry buffer storage tubes and interim storage ponds.

For short to medium term fuel storage durations, IGA is the prominent defect mechanism for AGR fuel cladding. Unlike zirconium based alloys, if the storage durations become prolonged (i.e., hundreds of years) general waterside corrosion becomes a significant factor, especially where initial in-reactor cladding wall thinning has been significant. This failure mechanism also affects and is dominant in the fuel element stainless steel structural materials (braces, etc.).

Sensitization of stainless steel is a widely recognized and researched topic. It is caused by the free carbon in the alloy, reacting with the chromium in the alloy, to form chromium carbides at the metal grain boundaries. The formation of chromium-rich carbides on the grain boundaries denudes them of the chromium alloying additions, and the stainless steel becomes sensitized to localized grain boundary corrosion in environments where the bulk material is passive.

The specification of AGR cladding steel is set to avoid chromium carbide precipitation by firstly including a low carbon limit and secondly by inclusion of niobium. The niobium constituent is added specifically to stabilize the steel against the precipitation of chromium carbides, by allowing preferential reaction of carbon with niobium. A 30 minute 930°C anneal allows this preferential reaction to occur and the niobium concentration is specified to ensure an excess over (carbon + nitrogen). The concentration of carbon left in solution in the steel at the start of irradiation is thus very low. Clearly, the carbon deposit on the coolant side of AGR cladding is a potential source of carbon, but diffusion of carbon is not considered fast enough to be able to sensitize material at depth in the cladding in the relevant temperature range; the inability of carbon to diffuse deep into the cladding at the relevant temperatures has been confirmed experimentally [41].

Radiation induced segregation, however, has been found to be the overriding factor in AGR cladding sensitization. Fast neutrons are capable of generating defects in metals by ‘non-elastic’ displacement of atoms. An atom can be knocked from its normal lattice site into an interstitial location and a vacancy created. Vacancies are mobile and can be removed from the lattice at sinks. A grain boundary is a good sink. In moving in the lattice, a vacancy needs to exchange positions with another atom. The diffusion coefficients of iron, chromium and

nickel in an austenitic steel are such that chromium diffuses fastest. There is thus a slight bias in favour of vacancies exchanging with chromium as they move towards a sink. The net effect is to move chromium away from the grain boundary. Nickel diffuses the most slowly of the three main steel constituents, and, as a result, nickel tends to become enriched at grain boundaries.

Chromium-depleted zones on grain boundaries can only be maintained if the supply of chromium from within the grain is not fast enough to replenish the boundary region. When vacancy mobility is very low, very few vacancies will reach sinks. Thus, a window in irradiation temperature exists, above and below which irradiation-induced sensitization is not observed. Some important points follow. First, with continued irradiation at constant neutron flux, there will be a move towards a steady state chromium depletion profile at a grain boundary. The steady state results from a balance between vacancy migration rate (number and mobility) and chromium diffusion rate (gradient and mobility). Based on the modelling of experimental observations, predictions were made of the likely AGR fuel burnups at which radiation induced sensitization might level off. Second, the nature of the chromium depletion profile at a grain boundary (width of depleted zone and reduced chromium concentration on the grain boundary itself) is likely to influence the occurrence and rate of intergranular corrosion.

Figure 45 provides data from two AGR reactors showing depth of attack vs. cladding irradiation temperature from fuel having achieved different burnup levels. As mentioned earlier, depth and width of chromium-depleted grain boundaries are expected to stabilize with burnup, possibly after ~20 $GW \cdot d \cdot tU^{-1}$.

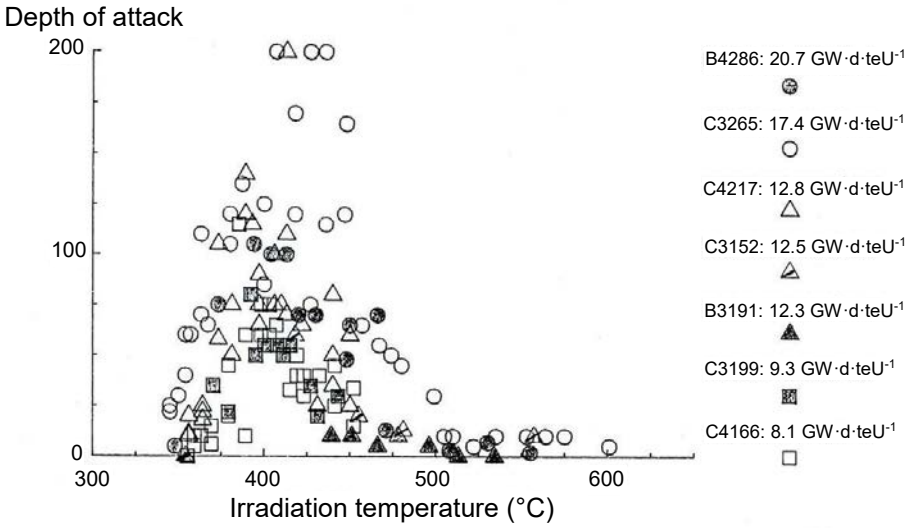

FIG. 45. Stringer-to-stringer variation in mid-wall attack after 72-hour Strauss Testing (Sample exposed to boiling sulphuric acid in contact with copper powder for 72 hours) (figure courtesy of Sellafield Ltd. [4]).

The problem caused by in-reactor IGA initiation, during spent AGR fuel wet storage, has been inhibited by sodium hydroxide dosing to a pH of 11.4. Inhibitor levels are a function of both chloride ion content and pool water temperature; a pH of 11.4 represents an optimized level for pool storage conditions at Sellafield. Although the long term use of sodium hydroxide as an inhibitor was originally thought to have implications, through dissolution of

the protective oxide film on the steel with a resultant increase in general waterside corrosion, corrosion studies have not seen any evidence of accelerated general corrosion.

4.3. MAGNOX FUEL

4.3.1. Wet storage

In wet storage, MAGNOX cladding corrodes according to the reaction with water, forming $Mg(OH)_2$ and hydrogen. In principle, if the pH is increased to greater than 11.5, the solubility of the magnesium hydroxide layer is low, effectively forming a passive surface film on the metal. Research work, however, shows that this is not the full story and other factors, such as micro-cracking and the presence of carbon in the oxide layer, result in corrosion rates being up to three times higher than unirradiated material. Cladding corrosion is also influenced by the presence of water impurities, notably chloride, which leads to pitted areas even at low concentrations. To minimize these effects, chloride and sulphate ion levels are maintained at levels <1 ppm in pond purge water. Pitting corrosion may cause failure of the cladding during longer storage. Crevice corrosion between the splitter blades and the cladding may also occur. For the reasons outlined above, MAGNOX spent fuel is usually reprocessed within two years of reactor discharge; however, current storage practices show good performance and storage periods >5 years are feasible.

4.3.2. Dry storage

MAGNOX cladding was developed for gas reactor use and therefore is ideally suited for dry storage. Normal storage is initially carried out in CO_2 until the clad temperature drops below the level at which uranium hydride could ignite (if present and if there is a restricted supply of oxygen); application of safety hierarchy. For storage in CO_2, corrosion rates are negligible for temperatures below 350°C. Storage in dry air has been practiced for several decades, at fuel temperature below 150°C. In air, fuel deterioration will occur through pitting attack, if the relative humidity is >50% and aggressive ions are present, or if there is water ingress.

4.4. CANDU FUEL

4.4.1. Wet storage

Potential fuel degradation mechanisms are the same as LWR fuel, see section 4.1.1.

4.4.2. Dry storage

The potential mechanisms of concern for degradation of CANDU fuel, during long term dry storage, are principally related to hydrogen effects. Spent CANDU fuel has much lower burnup than LWR fuels; this results in lower fission product inventories and lower residual heat, leading to lower storage temperatures. The effect of the lower temperatures is beneficial for most cladding degradation processes, except for some phenomena associated with hydrogen effects. Hydride precipitation and thermal cycling effects are enhanced in a temperature range close to the ductile–brittle transition, which is expected to prevail from the start of the dry storage period.

For fuel elements with cladding defects developed during reactor operation, the potential exposure to oxygen, under abnormal storage conditions, could lead to cladding rupture as a result of fuel pellet oxidation and expansion. Tests on intentionally defected fuel bundles

stored in a variety of storage environments have not reported any issues with fuel pellet swelling or clad splitting due to exposure to air; see section 9.4.2.

The possibility of cladding failure by creep rupture has been extensively examined [42] and summarized in Ref. [2]. Given the low storage temperatures (<200°C) and cladding hoop stresses (<100 MPa), creep rupture is not considered to be a limiting mechanism for CANDU fuels. For CANDU fuel, delayed hydride cracking (DHC) of the endcap/endplate welds is considered to be the most critical mechanism that could affect fuel bundle integrity during dry storage.

4.4.2.1. Delayed hydride cracking studies

To improve the understanding on fuel bundle endcap/endplate weld properties and to determine whether DHC could be a concern, an apparatus and methodology were developed that could be easily implemented in a hot cell to test endcap/endplate welds of irradiated fuel. Parameters of interest include the stress intensity factor that can lead to endcap/endplate crack formation and a determination of the crack velocity of endcap/endplate welds of irradiated fuel as a function of temperature in the range from -50°C to 150°C relevant to dry storage conditions.

The first phase of the programme was completed in 2007 by developing the apparatus and testing the methodology on unirradiated endcap/endplate welds from a commercial CANDU fuel bundle. The methodology is based on a bending test which consists in essentially peeling off the endplate from the endcap by applying a torque on the weld. The loading supplied by the torque is measured and the growth of the crack is followed by measuring the potential drop along the crack and by acoustic emission. A photograph of the DHC test apparatus is shown in Fig. 46.

The test apparatus was successful in initiating and following crack growth of the endcap/endplate weld. A typical crack is shown in Fig. 47.

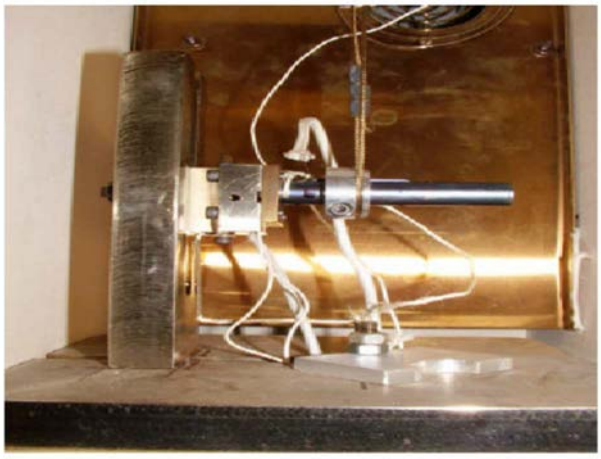

FIG. 46. DHC test apparatus showing an endcap/endplate sample being loaded by the cable (picture courtesy of OPG [4]).

TENSION SIDE

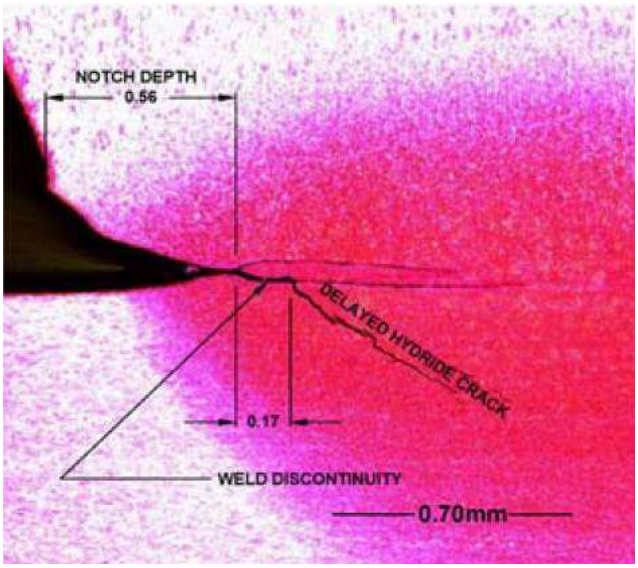

COMPRESSSED SIDE

FIG. 47. Metallographic section showing the weld notch, weld discontinuity and DHC crack (picture courtesy of OPG [4]).

The crack begins at the notch of the endcap/endplate weld before proceeding into the weld material in the direction of the endplate as loading from the bending stress is increased. The weld notch acts as a stress raiser from where the crack grows.

The first test was used to commission the apparatus and demonstrate the methodology. The test material from the fuel bundle had concentrations of hydrogen in the Zircaloy matrix of about 10 ppm and was used to confirm whether DHC could be operative at concentrations of hydrogen which are nominal for a manufacturing bundle, and, also, to scope a series of tests with endplate/endcap welds with concentrations relevant to those found in irradiated fuel.

The results confirmed that DHC could be operative in endcaps/endplates with low concentrations of hydrogen and a stress intensity factor of 13.9 $MPa \cdot m^{1/2}$ at 130°C. In preparation for testing of irradiated endcap/endplate welds, a series of tests were done at various temperatures and loadings to further develop the methodology and provide benchmarking results.

For these tests, the unirradiated bundle cladding and endcap/endplate welds were loaded electrochemically with hydrogen to a level of about 40 ppm. The tests results were assessed with both analytical stress intensity factor equations relevant to the geometry of the test samples and with a finite element code developed for the purpose. The finite element code calculated stress intensity factors that are in agreement with the analytical models. Delayed hydride cracking was confirmed through analysis of the crack morphology through SEM. Stress intensity factors (K_{IH}) from the tests are about 7.6–13.6 $MPa \cdot m^{1/2}$ at 150°C and crack velocities of the order of 10^{-9} $m \cdot s^{-1}$. Further information on these studies is provided [43].

4.5. RBMK AND WWER-440/1000

This section uses only the references cited.

4.5.1. Wet storage

Potential fuel degradation mechanisms are the same as LWR fuel, see section 4.1.1.

4.5.2. Dry storage

As RBMK and WWER-440/1000 fuel would be expected to be susceptible to similar degradation mechanisms as those considered for LWR fuel (section 4.1.2.), the assessment of cladding degradation under dry storage conditions has focused on the creep behaviour of the Zr-1%Nb cladding; used in all reactor types. The following studies have been undertaken to demonstrate the performance of Zr-1%Nb clad [2, 4]:

- Testing of Zr-1%Nb tube pieces (80 mm in length) which were pressurized with argon and then irradiated to various fluences in the BOR-60 research reactor. Creep tests were conducted in a vacuum for 20 days at 400°C. It was noted that irradiated material underwent radiation induced hardening, similar to other zirconium alloys, which reduced thermal creep; i.e. testing of unirradiated samples would be worst case [44].
- Creep tests on unirradiated Zr-1%Nb cladding tubes at a range of temperatures and hoop stresses have been performed in the Czech Republic to establish the maximum allowable temperature for the storage of WWER-440 fuel in a CASTOR 444/84 cask. The study is reported in Ref. [45].
- A CASTOR 'WWER-1000' cask was loaded with three cans containing 3 WWER-440 fuel rods (in each can) at the Novovoronezh NPP; rod burnup was 36 $GW \cdot d \cdot t(HM)^{-1}$. Twelve spent WWER-1000 FAs were used as a heat source in the cask and temperatures in the range of 330–380ºC were reported for rods removed from the cask after 2.5 months storage [46]. The post-test investigation showed no alteration of the fuel rods, especially no diameter increase beyond the detection limit [2, 4]. The total duration of the test was planned for 12 months.
- Two WWER-440 fuel rods with a burnup of 48.2 $GW \cdot d \cdot t(HM)^{-1}$ were subject to simulated dry storage in sealed capsule filled with argon and externally heated at 350°C for two months and 390°C for a further two months in a hot cell at the Scientific Research Institute for Atomic Reactors (RIAR), Dimitrovgrad [47]. Three control rods from the same FA were subjected to a series of non-destructive and destructive analysis. Post-test examinations concluded that:

  > "*The external appearance of the fuel rod cladding surface, oxide film thickness, fuel rod length and distribution of fuel fission products remained the same after testing. A statistical assessment of all measured diameter changes resulted in a diameter change of 2.6 μm. Furthermore, calculated cumulative hoop strain (around 0.02%) under realistic conditions of decreasing clad temperature leads to creep being saturated after 10 years*" [47].

5. FUEL BEHAVIOUR IN WET STORAGE

The information in the chapter has been sourced from Refs [2, 4, 6] Other references are cited within the text as appropriate.

5.1. GENERAL PERFORMANCE

The experience in wet storing spent nuclear fuel now spans approximately 60 years. The benefits provided by this technology are mainly associated with cooling efficiency and shielding. Water also facilitates safeguards, fuel inspections/examination exercises, operational flexibility (particularly in respect of reprocessing operations), through pool water analysis enables ongoing fuel clad integrity to be established, and readily enables specific fuel assembly data to be collected.

The factors which could impact on fuel assembly/clad integrity, apart from routine fuel handling operations, were outlined in Section 4.

In general, wet storage of spent fuel only appears to be limited by adverse pool chemistry conditions or deterioration of the fuel storage pool structure. In the case of AR facilities, the factors that influence fuel removal are to maintain a reserve capacity for future fuel off loads from reactor or complete closure on economic grounds at the time of reactor shutdown.

The standard techniques for confirming ongoing spent fuel performance are destructive analysis (physical measurements on cut samples undertaken in hot cells) and non-destructive analysis (techniques which can be used in situ). The latter is discussed in Section 8.

5.2. LWR (BWR, PWR) FUEL

The performance of LWR fuel in wet storage in general has been excellent, with only occasional operational problems or incidents. For zirconium alloy clad fuel, data exists for continuous pool storage for greater than 50 years and stainless steel clad fuels for 32 years.

The basis for wet storing water reactor fuels in water pools was mostly established at the beginning of the project with only the impact of increasing fuel burnup needing further investigation. By the early 1980s cladding integrity investigations, both destructive and non-destructive analysis, had been conducted in a number of participating countries including Finland, Germany, the UK and the USA. The longest wet stored fuel was low burnup Zircaloy clad which had been in deionized water for >20 years. The longest stored stainless steel clad fuel had been stored in borated water for 6 years at the time of examination. In Germany, the performance of high burnup fuel (up to 39 $GW \cdot d \cdot t(HM)^{-1}$) was being investigated; benchmarked fuel had been re-examined after 1, 3 and 6 years of storage. The overall conclusion from these national studies was that no detectable cladding degradation had been observed [1, 3]. There was, however, some evidence that crud was beginning to soak loose from PWR fuel cladding after 8 years of storage.

In subsequent years the number of repeated post storage fuel examinations has been limited. Fuel integrity inspections/monitoring, however, are routinely performed during pool offloads and in support of reprocessing operations. For example, in the USA there is a requirement that all fuel assemblies must be visually inspected prior to handing [48]. Table 17 provides two examples of the data collected during recent pool offloads in the USA [49–50].

TABLE 17. EXAMPLES OF THE INFORMATION COLLECTED ON SPENT FUEL INTEGRITY IN SUPPORT OF AR POOL OFFLOADS IN THE USA

NPP	FAs inspected	FAs modified	FAs sipped	FAs placed into damage fuel cans	Oldest fuel	Comment
Zion	2226	1478	1369	98	1973	Modified with instrument tube tie rods
Kewaunee	887	241	161	3	1974	Modified with guide tube anchor pins No structural anomalies

The condition of long stored LWR fuel (40+ years) has generally been found to be good when retrieved in support of reprocessing operations or pool offload into dry storage casks. There is no evidence to suggest that there has been any fuel assembly degradation as a result of the wet storage regime employed. No limiting effects have been found during AR wet storage either; including the storage of high burnup fuels with new corrosion resistant structural materials.

Sleeve corrosion subsequently leading to top nozzle separation during fuel handling, however, has been reported for some PWR fuels with Zircaloy guide tubes and 304 stainless steel bulge joints containing higher than normal carbon levels. The degradation mechanism was identified as intergranular stress corrosion cracking of the stainless steel bulge joints (either sensitized during manufacture or in-reactor core and initiated through exposure to adverse pool chemistry conditions). Since these observations in the 1990s, design and materials changes have been implemented in later PWR designs. To minimize the corrosion of spent fuel structural materials in wet storage, chloride, fluoride and sulphate concentrations are also limited to 0.1 ppm, sodium and calcium contents have to be below 0.5 ppm, while the minimum value for pH is 4.5.

In support of reprocessing operations in the UK a number of PWR fuel assemblies susceptible to bulge joint corrosion were inspected prior to handling. Repeated examination, over many years, of one fuel assembly with observed bulge joint corrosion did not show any deterioration in condition with time, and has subsequently been retrieved and reprocessed without the top nozzle separating. Experiences in Spain in re-racking around 13 000 spent fuel assemblies provide further support to the UK observations.

The potential for top nozzle separation, however, still remains an issue for the retrieval of long stored fuel. To avoid any potential for top nozzle separation procedural controls and/or hardware fixes have been implemented for managing susceptible fuel assemblies. For example, in the recent retrieval of 887 fuel assemblies from the AR pool at the Kewaunee NPP (USA). There were 241 fuel assemblies known to be susceptible to bulge joint corrosion and remedial action was taken before the fuel was transferred to dry storage canisters [50]. The remedial steps included inserting six anchor bolts into the guide tubes and load testing to 450 $Kg \cdot m^{-1}$.

In recent phases of SPAR, AR spent fuel performance has been assessed in response to the September 11, 2001 (‘9/11’) events and, more recently, the events at the Fukushima Daiichi

nuclear power plant (2011). In the USA, the potential for rapid loss of water from a storage pool and uncontrolled reaction of zirconium based alloy components with air (zirconium fires) was assessed for BWR and PWR fuels resulting in strategies for mitigating the impact of an extended loss of pool cooling being introduced [51, 52]. A study of spent fuel pool safety at a reference BWR plant indicated that there is about a one in 10 million year chance that a severe earthquake would cause a radioactive release from a spent fuel pool. The regulatory evaluation confirmed that these results would apply to all U.S. plants [53].

Similar studies have also been undertaken in other SPAR countries. The most recent summary report on the findings from such investigations is provided in the Organization for Economic Cooperation and Developed (OECD) Nuclear Energy Agency (NEA) committee on safety of nuclear installations (CSNI) report on 'Spent Fuel Pools under Loss-of-Cooling and Loss-of Coolant Accident Conditions' [54].

5.3. CANDU FUEL

Canada has been storing research reactor fuel under water since the 1950s. CANDU power reactor fuel has been stored in water pools at the reactor sites and there has been continuous storage for about 45 years. Experience in wet storage has been excellent.

In 1977/78, AECL and Ontario Hydro initiated an experiment at AECL's Chalk River Laboratories (CRL) to assess the feasibility of storing irradiated zirconium clad CANDU fuel in water for at least 50 years. One hundred and seventy six fuel rods from 19 fuel bundles were originally selected for the programme. They included prototype generating station fuel irradiated in the national research universal (NRU) reactor at CRL and production fuel irradiated in the nuclear power demonstration reactor (NPD), Douglas Point and Pickering. The oldest bundle selected for the programme was discharged from the NPD reactor in May 1962. All 19 bundles were dismantled and the fuel stored as individual fuel rods in open ended stainless steel tubes. Groups of eight tubes were loaded into either aluminium or stainless steel storage cans. Stainless steel and aluminium storage cans were selected for the programme to investigate differences in storage material behaviour.

The fuel originally selected for the programme was characterized in 1977/78, which consisted of a destructive examination of specific fuel elements from each of the bundles plus a non-destructive examination on the remaining elements. The examination revealed no changes in the condition of the fuel or sheath from the original post irradiation examinations after 16 years of wet storage.

In 1988, specific fuel elements from each of the bundles were retrieved for a detailed interim storage examination. That examination revealed no apparent change in the condition of the fuel or cladding in any of the intact fuel elements after 26 years of wet storage. The condition of intentionally defected fuel is reported in Section 9 of Ref. [55]. No further examinations of this fuel have been reported.

5.4. RBMK, WWER FUEL

Prescribed AR conditions for wet storing Russian Federation origin fuels are: boric acid maintained within 12–16 $g \cdot kg^{-1}$; the concentrations of halides (Cl^- and F^-) are kept below 0.1 $\mu g \cdot kg^{-1}$; and pH in the 4.3–6.5 range. AFR pools are filled with demineralized water, halide concentrations are kept below 0.15 $mg \cdot kg^{-1}$, and pH within the 5.5–7.0 range.

Over ~50 years' experience of wet stored Zr-1%Nb clad WWER and RBMK fuel exists. There have been no reported fuel cladding failures in wet storage, under normal operating conditions, based on pool water activity monitoring. The corrosion of stainless steel spacer grids, however, has been reported. Spacer grids have now been replaced by zirconium alloy components to overcome the problem.

Corrosion studies have been conducted on Zr-1%Nb alloy cladding specimens cut from RMBK and WWER spent fuel assemblies of different burnup and cooling times. The results showed that burnup has a significantly greater influence on cladding plasticity than storage duration.

For RMBK fuel, a maximum oxide layer growth rate of 3–5 $\mu m \cdot year^{-1}$ has been observed in the spacer contact area for spent fuel stored in open canisters with uncontrolled chemistry; storage duration up to 15 years. For WWER-440 fuel, the measured oxide film thickness is distributed uniformly along the total cladding; its average value is 0.01 mm. In the location of the spacer grids, a local increase in the oxide film thickness by 0.005 mm has been observed [2].

5.5. AGR FUEL

For 20Cr:25Ni:Nb stainless steel clad AGR fuel, storage experience of 38 years exists. Although the general cladding corrosion rates for these fuels are significantly higher than for zirconium based alloys (at ~0.1 $\mu m \cdot yr^{-1}$), general corrosion is not a time limiting factor for the storage durations currently envisaged (up to 100 years).

For AGR fuel, particular attention to pool water chemistry is required as parts of the fuel stringer become sensitized during reactor operation (see Section 4.2) resulting in the cladding becoming susceptible to intergranular attack (IGA) in the presence of aggressive anions; particularly chloride. To inhibit IGA, the recommended wet storage regime for the fuel is sodium hydroxide dosed pool water at pH 11.4. Continuous storage experience in this environment for up to 24 years exists. No detectable cladding failures have occurred for fuel stored in sodium hydroxide dosed pools. As reported in SPAR-II, studies were initiated to evaluate alternative storage chemistry for AGR fuel to facilitate the co-storage of aluminium containing materials associated with LWR fuel storage in the THORP Receipt & Storage pool. Sodium nitrate was initially taken forward for further development, including active laboratory scale testing with high burnup brace material and a series of controlled studies on a limited number of storage containers containing AGR fuel isolated from the bulk pool water. It was subsequently decided to abandon the implementation of nitrate dosing on the basis of a lack of operational experience, some uncertainties in the ability of nitrate to absolutely arrest corrosion during controlled testing and concerns over the potential to promote algal blooms.

Short term dosing of the THORP Receipt & Storage pool with sodium hydroxide to pH 9 has subsequently been identified and implemented as an alternative water chemistry that is both protective to sensitized AGR cladding in wet storage and compatible with aluminium components currently stored in the pool. This offers a number of advantages, including utilising the extensive experience of using sodium hydroxide in storage pools at Sellafield.

5.6. MAGNOX FUEL

Magnesium alloy (MAGNOX Al80) clad fuel is particularly susceptible to cladding corrosion under wet storage conditions. Although a protective magnesium hydroxide film is initially

formed, the presence of any aggressive ions in the water promotes the dissolution of the protective oxide film and leaves the cladding open to pitting attack. For this reason, MAGNOX fuel is stored in high purity caustic dosed water to a minimum pH of 11.4 and storage duration tends to be limited; normally <5 years. Away from reactors, MAGNOX fuel is stored within containers initially dosed to pH 13.0.

Work is also ongoing to establish the feasibility of wet storing MAGNOX fuel beyond the currently accepted durations. Investigations are aimed at supporting the contingency options in the event of a major failure of the MAGNOX reprocessing facility [56].

6. FUEL BEHAVIOUR IN DRY STORAGE

6.1. GENERAL PERFORMANCE

Almost 40 years of favourable experience exists with the dry storage of spent power reactor fuel and about 50 years with the dry storage of research reactor fuel. Dry storage experience exists with fuel from a variety of reactor types (CANDU, HWR, PWR, BWR, WWER, RBMK, MAGNOX and HTGR). Since its conception, dry storage of spent fuel has evolved into a wide variety of systems (Section 3.2. provides further details). Almost all countries which have participated in the different BEFAST or SPAR programmes (Argentina, Canada, France, Germany, Hungary, Japan, Republic of Korea, Russian Federation, Spain, Switzerland, United Kingdom and the United States of America) are engaged in various dry storage technologies. Almost all participating countries are also actively pursuing a dry storage research and development programme. So far, the results of the research indicate that fuel can be stored safely under the present conditions for many decades [2, 4, 6].

The quantities being placed into dry storage have increased significantly over the last 20 years. At the end of 2013, there was around 52 500 t(HM) in dry storage [4]; for some countries this represents around 30% of the total fuel inventory.

The basis behind the choice of operating environment (cover gas) and conditions for the dry storage of spent fuel is reported in Ref. [3]. Studies in air and inert gases led to the adoption of one of two approaches: Loading spent fuel in air at a temperature whereby oxidation of any exposed fuel would not be affected; Loading spent fuel into an inert gas environment (to avoid any oxidation of exposed fuel and the fuel clad).

Helium is mostly used for the dry storage of LWR fuels, where to facilitate a timely removal of spent fuel from AR pools relatively high residual clad temperatures have to be accommodated [2]. Helium was chosen because of its thermal properties being 5–6 times more conductive than air, nitrogen, carbon dioxide or argon. Studies evaluating the thermal behaviour in a cask or closed system also showed that increasing the cover gas pressure improved heat transfer efficiency, for the pressure range 0.1–0.5 MPa [3].

The exceptions are CANDU fuel which is stored in dry air, MAGNOX fuel, which is stored initially in carbon dioxide and then transferred to air once the fuel has cooled, and nitrogen which is used in the MVDS technologies[9].

Dry storage of spent LWR fuel in an inert atmosphere is licensed dependent on burnup and type of cask for temperatures up to 400°C (and higher than 400°C for low burnup fuel if it can be shown that the cladding hoop stress can be maintained below 90 MPa) in the USA and Spain. Dry storage in nitrogen is licensed for a temperature of 410°C in Hungary for Zr-1%Nb clad fuel [2, 4, 6].

In Germany, no specific temperature for the licensing is required. Instead the following two criteria should be met to exclude systematic fuel rod cladding failures during dry storage:

- The maximal tangential stress of the cladding shall not exceed a value of 120 MPa; and

[9] A mixed nitrogen and helium environment is used in the new MVDS at the Mining and Chemical Combine, Zheleznogorsk, Russian Federation

- The residual tangential strain of the cladding shall not exceed a value of 1% at the end of the dry storage period [2].

In the case of a fuel assembly with a burnup of 55 GW·d·t(HM)$^{-1}$, which has been cooled in water for around 5 years, this leads to a temperature limitation of 360°C at the cladding surface [2, 4].

Most of the fuel in dry storage is clad with a zirconium alloy (Zry-2, Zry-4, and Zr-1%Nb); however, dry storage experience also exists for magnesium and aluminium clad fuels [2, 4].

Maximum burnups reach up to 65 GW·d·t(HM)$^{-1}$. There is an almost universal tendency towards increasing the discharge burnup of the fuel elements. In Germany, for instance, average discharge burnups for PWR fuel assemblies have increased from 35 GW·d·t(HM)$^{-1}$ in 1983 to 50 GW·d·t(HM)$^{-1}$ in 1998, and a value of 65 GW·d·t(HM)$^{-1}$ is achieved presently. In the USA and other SPAR countries, most of the spent fuel assemblies are being discharged with burnups in excess of 45 GW·d·t(HM)$^{-1}$. Despite this, the majority of dry storage systems are limited to maximum fuel burnup in the range 45–65 GW·d·t(HM)$^{-1}$ for LWR fuel [2, 4].

Apart from MAGNOX fuel which has been routinely retrieved from the dry storage facilities at Wylfa NPP, in support of reprocessing activities, data to confirm ongoing spent fuel performance in dry storage is limited [2]. In most cases confirmation that spent fuel has not degraded in storage will only be confirmed once the system is opened. The design basis, for the majority of these systems, is that the fuel will remain intact provided that the storage system has remained leak tight and it is this function which tends to be monitored to infer ongoing fuel integrity. The main exception is bare fuel stored in modular vault systems where periodic monitoring of the storage tube cover gas can be exercised.

6.2. LWR (BWR, PWR) FUEL

The performance of LWR fuels in dry storage was originally established through short term demonstration tests carried out in the 1980s [3]. For example, Germany undertook a number of demonstration tests between 1 week to 30 months using CASTOR and TN transport casks where benchmarked fuel assemblies were retrieved and inspected to establish if any changes had occurred [57].

A list of more recent fuel and cask inspections is summarized in Table 18.

A demonstration programme, in support of LWR fuel dry storage in the USA, was initiated at Idaho National Laboratory in 1984 [58]. The initial phase of this programme involved periodic internal cask cavity gas sampling to confirm ongoing fuel clad integrity [58], after 14 years one of these casks, a CASTOR V/21, was inspected and reopened in 1999. The examination included removing all 21 fuel assemblies and undertaking non-destructively examinations to confirm spent fuel condition. The findings of these examinations are summarized:

> *"...there was no evidence of cask, shielding or fuel rod degradation during long-term (14 years) storage that would affect cask performance or fuel integrity. There was no evidence of exterior or interior cask deterioration during storage period, nor were there any signs of seal or shielding failure. The fuel was intact, and there were no indications of any significant cladding creep or rod bow. ...." [59].*

TABLE 18. SUMMARY OF SPENT FUEL INTEGRITY STUDIES IN DRY STORAGE CASKS

Year of examination	1985-1998	1999	2000	2005	2009	2013
Type of programme	Demonstration	Demonstration	Regulator requirement	Regulator requirement	Regulator requirement	Integrity checks after design base event
Scope of examination	Cavity gas sampling	Cask and fuel integrity	Cask and fuel integrity	Cask and fuel integrity	Cask and fuel integrity	Cask and fuel integrity
Programme owner	DoE/Virginia Power/EPRI	DoE/Dominion/ EPRI	TEPCO	TEPCO	JAPC	TEPCO
Country	USA	USA	Japan	Japan	Japan	Japan
No of Casks	5	1	1	5	1	9
Storage duration prior to examination (years)	Performance testing up to 1 year –all casks 10–13 – CASTOR V/21 7–11 – VSC-17	14	5	10	7	18
Cask type	CASTOR V/21, MC-10, TN-24P, REA-2023, VSC-17	CASTOR V/21	TN-24 (37 BWR)	TN-24 (52 BWR)	Hitachi-Zosen (61 BWR)	TN-24 (37 & 52 BWR)
Decay heat at loading (kW)	12.6–28.4	28	N/A	N/A	13	N/A
Cavity gas sampling	^{85}Kr not above background – CASTOR V/21, VSC-17, MC-10 Single rod failures detected in REA-2023, TN-24P during performance testing	^{85}Kr not above background	^{85}Kr not above background	^{85}Kr not above background	^{85}Kr not above background	^{85}Kr not above background

TABLE 18. SUMMARY OF SPENT FUEL INTEGRITY STUDIES IN DRY STORAGE CASKS (cont.)

Year of examination	1985-1998	1999	2000	2005	2009	2013
Inner lid leak rate ($Pa \cdot m^3 \cdot s^{-1}$)	N/A		5.3×10^{-8}	1.6×10^{-7}	No change c.f. loading	$<1 \times 10^{-6}$ (1× casks)
Condition of seal surface/gaskets	N/A		Whitening of secondary lid gasket observed[a]	Whitening of the secondary lid gasket observed[b]	No changes observed	Secondary lid gasket corroded by sea water[c]
Burnup of examined fuels ($GW \cdot d \cdot t(HM)^{-1}$)	24–35	24–35	32	28	33.5	
Fuel condition c.f. loading	No evidence of fuel rod degradation during storage based on gas sampling	No evidence of fuel rod degradation	No change observed	No change observed	No change observed	No deformations or abnormalities observed

[a] Gasket of all stored casks changed in 2001.
[b] A different cause is cited to the one given in 2000.
[c] All secondary lid gaskets replaced.

In Japan, cask and fuel integrity inspections have also been undertaken by TEPCO and JAPC. The objectives of these inspections were to confirm the containment of the metal gasket and spent fuel integrity. As for the containment, visual inspection on the seal surface and gasket did not show abnormal condition on the cask at Tokai Daini site [4]. The Fukushima Daiichi 2000 inspection, however, showed some colouring of part on the metal gasket surface used in the primary lid seal; this colouration had increased by the 2005 inspection. During the inspection in 2000, a white product on the surface was observed; it was concluded that a reaction had taken place between the aluminium material of the gasket and residual water. In 2005, the white colouration change occurred during immersion of the cask in the reactor pool for several days before opening the primary lid [60]. In the case of spent fuel integrity, no ^{85}Kr gas was detected by gas sampling of the cask cavity, and visual inspection of the fuel assembly surface did not show any abnormal condition [4].

During the earthquake and subsequent tsunami (2011) the cask storage facility at Fukushima Daiichi NPP was affected by a vast amount of seawater, sand and debris which was deposited into the building. The nine stored casks after confirmation of the safety performance by the external appearance of the cask bodies were transported from the dry storage facility to the common pool at the site, and further inspections were carried out to confirm containment, subcriticality and fuel integrity. The investigation confirmed that there were no abnormalities on the cask bodies or any abnormalities in the external appearance of the three representative spent fuel assemblies that were taken inspected. Removal of the primary lid of the other eight casks was only considered if the primary lid seal was found to be leaking or ^{85}Kr was detected; no further action was required. In all cases the secondary lid seal was replaced due to sea water corrosion [61].

6.3. CANDU FUEL

Demonstration programmes in support of the dry storage of CANDU fuel were carried out by AECL and Ontario Hydro at AECL's Whiteshell Laboratories between 1978 to 1996 [2, 4]. Details of the fuel histories, scope of studies and findings are provided in Table VI of Ref. [5].

Characterized fuel elements from the then OPG's Pickering and Bruce NPPs were periodically removed from storage and subjected to post storage examinations. Both non-destructive and destructive examinations were performed. The main conclusion from these studies was that no noticeable changes were detected.

No examination of dry stored CANDU fuel was reported by the participants from Argentina and Republic of Korea.

6.4. RBMK FUEL

The storage of 8–10 year water cooled RBMK fuel elements in air for 3 years was reported not to cause any serious impact on the corrosion resistance and mechanical properties. Furthermore, due to the relatively low decay heat of RBMK fuel after 5 years wet storage, the temperature in the centre of a dry storage cask was predicted not to exceed 270°C [5].

6.5. WWER FUEL

See Section 4.5.2.

It was also reported [5] that a demonstration loading of a TK-13 cask with 12 WWER-1000 FAs was performed at the South Ukraine NPP between 1988 and 1989; no leakers were reported.

6.6. MAGNOX FUEL

The general experience with dry storage of MAGNOX fuel at Wylfa NPP since the 1970s, both in the short term CO_2 cooled stores and in the two longer term air filled stores, has been very good [2, 4]. As the last operating reactor on the Wylfa site was shut down on 31 December 2015 and it is government policy for all MAGNOX fuel to be reprocessed; the site is currently being defuelled to Sellafield.

The only reported fuel integrity issues have been due to water ingress into one of the air cooled stores; see Section 9.4.2.

6.7. AGR FUEL

Although a number of R&D studies into the behaviour of AGR fuel under dry storage conditions (AFR storage) have been undertaken [62–63], there is currently no industrial experience.

The design of the AGR AR fuel route, however, includes an initial period of cooling in CO_2 forced cooled storage tubes. The capability to store fuel AR dry for most AGR NPPs is very limited, hence the fuel route involves dismantling of the fuel stringers after being initially cooled in CO_2 and then AR wet storage prior to transport to Sellafield.

7. STRUCTURES WET AND DRY STORAGE

Structures associated with fuel storage have to be resistant to irradiation, heat and corrosive attack for many decades. A variety of materials are used in spent fuel storage. Wet storage of fuel commonly occurs in specially designed racks stored in deep water filled pools with thick concrete walls which are normally stainless steel lined; to minimize corrosion of the concrete/re-bar and to aid decommissioning. Dry storage mainly involves self shielded storage systems (metal or concrete casks), canister based storage systems (unshielded sealed stainless steel canisters placed in a concrete structure) or a purpose built shielded storage building which can accommodate single or multiple FAs in storage tubes. Casks may have all or some of the following features: body; external cooling fins; trunnions for lifting; lid system single or multiple; seals (metal and/or elastomer or welds); a basket to position the spent fuel assemblies; and neutron absorbers. In contrast, the other types of storage system are intended primarily for spent fuel confinement and heat transfer; the concrete structure ensures shielding and physical protection of the canistered fuel or fuel in a storage tube and facilitates heat transfer from the stored fuel.

The following sections summarize the main materials used in spent fuel storage systems, their degradation mechanisms and materials R&D reported to BEFAST and SPAR CRPs.

7.1. MATERIALS

7.1.1. Stainless steel [2, 4]

Stainless steel components are highly resistant to corrosive attack due to the formation of protective oxide films. For example, corrosion as a consequence of pitting or galvanic attack have been shown to be negligible, and the rates of general (or uniform) corrosion only become significant over extended time periods (100s of years). To put the latter in context the short term measured corrosion rate of stainless steel in radiolysed water is ~0.3 $\mu m \cdot year^{-1}$ and <0.1 $\mu m \cdot year^{-1}$ in demineralized water dosed with sodium hydroxide to pH 11.4. The most significant failure mechanisms affecting stainless steel, under the right conditions, are stress corrosion cracking and microbial failure.

7.1.2. Aluminium alloys

Aluminium alloys in wet storage have a wide range of corrosion phenomena, from rapid penetration to minimal corrosion over decades. In general, the stability of the material is very much dependent on retention of the protective oxide barrier. For example, uniform or general corrosion of aluminium is low in the pH range 4–8.5, but at higher or lower pHs becomes significant because of dissolution of the protective film. The most significant degradation mechanism is from pitting attack; however, other mechanisms such as crevice, galvanic and microbial corrosion have also been reported; particularly in association with pool water chemistries with conductivities >3 $\mu S \cdot cm^{-1}$ [2].

During dry storage, aluminium alloys are mainly used as an efficient heat conductor inside the casks. Due to the low density compared to other metals, aluminium is a suitable base material for baskets, in order to increase the number of fuel assemblies to be loaded into the cask for efficient transport and storage. Besides that, borated aluminium alloys and composites are used as neutron absorbers. Under dry storage conditions, corrosion is excluded or minimized, since the aluminium parts are anodized or made of low corrosion alloys, respectively.

There is no external mechanical load on the parts made of aluminium alloys, since the load on casks is restricted to vertical or horizontal handling and dead load due to upright standing or lying horizontally. Usually, changes of mechanical properties of aluminium alloys do not occur at neutron fluxes of fast neutrons below 10^{20} n·cm^{-2}. The amount of emitted neutrons by the inventory over the foreseen interim storage time is several orders of magnitude smaller. Therefore, no significant changes of mechanical properties of the aluminium alloys due to radiation effects are expected.

7.1.3. Borated stainless steel or borated aluminium alloys and composites as neutron absorbers [4]

Neutron absorbers are deployed in spent fuel storage racks, transportation baskets etc., as a means of maintaining subcriticality. The commonly used borated absorber types are listed below:

- Boron carbide in a silicone rubber binder; for example, Boraflex;
- Boron carbide dispersed between aluminium alloy cladding; for example, Boral;
- Borated aluminium alloy, e. g. BC-A6N01SS-T1 and 1%B-A6061-T6/T651;
- Borated stainless steel alloy; and
- Cadmium metal in a leak proof cladding; for example, Cadminox.

The latest designs for transportation and storage casks has called for new neutron absorbing materials to attenuate the higher enriched (up to 5% ^{235}U) and higher burnup fuels (>55 GWd·t (U)$^{-1}$); i.e. a requirement for better thermal and neutron efficiency, for example, metal matrix composites which can accommodate significantly higher loadings of boron compared with borated stainless steels. Derived from aluminium alloys, they act as both neutron absorber and structural component for spent fuel baskets. Aluminium offers excellent thermal conductivity.

One of two technologies deployed to incorporate the neutron absorbers:

- Adding boron into molten aluminium (ingot metallurgy); and
- Mixing the stable compound such as B_4C with aluminium alloy powders (powder metallurgy).

Generally, the borated aluminium needs properties as follows:

- Uniformly dispersed boron (or boron carbide) particles in the materials to control the criticality;
- High thermal conductivity to remove decay heat from spent fuel; and
- Keeping the required mechanical strength for long period (more than 60 years) under high temperature (>200˚C).

7.1.4. Concrete [4]

Concrete is by nature a non-uniform non-homogeneous material. It is relatively inexpensive and, though it has high compressive strength, is weak in tension. Steel, which is more expensive, has very high tensile strength, is incorporated into concrete in regions of tensile stress, thus taking over from the concrete in carrying these tensile effects. Steel also has the beneficial effect on concrete by controlling the width of cracks associated with tensile strains

in concrete. Such tensile strains may be caused by mechanical and thermal loading, and/or the effects of restrained drying out shrinkage (soon after casting), as well as surface thermal contraction strains due to temperature gradients during curing conditions. Good quality modern concrete in a benign environment can be expected to last indefinitely without any serious deterioration in structural properties.

7.1.5. Cast iron [2]

Similar to untreated carbon steels, cast iron has relatively poor corrosion resistance. Its application is mainly in the manufacture of transport/storage casks and cask handling equipment. The material behaviour, however, is taken into consideration in the design of storage components, such as dry casks, where cask body thickness is derived from the shielding requirements; proposed duty, assuming a uniform corrosion rate; and a safety margin (e.g. 100%). To mitigate against uniform corrosion, cast irons are usually treated with several coatings of epoxy. Nevertheless, it should be mentioned that long term corrosion tests with ductile cast iron have been made under extreme conditions in salt water and showed an equilibrium corrosion rate of about 0.1 $mm \cdot year^{-1}$. This is the result of the good adhesion of the oxide layer, due to the high carbon content in the cast iron.

7.1.6. Carbon steels [2]

Untreated carbon steels have relatively poor corrosion resistance in oxygenated waters at low temperatures, and therefore do not find general application. To overcome this effect, carbon steels are normally treated with zinc and/or coated with epoxy paint systems. The main degradation mechanism to be considered, therefore, is pitting corrosion, where the protective coating has been damaged during operation or the original material preparation was poor. Where such defects occur, pitting corrosion will proceed in the presence of aggressive ions, such as chloride. Once again, the maintenance of good water chemistry conditions will minimize this effect.

7.1.7. Polymers [4]

In wet storage, polymers can be used as water retaining flexible wide polymeric strips or ‘water bars’ in unlined water retaining structures. Water seepage at the expansion joints is prevented by the incorporation of for example polyvinyl chloride bars. The gaps between the joints are also filled with polymeric sealants for example polysulphides or polyurethanes.

In dry storage, a variety of polymers have been used as neutron shielding materials. These include polypropylene, polyethylene, polyesters, epoxy resins, and a variety of mixed polymers. As the name implies, the purpose of neutron shielding materials is to stop neutrons. This means that fast neutrons have to be slowed down first before they can be captured by neutron absorbers. The slowing down of fast neutrons is achieved by polymers due to their high concentrations of hydrogen atoms.

7.2. DEGRADATION MECHANISMS

7.2.1. Degradation mechanisms in metals

7.2.1.1. Radiation damage

Radiation damage of metals, e. g. cast iron, stainless steel, is mainly due to fast neutrons; i.e. neutrons with energies above 100 keV. A considerable modification of the mechanical properties of metals is expected at neutron fluxes above 10^{18} n·cm^{-2}. The typical absolute amount of emitted neutrons, however, results in a flux which is well below this value. For example, the full energy spectrum of a CASTOR® cask inventory over 40 years is shown by Eq. (6):

$$N(40y)= 10^{19}–10^{20}\ n\cdot(cask)^{-1} \quad (6)$$

7.2.1.2. Stress corrosion cracking

Stress corrosion cracking commonly occurs in stainless steels with a depleted chromium content (the chromium content in the grain boundary has decreased below 12%) when they are simultaneously exposed to mechanical stress and aggressive ions, such as chloride [2, 4].

Under dry storage, sensitization of stainless steel may be induced in a certain temperature range. Sensitization is a process where the chromium in some stainless steels can migrate from the grain boundaries into the bulk metal and react with any free carbon to form particles of chromium carbide. Thermal annealing processes are sufficient to re-establish a homogeneous distribution of chromium [2, 4]; thus, thermal sensitization is a reversible process.

Stress corrosion cracking has been identified as a potential issue for canister based dry storage systems located at marine sites. This is because the inner welded canister is normally fabricated from austenitic stainless steel with non-stress relieved welds, and there is potential for salt to be entrained into the welds during cool down processes.

7.2.1.3. Microbial attack

Over time, microbial colonies may become attached to pipes etc., establishing local environments that favour the growth of species, which would not otherwise survive. Established colonies are also highly resistant to fluid forces and most chemical treatments, making removal difficult. The microbial colonies effectively shield the metal surface from water treatment chemicals, rendering corrosion inhibitors ineffective. It has been demonstrated that welding of austenitic stainless steel increases their susceptibility to MIC compared to smooth pipe surfaces. In fact, the weld and the associated heat affected zones become the primary area of MIC attack. The impact of MIC has generally been ignored, as it is hard to detect, and this mechanism is usually masked by general corrosion. The only indicator of its influence is that components under periodic replacement programmes have to be locally replaced at slightly greater frequency than originally anticipated [2, 4].

To avoid MIC, periodic sampling to establish whether any microbial species which can cause corrosion are present is recommended. Corrective action involves the removal of sources such as light, carbon etc. which would promote colony growth.

7.2.1.4. Pitting corrosion [2]

Pitting corrosion is most prominent in high chloride environments. Pits tend to develop at defects in the passive film, where chloride ions not only promote local dissolution of the protective oxide film, but also stimulate metal dissolution and hence promote growth of the resulting cavity or pit. The attack is generally limited to small areas, where local chemistries develop in the pits. In some cases, the chemistries are isolated from the bulk water by crusts that are formed over the pits. Improving the water chemistry in such cases may only slow the mechanism rather than totally inhibit the attack.

A specific case of pitting corrosion has been experienced with the outer high-grade aluminium cask seals. The 1000 series alloys are high purity aluminium alloys that in most environments provide a high level of corrosion resistance, due to the rapid formation of a thin, tight and protective aluminium oxide film. However, in some environments, such as those containing boric acid, with chlorides present, the alloys can approach or even exceed their pitting potentials. In this situation, chlorides can destroy this passive protective oxide film, leading to pitting. Aluminium in this condition, which is then placed in close contact with a metal that is more cathodic, will undoubtedly experience corrosion as a result of the galvanic cell that is formed once pitting has occurred.

7.2.1.5. Galvanic attack [2]

Aluminium alloys lie at the active end of the galvanic series. Galvanic corrosion of aluminium alloys has been observed in fuel storage environments when coupled to stainless steels, and even with different aluminium alloys, in waters with high conductivities >100 $\mu S \cdot cm^{-1}$. In highly pure waters (1–3 $\mu S \cdot cm^{-1}$), galvanic effects have not appeared to degrade the service capability of aluminium alloy components; except in dissimilar metal crevices, that facilitate development of low pH and concentration impurities.

7.2.1.6. Crevice corrosion [2]

Crevice corrosion is a localized form of attack, occurring in closely fitted surfaces that are sufficiently offset to allow water entry. The suggested mechanism of attack is where chloride ions are drawn into the crevice, causing metal dissolution to proceed and acid conditions to develop.

As with galvanic attack, mitigation of crevice corrosion can be achieved by maintaining water conductivities in the 1–3 $\mu S \cdot cm^{-1}$ region.

7.2.2. Concrete degradation

Conversely, unlike plain concrete, reinforced concrete is generally not as inherently durable, owing to the propensity of its steel reinforcement to corrode. ‘Cover’ is the specified minimum thickness of concrete from the reinforcement to the external concrete surface. Once the concrete in this cover zone to the reinforcement loses its alkalinity, and given that moisture and oxygen can get to the reinforcing steel, the reinforcing steel will start to corrode. There are many possible causes of degradation in reinforced concrete structures; they include) physical conditions (such as movement of the foundations, structural overloading, accidental impact damage), thermal cycling, and chemical/environmental effects (for example carbonation or chloride ingress). It is, therefore, imperative that concrete structures are

regularly inspected (this is usually done on an annual basis for large wet storage pools) so that warning signs can be detected and the causes of defects identified [2, 4].

7.2.2.1. Carbonation of concrete

During the hydration of concrete there is a formation of calcium hydroxide ($Ca(OH)_2$), which is responsible for the high alkalinity of the concrete (pH≥ 12). $Ca(OH)_2$, however, is gradually converted to calcium carbonate ($CaCO_3$). The reaction with CO_2 from the air causes a lowering of the pH to about 9. In a humid environment the surface starts to 'corrode'; associated with a volume enlargement. Depending on the density of concrete CO_2 can penetrate some millimetres or some centimetres in the concrete.

7.2.3. Polymer degradation

Polymer degradation impairs mechanic properties of polymers and reduces their capacity for slowing down fast neutrons. The changes in properties are often termed as 'ageing'; therefore, the potential for aged polymers to lose their specified properties increases. Polymers will degrade with time due to the combined effects of irradiation and further environmental factors, primarily chemical agents (acids, alkali and certain salts) in moisture and heat under dry storage conditions. Likewise, polymer degradation depends on i.e. whether the polymer is in contact with water or exposed to air or oxygen-free atmospheres. The degradation of various polymers follows the same pattern, they lose weight by releasing relative small chemical molecules such as hydrogen, hydrogen chloride, water and oxidized compounds. The chemical molecules released are polymer composition dependent. Wherever the polymers are in contact with pool water, the small chemical molecules will be leached to the bulk pool water, associated with a potential impact on water treatment systems [4].

A variety of polymeric materials such as polypropylenes, polyethylene, polyesters, epoxy resins, and a variety of mixed polymers have been used as neutron shielding materials [4]. For example, ultra high molecular weight polyethylene (UHMW-PE) is implanted in the cask wall and both ends of CASTOR® casks; allowing enough space for thermal expansion and under exclusion of oxygen. Therefore, only two possible degradation mechanisms have to be considered. This is the influence of high-energetic radiation on UHMW-PE, which leads to a release of mostly hydrogen and the generation of cross-links. Thus, bonds between separate polymer chains are formed. The amount of generated radiolysis gas and cross-links depends solely on the absorbed dose in the material during the storage period. Possible increase of the pressure in the vicinity of the moderators is considered in the cask design.

As a shielding material in transport/storage casks, it is anticipated that the implanted polymers are able to withstand high temperatures for short time periods like in case of fire i.e. 800ºC for 30 minutes. With a move to increased fuel burnups and mixed oxide fuels the importance of their long term thermal stability increases in view of an increasing cask operating temperature. The increased demand for long term thermal stability together with a high neutron/gamma dose resistance has called for the development of new materials [4].

7.3. INVESTIGATIONS AND RESULTS

A review of materials performance in wet storage environments is provided [64]. The review includes corrosion data and represents the state of knowledge up to 1997; for most materials this is still a useful reference publication.

7.3.1. Stainless steel

On behalf of Jaslovské Bohunice spent fuel interim storage facility (SFIS), a surveillance programme has been evaluating the corrosion rates and behaviour of materials used in spent fuel storage baskets and the pool liner [7]. The materials were fabricated into corrosion coupons comprising:

- Standard corrosion coupons;
- U-bend;
- Circular bead welded;
- Crevice bent beam (CBB); and
- Special types, for example hexagonal welded joints.

The behaviour of these materials in the storage environment has been monitored through standard weight loss measurements and analysis of the coupons by microscopy.

In the case of the pool liner, manufactured from ANSI 321 stainless steel, the results are in-line with expectations (see Fig. 48). There is some variability in the reported results due to sample variations and the weight measurements being at the measuring limit.

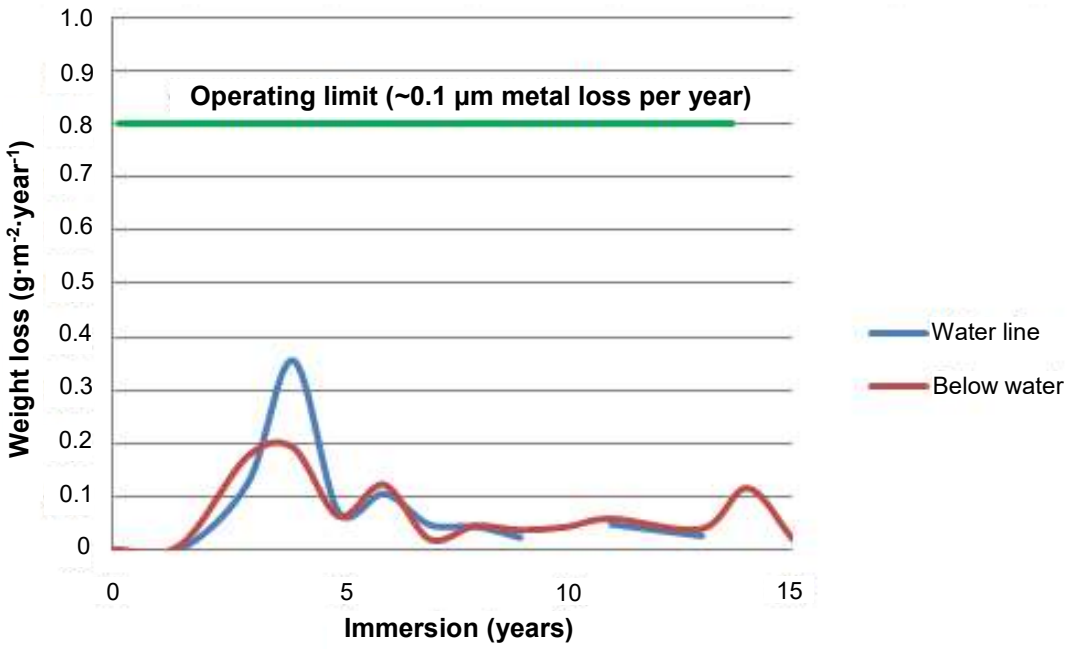

FIG. 48. Weight loss measurements for ANSI 321 stainless steel used in the pool liner.

7.3.1.1. Stress corrosion cracking of fuel canisters

There is potential for SCC to occur in austenitic stainless steel fuel canisters used in ventilated concrete cask storage systems. SSC may be initiated in the weld zones of these canisters if there is residual stress and aggressive ions, such as chloride, are present. Studies evaluating the minimum concentration of salt to initiate SCC, crack growth rates and salt disposition/transport are reported [4, 7]. The main results are summarized here.

Japanese studies on 304 L stainless steel concluded that the minimum concentration of salt to initiate SCC was 0.8 $g \cdot m^{-2}$ as Cl- under the applied test conditions (Fig. 49). A limitation of the surface crack length to ≤ 100 μm was identified as a criterion for achieving damage control after SCC initiation.

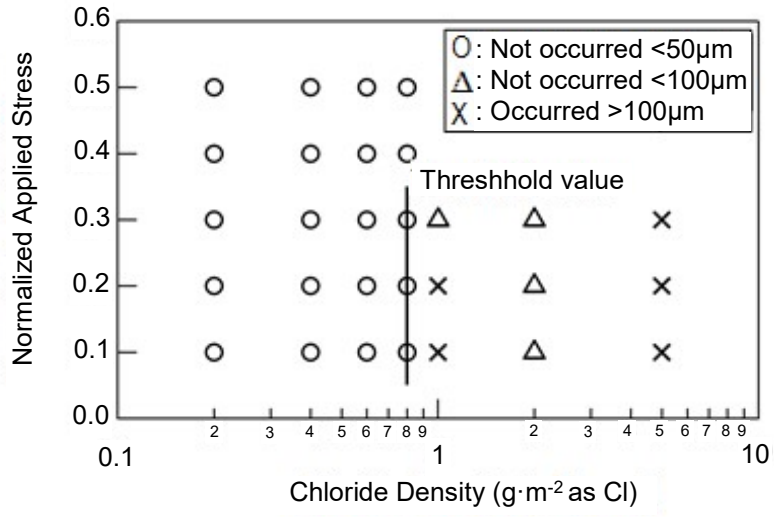

FIG. 49. SCC Initiation Test Results - Specimen B for 5000 hr, Hardness 247 Hv (figure courtesy of CRIEPI).

U.S. studies under plausible natural atmospheric conditions, with a maximum absolute humidity of 30 $g \cdot m^{-3}$, observed SCC initiation in Type 304 U-bend specimens at temperatures ranging from 35–60°C; when the relative humidity (RH) during exposure was above the measured RH for deliquescence of simulated sea salt. SCC initiation was observed on specimens deposited with as little as 0.1 $g \cdot m^{-2}$ of simulated sea salt compared to 0.8 $g \cdot m^{-2}$ (Japanese studies). The extent of cracking increased with increasing salt surface concentration. Because no testing was conducted at salt concentrations below 0.1 $g \cdot m^{-2}$, the threshold surface salt concentration for SCC was not determined. Furnace sensitized material was more susceptible to SCC. The heat affected zones of welded U-bend specimens showed SCC susceptibility and had a microstructure similar to the as-received material.

SCC was also observed on Type 304L C-ring specimens that were strained to 0.4 or 1.5%, with deposited surface salt concentrations of 1 or 10 $g \cdot m^{-2}$ at temperatures of 35–52°C. No tests at higher or lower temperatures were conducted. At the strain of 0.4%, the stress on the C-ring specimen is approximately equal to the material yield stress.

No SCC was observed on Type 304 U-bend specimens with deposits of NH_4NO_3, NH_4HSO_4 and fly ash which would be expected from agricultural, commercial and industrial activities. SCC was observed on Type 304 U-bend specimens that were exposed to mixtures of NH_4NO_3 and NaCl with NO_3^-:Cl^- mole ratios of 3.0 and 6.0, but less than 10 $g \cdot m^{-2}$ of NaCl indicating that NO_3^- is not an effective inhibitor for chloride SCC.

The crack growth rate (CGR) under various conditions has been measured in Japan by using a four point bend test specimen made from 304L stainless steel (304L SS). Figure 50 shows the results for a test specimen placed under conditions of constant temperature and RH; i.e. 80°C and 35% RH. The measured CGR shows that the crack initially propagated fast, whereupon the propagation rate declined. Assuming an initial crack size as a result of the initial fast crack propagation, the remaining canister wall can be evaluated with slow propagation rate data. An example of the calculated RH on the canister surface with time is shown in Fig. 51. According

to this calculation, the accumulated time period where the RH exceeds 15% (threshold for SCC to occur) would be approximately 15 000 hours (i.e. <2 years) during a 60 year storage period. Using a CGR of 1×10^{-11} m·s^{-1}, the estimated crack propagation value during this period is only 0.5 mm.

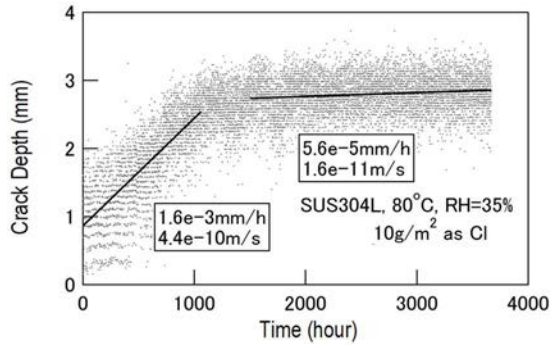

FIG. 50. Crack growth test results (figure courtesy of CRIEPI).

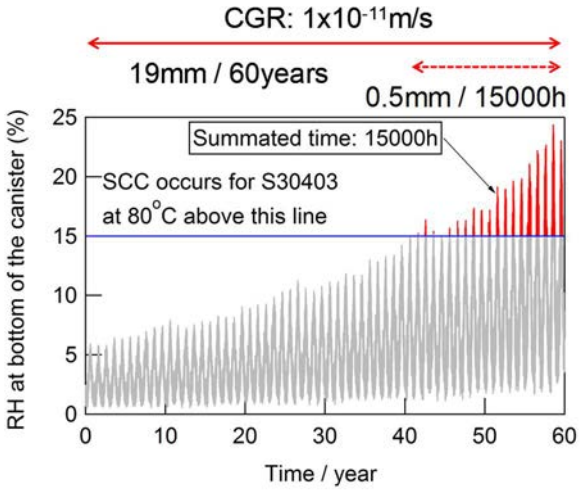

FIG. 51. Relative humidity change at the canister bottom with time (figure courtesy of CRIEPI).

The use of surface treatment techniques such as shot peening, laser shot peening and low plasticity burnishing to relieve stress in weld regions has also been studied. Further information on this can be found in Ref. [7].

7.3.2. Borated stainless steel

The neutron absorbing material used in the spent fuel storage baskets at Jaslovské Bohunice is ANSI 304 stainless steel alloyed with a minimum of 1.1% boron (called ATABOR). This material has been subjected to the same surveillance programme as described in Section 7.3.1. The results from the weight loss measurements of this material are shown in Fig. 52.

Analysis of this material, however, has shown several micro-cracks in the base metal associated with areas of high chromium content. The cracks were found to be corrosion free and are the result of initial sample preparation due to the brittle nature of the Cr–B bonds. There has been no evidence to support crack propagation [7].

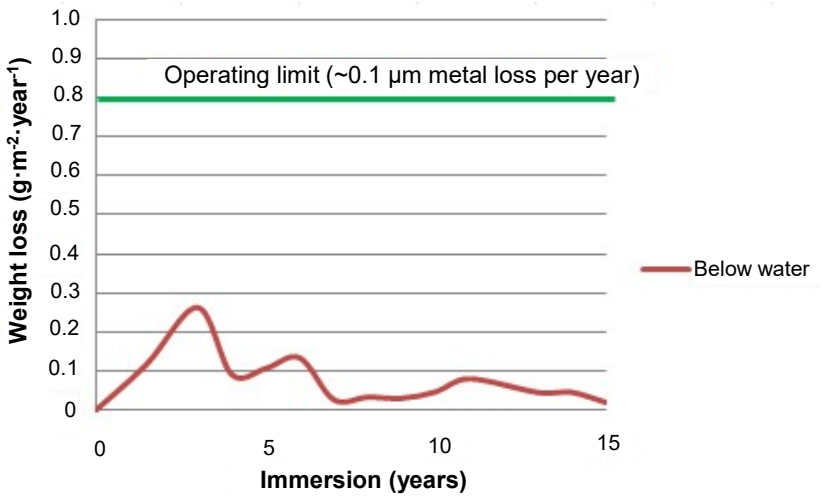

FIG. 52. Weight loss measurements for ATABOR stainless steel used in storage racks.

7.3.3. Borated aluminium alloys

The mechanical properties of borated aluminium materials have been investigated in Japan [7]. The effect of irradiation, testing performed in a research reactor, was concluded to be negligible.

Additional information on the use of borated aluminium alloys in transport/storage baskets is provided in Ref. [65].

7.3.4. Concrete

7.3.4.1. Ventilated concrete casks

R&D interests have mainly been focused on reinforced concrete overpacks used in ventilated concrete cask systems for the dry storage of LWR fuel [2, 4]. Studies in Japan have looked at the rates of diffusion of carbon dioxide and chloride at a variety of operating conditions (temperature and humidity) for concrete samples with a range of water–cement ratios. Through studying these parameters an indication of the minimum 'cover' required for a given set of operating conditions and design life can be established. Results from these studies are reported [2, 4, 7]. A full account of the studies is provided in Ref. [66].

The studies concluded that the chloride ion concentration required to initiate corrosion of the reinforcement bar was ~1.2 $kg \cdot m^{-3}$ in the temperature range 20–90°C. The chloride ion diffusion coefficients were obtained by immersion tests of concrete samples in 10% sodium chloride solution at a range of operating temperatures. For the applied test conditions and samples used, it was concluded:

- The diffusion coefficient for chloride increases with increasing temperature;
- There is a linear relation between the logarithm of the diffusion coefficient and the reciprocal of the temperature; and
- The concrete samples with a larger water–cement ratio had a tendency to have a larger diffusion coefficient.

The results of these tests were used as the basis for proposing a diffusion coefficient evaluation equation. The equation is provided in Refs [7, 66].

In terms of ageing management, the analysis of small core bore samples taken from non-critical areas can be used to establish the depth of carbonation and chloride in deployed systems. The depth of carbonation and chloride ingress is dependent upon site operating conditions, concrete mixture composition and quality of the manufactured system

7.3.4.2. Concrete casks

In the case of concrete casks where the reinforced concrete is sandwiched between inner and outer metal plates, the loss of concrete alkalinity is not considered an issue. The visual inspection of a reopened CONSTOR® cask did not show any significant corrosion effects on the walls [2].

Change in cement grade used in Ontario Power Generation dry storage casks [4]

Canadian Standards Association (CSA) Type 20 cement is used in the manufacture of OPG DSCs. Due to concerns with the long term availability of Type 20 cement (i.e., moderate heat of hydration), studies have been performed to evaluate the use of:

- CSA Type 20E or Type 50E equivalent cements. In particular, replacing about 20% Ordinary Portland cement with ground granulated blast furnace slag; and
- CSA Type 50 cement (i.e., high sulphate resistant cement).

For cement formulations incorporating slag, a concern was raised that there could be potential for the carbon steel reinforcement to corrode as a result of slag sulphide content. A follow-up thermodynamic study concluded that sulphide could convert to hydrogen sulphide under a given set of conditions; i.e. if there is sufficient residual water to form an aqueous phase in the concrete matrix. If a water vapour phase only remains, then the generation of H_2S would be expected to be insignificant. The study pointed out the importance of a low residual moisture content to reduce the risk of enhanced corrosion of the reinforcement and DSC steel components. Kinetic rate studies to confirm the thermodynamic findings were not undertaken.

As a result of the above findings a development programme looking at Type 50 cement was initiated. The programme included multi-phase laboratory testing and a field trial. The purpose of the laboratory tests was to develop, optimize and test a candidate high density concrete using Type 50 cement. The field trial was designed to confirm full scale performance of the concrete, as well as to address practical aspects of its processing such as mixing, batching and curing.

Satisfactory results were obtained with the Type 50 cement, and, the experimental findings met the specifications for the DSC, as well as the requirements for long term performance and durability. Type 50 cement met a 7 day heat of hydration limit set at 300 kJ·kg cement, as per the DSC specification. Results from the field trial indicated that some localized honeycombing/layering was observed in the hardened concrete, which was attributed to inadequate compaction during placement, and was later resolved.

The main conclusion of the development programme proved that Type 50 cement can be recommended for use as a replacement for Type 20 cement.

7.3.5. Polymers

7.3.5.1. Polymers (PVC) used to seal large constructions [4]

The degree of PVC degradation is affected by a number of parameters which include thickness, composition (presence of other materials), dose rate, medium they are in contact with (air, water, boric acid, etc.). For example, degradation is greater if the material is irradiated at a low dose rate for a long time, compared with the degradation produced by irradiation to the same total dose at a high dose rate over a shorter period of time.

Accelerated radiation testing of the PVC water bar material used in the expansion joints of the THORP Receipt & Storage (TR&S, Sellafield, UK) pools showed that the material experienced a moderate to severe damage up to 1×10^6 Gy, and was degraded at 5×10^6 Gy; when irradiated in water at a temperature of 35ºC with an applied dose rate of 10^4 Gy·hr^{-1}. After considering a number of factors, for example a low dose uptake correction, the difference between irradiation in air and water etc., a safety margin of two orders of magnitude has been applied, which leads to a working dose uptake limit of 2×10^4 Gy.

The impact of extending the service life of TR&S, in terms of water bar service life, has been evaluated for continued operations up to 80 years. The assessment used data on past and future fuel storage planning models and gamma data derived from FISPIN calculations for the most demanding fuels that have and will be positioned over the expansion joints.

The assessment concluded that a number of the water bars will not approach the 2×10^4 Gy limit, there is, however, potential for it to be exceeded in one area. A number of management options have been suggested to ensure the limit is not reached.

7.3.5.2. Polymers used for neutron shielding

To meet current and projected fuel burnups, in France, new shielding resins for their application in transport/storage casks have been evaluated [7]. High performance shielding materials are required to protect against severe neutron and gamma sources. The new requirements are to accommodate [4]:

- Greater neutron shielding efficiency (through higher hydrogen and boron content);
- Fire resisting (M1); and
- Resistance to long term high temperatures (160°C to 180°C).

A polymer Vyal resin has been evaluated. Vyal is produced by reacting a vinylester polymer with styrene (vinylester resin in solution of styrene). The resulting polymer is highly cross linked and solid. The mineral fillers, aluminium hydrate (fire retardant and source of hydrogen) and zinc borate (fire retardant and source of boron), are dispersed within the polymer matrix to provide the shielding ability of the Vyal resin to neutron radiation [4].

When compared to other neutron shielding materials, polyester resin and ethylene propylene rubber (EPR), Vyal resin shows less weight loss at the same temperature for the same sample size and test duration. At 160ºC Vyal resin lost ~2.5% of its weight after 10 000 hours, this weight loss is lower than EPR (~3%) and the existing polyester resins (>4%). Similarly, the fire resistance was found to be excellent, as the material was found to be self-extinguishing and only lost 7% of its weight [4].

In-service, changes in neutron shielding material performance are caused by irradiation and thermal processes. Experimental results have shown that oxidation is by far the most predominant process. Oxidation in thermoset matrix based neutron shielding materials has been studied through:

- Accelerated ageing tests on neutron shielding samples at various temperatures and O_2 partial pressures;
- O_2 permeation tests to estimate both O_2 diffusivity and solubility in neutron shielding films; and
- Application of a non-empirical model in order to investigate the long term properties. For this purpose, oxidation kinetic is coupled with oxygen diffusion. The model simulates weight losses (which are then converted into hydrogen atom loss) and oxidation profiles.

The following was concluded:

- A diffusion limited oxidation characteristic was observed; as shown in Fig. 53;
- Increasing temperature and O_2 pressure accelerates sample weight loss;
- There is a linear relationship between hydrogen atom loss and overall weight loss; and
- Simulated data was in good agreement with experimental results for all conditions studied. This allowed the in-service Vyal B hydrogen atoms loss over decades to be predicted; as shown in Fig. 54.

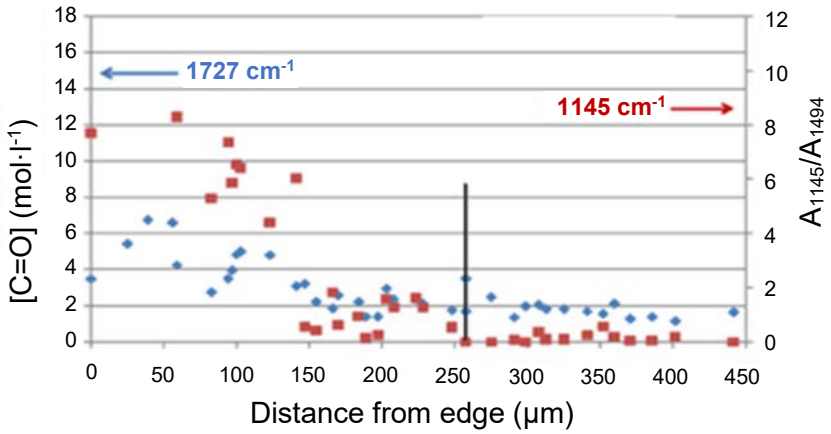

FIG. 53. Vyal B samples exposed to 160°C, 2 bar O_2 display a superficial layer (roughly 250 µm) while the core is not affected (figure courtesy of AREVA TN [7]).

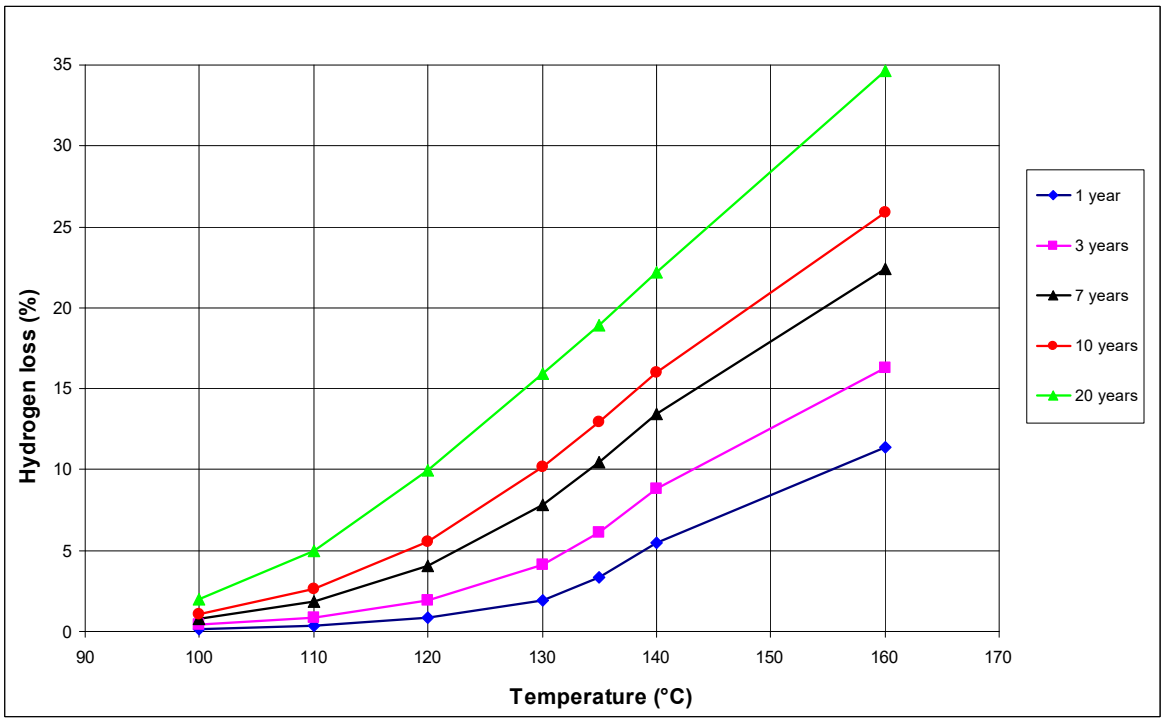

FIG. 54. Plot of hydrogen loss versus temperature and time (picture courtesy of AREVA TN [4, 7]).

7.3.6. **Metallic seals**

Metallic seals or gaskets are commonly used to seal dry storage casks. One of the most widely used seal is a spring energized O ring. The type used for dry spent fuel storage applications comprise an inner helical spring which creates internal sealing stress, an inner stainless steel sheath which evenly distributes the springs force and an outer ductile sheath, aluminium (Al) or silver (Ag), which compresses into the lid flange to absorb inflections. Metal seals of this type are characterized by excellent resilient properties which ensure useful elastic recovery. Elastic recovery is a precondition to accommodate minor distortions in the lid closure assembly due to changes in internal and external loads; even under accidental conditions of transport. Figure 55 shows the typical compression and decompression cycle for a HELICOFLEX® (spring energized) seal.

The accumulated operating experience (CASTOR® type casks) has shown no indication of any ageing effect in containment performance for HELICOFLEX® seals.

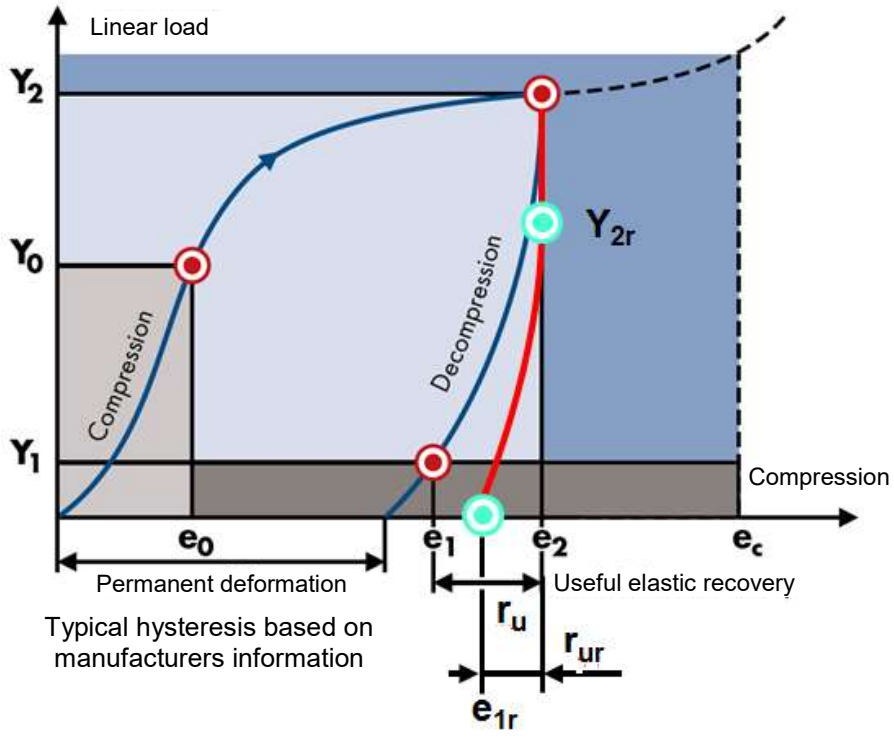

FIG. 55. Load–compression behaviour of a HELICOFLEX® seal (courtesy of GNS [7]).

7.3.6.1. Degradation studies

The dominant degradation mechanism for spring energized seals in the long term is thermal creep under mechanical load. Creep leads to changes in the linear load between the seal, the sealing surface and in elastic recovery. If we refer to Fig. 55., the impact of creep results in a drift towards lower load values (Y_{2r}) with time from the point of optimum compression. The additional permanent deformation of the seal reduces the useful elastic recovery with time. This is an important consideration for transport as the lower elastic recovery (r_{ur}) must be considered in the design of the lid closure assembly. The gap between the cask body and lid flanges must be limited to less than the elastic recovery remaining before transport; based upon intended storage period. The correlation between load–compression behaviour and the leak rate is important for any forecast of the cask behaviour with an extended storage period or transportation after long term storage.

A number of investigations have been conducted to explore the change in load–compression behaviour of spring energized seals versus time and temperature; see SPAR-II and III [4, 7].

The following summarizes the key findings from these studies:

- Using containment performance data collected over 19 years for seals kept at a constant 160°C, the Larson Miller Parameter (LMP) has been established for Al and Ag sheathed seals; LMP = 7942 (Al) and 7781 (Ag). The threshold at which leakage would occur was reported as 8050. Based on the assumption that long term estimations of sealing performance can be predicted from shorter term results, extrapolating to 60 years, predicts that sealing performance will be maintained for Al and Ag sheathed seals if the initial seal temperature is <134°C and <125°C;
- Other longer term tests 4+ years for seals kept at a constant 150°C concluded:

    - Both the load values (Y_{2r}) and the elastic recovery (r_{ur}) decrease with time. The decrease occurs more quickly with increasing temperature. It can be concluded that the initial temperature at cask loading has the greatest influence on the seal service life;
    - On a logarithmic timescale the behaviour appears as a linear function;
    - Extrapolation to a storage period of 40 years confirmed that the gasket has the ability to remain leak tight even at a constant temperature of 150°C; and
- Short term testing up to 250°C and 10 000 hours confirmed a leak rate[10] of $<10^{-10}$ Pa·m^3·s^{-1}.

Other studies have investigated the long term corrosion behaviour of seals with borated pool water trapped between the inner and outer sheaths and for a defect penetrating the outer sheath. Leak tightness has been confirmed in both cases. Thermal relaxation tests on metal seals have also been performed; see Ref. [7] for further details.

[10] A leak rate of $<10^{-10}$ Pa·m^3·s^{-1} is considered leaktight.

8. MONITORING (WET & DRY)

The information in the chapter has been sourced from Refs [2, 4]. Other references are cited within the text as appropriate.

In SPAR phases I & II [2, 4] part of the projects were devoted to collating information on monitoring technologies and techniques. The purpose of performance monitoring was outlined and brief descriptions of monitoring technologies in routine use were given. Additional Member State experience and practice in monitoring and surveillance is also reported in BEFAST-III [6].

The BEFAST and SPAR CRPs report monitoring activities in participating countries. The main aim of these technologies is to confirm ongoing spent fuel integrity or to provide an early indication of developing conditions which would impact on the long term spent fuel integrity if no corrective action is taken.

8.1. METHODS FOR CONFIRMING PERFORMANCE

The techniques employed range from basic visual inspections (through the biological shielding wet or dry (cave)) to sophisticated radiometric systems (such as a burnup monitors).

Examples of commonly used techniques in participating countries are summarized in Tables 19 and 20. The techniques are described in Ref. [2].

Most techniques for confirming spent fuel integrity during storage are retrospective or reactive; i.e. when you detect radionuclides for example caesium in-pool water or krypton in the cover gas the spent fuel has already failed. The plant operator then has to establish where the failure is, undertake some form of failure analysis and then make a decision on how to manage the failed fuel.

In the following sections newer/novel applications that have been deployed or tested for confirming spent fuel and storage system ongoing integrity are reported.

TABLE 19. SUMMARY OF MONITORING TECHNIQUES AND APPLICATIONS

Technique \ Function	Containment	Shielding	Criticality	Operability	R&D Data Confirmation	Other Safety Functions
Pressure Monitoring	✓				✓	
Fission Gas Sampling	✓					
Temperature				✓	✓	✓
Radiation Detection Systems		✓				✓
Liquid Sampling	✓			✓		✓
Visual Inspections	✓		✓	✓		✓
Gas Sampling (non-active)					✓	
In-pool Inspection Systems					✓	✓
Burnup			✓		✓	✓
Ultrasonic Test	✓			✓		

TABLE 20. SUMMARY OF CURRENT AND FUTURE MONITORING TECHNIQUES AND APPLICATIONS IN EACH COUNTRY

	ARGENTINA		CANADA		FRANCE		GERMANY		HUNGARY		JAPAN		KOREA		RUSSIAN FED.		SLOVAKIA		SPAIN		SWEDEN		U.K.		U.S.A.	
TECHNIQUE/FUNCTION	**W**	**D**	**W**	**D**	**W**	**D**	**W**	**D**	**W**	**D**	**W**	**D**	**W**	**D**	**W**	**D**	**W**	**D**	**W**	**D**	**W**	**D**	**W**	**D**	**W**	**D**
Pressure Monitoring	–	–	–	F	–	–	–	C	–	C	–	C	–	–	–	F	–	F	–	C	–	–	–	–	–	C
Fission Gas Sampling	–	C	–	F	–	C#	C	–	C	C	–	C	–	–	C	F	C	F	C	–	C	–	–	C	C	–
Temperature	C	C	C	C	C	–	C	–	C	C	C	C	C	–	C	–	C		C	C	C	–	C	C	C	–
Radiation Detection System	C	C	C	C	C	–	C	C	C	C	C	C	C	C	C	F	C	F	C	C	C	–	C	C	C	C
Liquid Sampling	C	–	C	–	C	–	C	–	C	–	C		C	–	C	–	C	F	–	–	C	–	C	–	C	–
Visual Inspection	C	C	C	–	C	–	C	–	C	–	C		C	C	C	F	C	F	C	C	C	–	C	C	C	C
Gas Sampling (non active)	–	–	–	F	–	–	–	–	–	C	–	C	–	–	–	F	–	–	–	–	C	–	C	–	–	C
In-pool Inspection System	–	–	C	–	C	–	C	–	C	–	C	–	C	–	–	–	–	–	C	–	C	–	C	–	C	–
Burnup Monitor	–	–	–	–	P	F#	–	–	–	–	P	F	F	F	–	–	F	–	–	F	F	–	P	–	–	F
Ultrasonic Testing	–	–	–	–	C	–	–	–	–	–	C	–	C	–	–	–	–	–	C	–	–	–	–	–	–	–
Corrosion Probes	–	F	–	–	–	–	–	–	–	–	–	–	–	–	–	–	–	–	–	–	–	–	F	–	–	–

W: wet storage, D; dry storage, C:current, F: future, P: prior to or in support of reprocessing

Transport casks

8.1.1. Technologies for confirming ongoing spent fuel integrity in wet storage

The confirmation of ongoing spent fuel integrity in wet storage is routinely carried out by pool water liquid sampling for the mobile fission products ^{134}Cs and ^{137}Cs. The ratio of ^{134}Cs to ^{137}Cs provides an indication of whether a fuel failure has occurred or where there are multiple fuel failures already present whether new fuel failures are occurring. The problem with this approach is that once caesium is detected it is usually too late. For some fuels/components, for example stainless steel, where storage is in demineralized water, an early indication of deteriorating conditions can be monitored through sampling for elemental nickel and for the activation products ^{54}Mn, ^{55}Fe, ^{60}Co and ^{63}Ni. If LWR fuel is present, detection of evolving storage conditions can be hampered by interference from crud.

In considering the above, practice the importance of trend monitoring and not solely relying upon trigger or action levels cannot be overstated. Notably, for example it can take multiple fuel pin failures in large pools before action levels or a trigger level are reached, and it is only through trending sampling results can deteriorating conditions be established.

The use of on-line corrosion probes, fabricated from fuel pin cladding or probes designed to simulate known fuel corrosion mechanisms, can provide a mechanism for bridging the gap between detecting failure and the initiation of conditions, that would lead to failure if no corrective action is taken. Techniques which have been investigated during SPAR include: Electrochemical Noise (EN), Electrochemical Impedance Spectroscopy (EIS), Zero Resistance Ammeter (ZRA), Field Signature Method (FSM) and Radiometric electrical resistance.

The use of on-line corrosion probes is of particular interest for spent fuels that are known to be susceptible to failure under abnormal operating conditions. Although zirconium clad fuels are not known to be susceptible to corrosion under most operating conditions, Zry-4 probes have been used to study the impact of changing pool chemistry on LWR fuel. Further development and maturity of these technologies, may offer application in providing supporting data to re-licensing or safety case review activities; as an alternative to undertaking post storage examination of long stored fuel.

Examples of the use of corrosion probes have been:

- The application of EN and EIS for confirming MAGNOX fuel passivity, see Section 10.2.4. [4]; and
- Use of intergranular attack corrosion probe using the techniques of ZRA and FSM for studying the onset of corrosion in AGR fuel, see Section 4.1.3. [4].

8.1.2. Technologies for confirming spent fuel integrity in dry storage

Apart from the vault technology, where the cover gas of individual storage tubes can be sampled in situ by a portable gas analyser for the presence of gaseous fission products, confirmation of spent fuel integrity in other dry storage technologies would require the containment to be broken to inspect or monitor the fuel. Ongoing spent fuel integrity for other systems is inferred through external temperature and containment monitoring (either pressure monitoring of the seals (bolted casks systems) and/or radiological/visual inspections of the outer cask or canister fabric), quality assurance during system closure and supporting R&D that provides the confidence that failure during storage can be discounted.

The specific investigations that have been performed with cask opening were discussed in Section 6.2, the following reports R&D on monitoring fuel failures in a closed systems.

To provide further reassurance to key stakeholders that the spent fuel is still intact during storage, a number of non-intrusive techniques have been proposed.

Gamma monitoring

Probably one of the most attractive options for monitoring the condition of spent fuel in dry storage is by direct measurement of the 514 keV ^{85}Kr γ-line. This technique is particularly attractive proposition for monitoring the condition of spent fuel during the early years of dry storage (which are probably the most onerous for Zircaloy clad fuels). If storage duration were to extend to 50+ years then the technique becomes less attractive given the half-life for ^{85}Kr (10 years).

This technique, investigated by CRIEPI, requires a modified lid arrangement. The studies showed that if ^{85}Kr $>7 \times 10^{10}$ Bq is released from a failed fuel rod or rods, it would be picked-up by a gamma detector; see Section 10.2.2. [6].

Acoustic monitoring

Monitoring the velocity of sound through the cover gas is an alternative mechanism for detecting the condition of the atmosphere inside a sealed system. Such a system was proposed for the TranStor™ Storage system [67] for the detection of oxygen in helium (indicator of air ingress) but, was not developed into a fully operational system.

8.1.3. Technologies for confirming storage system integrity

8.1.3.1. Wet storage

The use of acoustic emission for monitoring pool liner integrity

The technique involves listening to the natural energy waves released when a material undergoes plastic deformation. In the case of a metal pool liner, this results from changes in load, pressure or temperature. It is a qualitative technique for establishing damage within a structure and is used for monitoring the development of active defects. Defects are detected as the stress levels (and corresponding energy levels released) in front of the crack tip are several times higher than the surrounding metal.

At Jaslovské Bohunice (Slovakia), there are six sensors installed in each pool and measurements are performed periodically, using a portable data collection system. Comparison with archived data is used to establish if there any cracks or defects developing. To date there has been no significant defects detected.

8.1.3.2. Dry storage.

Temperature monitoring of dry storage casks in Canada

To confirm that the DSCs would not suffer from freeze-thaw damage to a significant extent, a programme to monitor the temperatures of both the storage facility and the DSCs was put in place. The monitoring took place at the Used Fuel Storage Facility – Phase 1 of the Pickering Station from the latter part of December 2000, to the end of March 2001, coinciding with the return of above freezing temperatures. The purpose of the monitoring was to record the minimum temperatures that could be experienced by the DSCs. To fulfil this objective, a total of 31 thermocouples were placed in various locations: outside of the storage facility to

measure ambient air temperatures, indoors within the storage facility including the concrete floor surface, on the surface of the DSC's outer shell for DSCs most exposed to the coldest temperatures, and, thermocouples located at the bottom of the DSCs to measure their temperature in contact with the concrete floor.

The observed temperatures indicated that the temperature outside of the storage facility on the coldest day was -17.5ºC, and, there were 31 freeze-thaw cycles over the monitoring period. Yet, at all times, concrete floor temperatures under the DSCs remained above zero, as well as the DSC's outer shell temperatures being about 2ºC above zero. In the facility itself, the lowest air temperature reached -4.5ºC and the lowest exposed concrete floor temperature was -0.5ºC. Inside the storage facility, ambient air between two DSCs freeze-thaw cycled seven times, while the most exposed wall of the facility freeze-thaw cycled four times.

The results of that monitoring showed that the storage facility provides significant protection against freeze-thaw conditions. Data indicated that the DSCs remained above zero at all times even though ambient air temperatures within the facility were on seven occasions below freezing. However, the low temperatures recorded inside the facility would suggest that as the stored fuel decays, the DSCs might experience some freeze-thaw cycles during their 50 year design life. In view of the 6% air-entrainment provided in the concrete, some freeze-thaw cycling of the concrete is not viewed to leading to a detrimental impact.

Surface analysis of welded storage canisters

In order to detect whether the environmental conditions, i.e. the presence of chloride, to induce SCC on non-stress relieved welded canisters are present, the technique of laser induced breakdown spectroscopy has been investigated by CRIEPI. The advantages of this technique are that it is non-contact and therefore would facilitate in situ analysis without taking samples. This enables canisters at high temperature to be analysed and potentially could reduce dose uptake to operators.

Using stainless steel samples treated with various amounts of chloride, the feasibility of this technique to provide a quantitative analysis for chlorine has been established. The study showed that the chlorine emission intensity normalized by oxygen emission intensity increased monotonically versus chlorine concentration in the range 0.05 to 0.4 $g \cdot m^{-2}$ (up to 1.0 $g \cdot m^{-2}$). Section 8.2.4.6. in Ref. [7] provides further information on this study.

Loss of containment - welded fuel canisters

In concrete cask storage systems spent fuel is loaded into stainless steel canisters, which are filled with helium gas and then welded leak tight. While the primary role of the helium is to store the fuel in an inert atmosphere, helium also enhances heat removal from the spent fuel. If the helium gas leaks from the canister, then convection of decay heat from the fuel to the canister surface will be affected; i.e. in principle the temperature at the canister surface would change.

The impact of a loss of helium on canister body temperature has been investigated by CRIEPI. While it was difficult to judge whether the surface temperature changes were caused by helium gas leak or not, the study, however, did show that for a failed canister there was a temperature difference between the bottom and top of the canister of around 8°C after 60 h. Section 8.2.4.6. in Ref. [7] provides further details of this study.

9. FUEL INTEGRITY (LEAKING/DAMAGED FUEL)

The subject of spent fuel integrity was covered in some detail in SPAR-II (see Section 6) [4]. In this section, the summary of BEFAST and SPAR reporting is limited to types of damage, at reactor techniques for detecting spent fuel failures and the operating experience in storing damaged or failed fuel. Techniques for the packaging and the transport of damaged fuel are covered in SPAR-II and are not reproduced here.

9.1. FUEL INTEGRITY DEFINITION AND CRITERIA [2]

The terminology used to describe fuel integrity, and specifically the definitions of 'damaged' or 'failed' fuel, varies between countries, with country specific criteria detailed in the SPAR-I and II reports [2, 4]. In general, the term 'failed' fuel is used within the CRP reports to describe any fuel assembly in which:

1. The cladding containment barrier has been breached, or;
2. Structural deformations that affect the handling of the SNF structure have occurred, or;
3. Mechanical defects of the SNF have occurred.

It should be noted that a fuel assembly can undergo minor mechanical damage or structural modification without necessarily being classified as 'failed'. It is also possible for cladding damage, detected during operation, to close during post-reactor storage by 'autogenous healing', or through corrosion product growth / deposition over the affected area.

9.2. EXAMPLES OF DAMAGED FUEL [4]

9.2.1. Damaged fuel rods

Figures 56 and 57 show examples of primary and secondary defects arising in PWRs and BWRs. Many primary defects are induced by small metallic debris. Due to rod vibrations, the cladding can be locally worn. A similar situation may occur in case of a very low holding force of a spacer grid mesh, if the rod interacts with a spacer grid vane, or with the spring itself. Secondary degradation can often be recognized by the appearance of a hydride blister at characteristic axial locations of the fuel rod. Occasionally, severe secondary degradation, such as long cladding splits, may be observed, see Fig. 57 [68].

9.2.2. Damaged structural parts

Structural parts may also show damage. During inspections in the spent fuel pool, great varieties of findings are observed, such as contact and wear marks at the tie plates, fretting marks at spacer grids up to damaged spacer grid corners or meshes, as well as broken guide tubes or slightly twisted fuel assemblies. Figure 58 shows on the left side a damaged corner and on the right side damaged outer meshes of a spacer grid. Damage may arise during operation or during handling of fuel assemblies. They generally do not affect fuel rod integrity, but may have an impact on the ability to further handle fuel assemblies in the reactor pool or under storage operations.

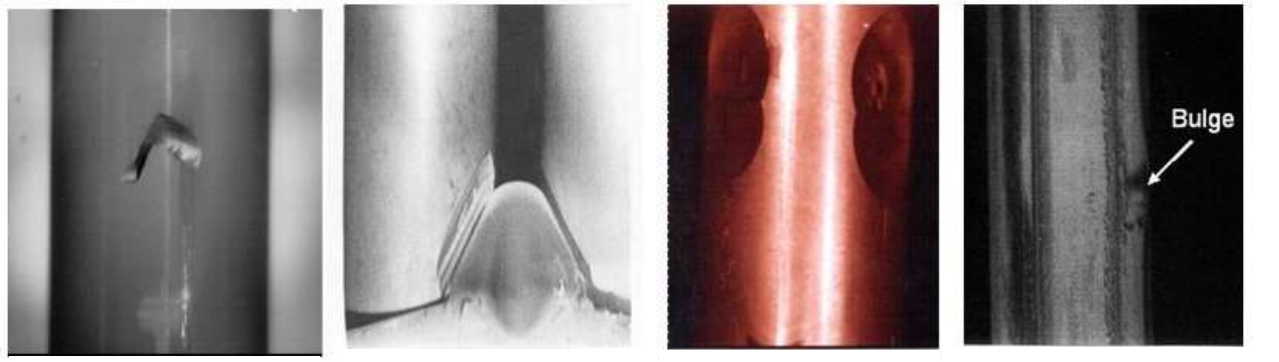

Fretting due to debris interaction | Fretting due to spacer grid vane-to-rod contact | Fretting due to spring relaxation | Secondary degradation (hydride blister)

FIG. 56. Fuel rod damage due to fretting and secondary degradation (photographs courtesy of Framatome ANP GmbH [4]).

Fretting mark | Axial split | Helical split

FIG. 57. Examples of fuel rod damage (photographs courtesy of Framatome ANP GmbH [4]).

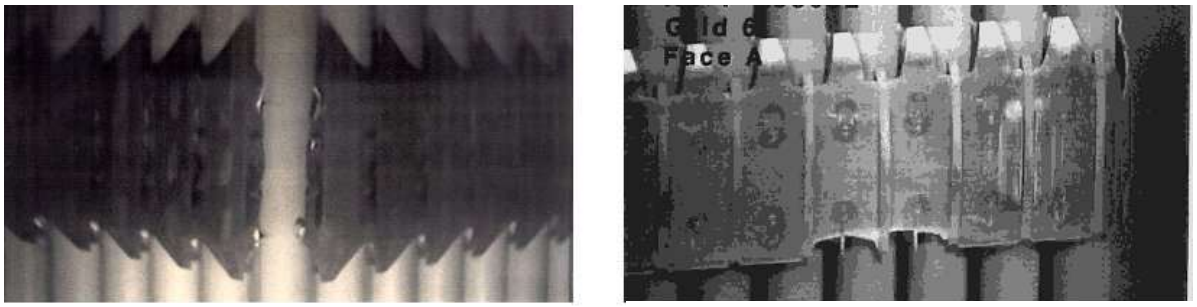

Damaged corner of a spacer grid | Damaged outer meshes (side wall and springs) of a spacer grid

FIG. 58. Examples of damaged spacer grids (photographs courtesy of Framatome ANP GmbH [4]).

9.2.3. Reconstitution of damaged fuel

The primary objective for reconstitution of fuel assemblies is to enable their reinsertion for further reactor operation. Main techniques of reconstitution are replacement of damaged fuel rods, repair of spacer grids and exchange of whole skeletons. Damaged fuel rods can be replaced by new fuel rods or by dummy rods made of stainless steel or Zircaloy. A wide variety of techniques is also available to reconstitute structural parts of fuel assemblies for further reactor operation. Some examples are repair of spacer grid corners and outer grid meshes (Fig. 59), recalibration of springs in spacer meshes, adjusting of vanes on spacer grids, exchange of tie plates and hold down springs, etc.

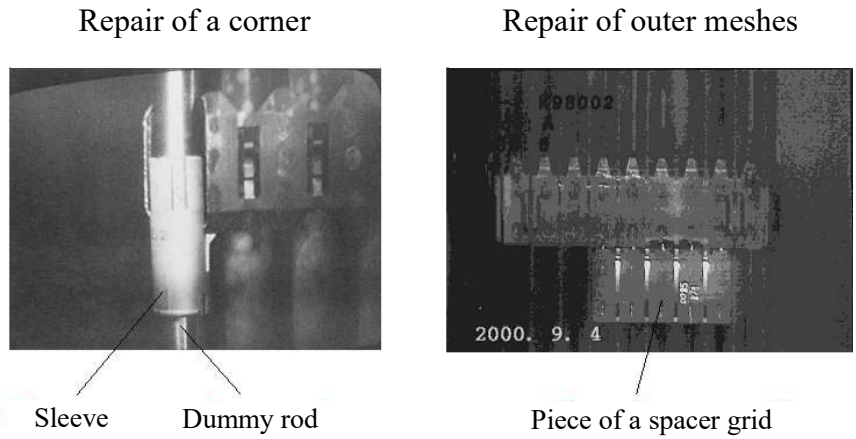

FIG. 59. Repair of a spacer grid corner and outer mesh (photographs courtesy of Framatome ANP GmbH [4]).

9.3. DETERMINATION OF SPENT FUEL INTEGRITY [4]

Typical techniques to monitor defective fuel are on-line monitoring, sipping and leaching tests and detailed examinations of fuel assemblies, such as visual inspection, ultrasonic examination or eddy current testing.

All reactors have at least one on-line monitoring system for the detection of in-core fuel failures as a means of controlling the contamination of primary cooling circuits and subsequent dose to personnel during maintenance operations. In LWRs, the onset of a fuel failure is usually detected by monitoring the gamma activity level associated with specific radioactive fission products in the reactor coolant or off-gas. A typical failure indication is an increase in Xe, Kr or I isotope activity. However, to characterize the failure it has to be distinguished between fission products coming from tramp uranium or defective rods. In CANDU reactors, the delayed neutron (DN) system measures the activity that comes from ^{137}I and ^{87}Br (they release neutrons and are also β and γ-emitters). An increase of the DN signal indicates uranium release to the coolant [69].

In addition to the in-core systems, most reactors also have secondary sipping systems associated with defueling and in-pool operations to check cladding/fuel assembly integrity. Fuel failure detection by sipping is based on the release of gaseous fission products from the leaking rod. The samples can be taken either from the top of the fuel assembly, or the fuel assembly can be inserted in a closed can. The driving forces for the release of the fission products during sipping may be heating up due to reduced water cooling, or the external pressure decrease associated with lifting of the fuel assembly to a shallower depth in the pool.

Further information on sipping systems and technologies for detecting failed fuel at reactors is provided in Section 6.3.1. of Ref. [4].

9.4. EXPERIENCE OF STORING DAMAGED FUEL

9.4.1. Wet storage

For wet stored fuel, the general experience is that the defect does not deteriorate or propagate during prolonged storage, with the exception of water logged or filled canned fuel [2, 4].

There is experience from many countries of handling failed Zircaloy clad LWR fuel after periods of wet storage.

An 18 year German programme involved the periodic inspections of Zircaloy clad fuel rods with incipient flaws and penetrating through wall cladding defects that were stored as part of a demonstration programme. The defects included cracks, hydride failures and wear spots [6]. No unanticipated effects or changes to the defects were revealed, providing strong evidence that wet storage of such fuels with adequate water chemistry and cleanliness was safe and reliable [2, 70–71].

The Republic of Korea conducted a long term study on the storage of deliberately damaged PWR rods. In the first series, 10 fuel rods, including 7 with intentional through-cladding defects, were examined after 1, 2.5, and 5 years of storage [6]. There were no indications of dimensional changes even after 5 years. However, some deposits were found around the defects. A white material (thought to be caesium hydroxide) was observed after 2.5 years, and an unidentified yellow material was observed after 5 years. Ultrasonic tests were used to determine the distance of water ingress at short times. The caesium release rate from defected rods was also assessed and found to increase rapidly over the first 30 days, increase at a slower rate up to 90 days and then remained nearly constant. The dissolution of ^{60}Co was also recorded, and the measured value of 0.0093 $Bq \cdot sec^{-1} \cdot rod^{-1}$ was found to be consistent with the reported value of 0.1 $Bq \cdot sec^{-1} \cdot rod^{-1}$. In the second series, two of the pins that had been stored 12 years were inspected and examined by PIE techniques. Again, there were no indications of any dimensional changes or eddy current signal changes at the defected positions. The yellow material which was found previously on another defective rod, was not identified on examination of these rods [2].

In Sweden, a study on the behaviour of a defective fuel rod was undertaken to ascertain the changes in chemical composition and structural integrity of the cladding and fuel pellet as a result of continued operation following cladding penetration [72]. When compared to an intact sibling rod, a large caesium loss of 30% was evident, especially between the cladding penetrations. The leachability of Cs, U and Cm in deionized water proved to be higher for the defected rod, with the results for Sr, Pu and Am more complex. The defective rod had also undergone a change of structure, with grain growth and structure reorientation, possibly due to increased oxygen content. The cladding on the rod was also hydrided in some parts.

Long cooled (up to 23 years) reactor failed LWR fuels in the UK were visually inspected and it could not be determined whether prolonged pool storage was propagating the failures. However, none of the fuels were considered to have structural defects that would impair handling. One assembly with known areas of corrosion stored within a multi element bottle (MEB) was inspected and assessed not to have deteriorated since the previous inspection nine years earlier.

Zircaloy clad PWR fuel assemblies with reactor induced defects were examined in the USA after up to 8 years of storage. No cladding deterioration around the defects or significant loss of fuel by dissolution was evident [73].

Deliberately defected CANDU fuel has been examined after 21 and 27 years of wet storage. It was determined that no measurable oxidation of the cladding surface had occurred and that no changes were observed in the condition of the fuel [6]. Examination of the UO_2 within the immediate area of the intentional defect of fuel that was stored wet for 21 years showed the surfaces of the fuel fragments were fully hydrated and significantly oxidized [2, 6]. However, the oxidation was restricted to a very thin layer (i.e., nanometres) on the surface [2], and there was no evidence of a diametral increase in the element due to UO_2 oxidation [6]. The evidence suggested that pool storage of defected bundles could continue for at least 50 years without significant degradation [6].

Defective WWER fuel has been wet stored in individual cans in both Hungary and the Russian Federation and in both cases no unexpected events have occurred and no further degradation has been noted [2, 4].

Spent MAGNOX fuel can undergo pitting corrosion during wet storage. These defects require fission product and actinide removal from the storage water, but otherwise do not cause handling problems, provided that the fuel is kept wet. To minimize corrosion, MAGNOX is stored in high purity caustic dosed water [4].

The storage of defective AGR fuel in the UK has shown little impact on wet storage operations, in that no handling problems were encountered and fission product release was low in comparison to failed MAGNOX fuel [6]. The presence of defective fuel was found to not affect rod consolidation by dismantling techniques.

The storage of failed MOX fuel was investigated by the CEA [74]. An irradiated MOX fuel sample was leached in pure aerated water with and without external gamma radiation under static conditions for 14 days. It was found that for the sample without external gamma radiation, the uranium and plutonium concentrations in the water increased steadily with time without reaching a steady state. On the other hand, the sample leached in the presence of gamma radiation quickly reached steady state conditions. A second set of experiments used Raman spectroscopy to characterize evolution of the fuel surface. The characterized fuel sample was leached for 3 months in pure aerated water in the presence of gamma radiation. It was found that only alteration of the UO_2 matrix was observed. The overall conclusion of the study was that in the event of a MOX fuel cladding breach, the behaviour will be no worse than what can be observed for standard UO_2 spent fuel.

9.4.2. Dry storage

A PWR assembly undergoing cladding integrity trials at the EMAD facility in the mid-1980s was found to have a failed rod after 2 months of storage at 275ºC with air cover gas [75]. The assembly was stored in air for a total of 2 years before the test was terminated without evidence of any further fuel degradation. The cause of failure was undetermined. It had been reported that there was evidence that larger reactor induced or intentional defects would allow fuel to oxidize and propagate the defects if exposed to air at sufficiently high temperatures [76–77].

The storage of spent fuel fragments and defected rod segments in humidified air was undertaken in the late 1980s to obtain oxidation data relative to the dry storage of spent fuel [2, 4]. High weight gains and cladding splitting due to oxidation of UO_2 were observed, while no dependence on burnup or cover gas moisture levels were observed. One example is where an intentionally defected zirconium clad rod segment failed by splitting after 23 000 hours storage in air at 150°C [78].

The effect of cover gas on the dry storage of Zircaloy clad BWR rods with reactor induced defects was assessed at Battelle-Columbus Laboratories by storing the rods for 2100 hours at 325°C. One rod was kept under argon, the other in air. The rod exposed to inert gas showed no change in the cladding defects. Marked fuel oxidation, fuel swelling and cladding distortion occurred on the rod exposed to air [79].

Intentionally defected CANDU fuel bundles were included in a long term experimental dry storage programme in concrete canisters in the late 1970s. They were stored in dry air at temperatures up to 150°C with no apparent increases in fuel diameters and the structural integrity of the cladding was maintained, even though a significant amount of the fuel had oxidized. Other intentionally defected CANDU fuel bundles that were stored in moisture saturated limited air for 8 years and moisture saturated unlimited air for a further 2 years (both at 150°C) were observed to have endcap fractures extending into the cladding. These fractures were attributed to DHC as a result of severe hydriding of the endcaps and positive cladding strain adjacent to the endcaps, which occurred during in-reactor operations, in combination with damage experienced by the fuel bundle prior to dry storage.

Dry stored MAGNOX damaged by water ingress at Wylfa were inspected in detail and found to be in a stable condition.

10. CONCLUSIONS

10.1. SPENT FUEL PERFORMANCE IN WET AND DRY STORAGE

For LWR spent fuels with either zirconium or stainless steel based clad, there is >50 years wet storage and >30 years dry storage experience. Performance in storage remains excellent with no generic failure mechanism identified or experienced.

The position with respect to stainless steel clad AGR spent fuel is >30 years of wet storage experience. Storage performance is good provided the fuel is stored in the presence of a corrosion inhibitor.

In the case of MAGNOX spent fuel, there is ~57 years' experience in handling and storage; this includes ~43 years of dry storage operations. The tendency is only to store for relative short periods of time in wet storage, but the fuel will remain intact for longer periods provided optimum pool storage chemistry is maintained. There has been no reported degradation of MAGNOX spent fuel retrieved from dry storage[11].

10.2. SPENT FUEL DEGRADATION MECHANISMS (WET AND DRY)

The potential degradation mechanisms that may affect zirconium based clad integrity in wet storage are [4]:

- Uniform (aqueous) corrosion;
- Pitting, galvanic, and microbial induced corrosion (MIC); and
- Hydriding.

None of these mechanisms has been demonstrated to be significantly involved under wet storage conditions as deducible from the studies carried out by BEFAST and SPAR participants (up to 30 organizations from 21 countries and the European Commission). It can, therefore be concluded that there is no evidence available to date or a theoretical mechanism has not been identified so far that would limit the dwell time of zirconium alloy clad fuel in wet storage, provided the pool chemistry is maintained within specified limits.

The potential degradation mechanisms that may affect zirconium based clad integrity in dry storage, subsequent handling and transportation operations are [4]:

- Air oxidation;
- Thermal creep;
- Stress corrosion cracking;
- Delayed hydrogen cracking (DHC);
- Hydride reorientation; and
- Hydrogen migration and redistribution.

Under normal dry storage conditions, the mechanisms which are currently receiving interest from CRP participants are thermal creep (although this is not considered as an issue in the USA), delayed hydride cracking that was an issue being investigated for CANDU fuel in SPAR-III and may have been addressed now, and the effect of hydrogen on the behaviour of

[11] Except the small amount of fuel which was affected by water ingress to one of the air cooled dry stores at Wylfa NPP.

zirconium clad. The latter is an area which is still under investigation and is potentially an issue under given operating/handling conditions.

For stainless steel and magnesium alloy based clad fuels the position is slightly different. In both cases neither clad is affected by hydriding, however, other mechanisms become dominant. For stainless steel clad material that has experienced reactor operating temperatures between 350-520°C, it is susceptible to intergranular attack in storage (both wet and dry). Mitigation is through adjusting the storage chemistry in terms of pool storage or total exclusion of moisture for dry storage.

MAGNOX clad was specifically designed not to oxidize in a gas and therefore should be robust to dry storage conditions. The evidence from fuel retrieval operations supports this view as no fuel degradation has been found. MAGNOX clad, however, was not designed for wet storage and reacts with water. Altering the pool chemistry slows this process down to an acceptable level. UK government policy is to reprocess MAGNOX spent fuel.

Based on good storage parameters, the evidence to date supports that transport following interim storage should not pose any concerns.

10.3. STRUCTURES WET AND DRY STORAGE

There are many materials in use in spent fuel storage, for example metals, concrete and polymers. Their long term behaviour has been studied during the BEFAST and SPAR projects and the results are summarized in this publication.

Areas which have been identified to date as requiring further consideration are ageing management and issues related to SCC in dry storage systems.

One area where there is a high level of knowledge is the long term behaviour of metal seals. The accumulated experience from metal seals deployed in the field and in-house long term testing has demonstrated their durability. Based on this experience, extrapolation to longer timeframes suggests that storage durations of 40–60 years should not be an issue. In order to improve this long term forecast, the current data set is being enlarged by performing further investigations.

10.4. MONITORING (WET AND DRY)

Spent fuel integrity in wet storage is routinely monitored through pool water sampling. Trending of the water samples is important to establish an early indicator of any deteriorating conditions.

Ongoing spent fuel integrity in dry storage is mostly inferred through external temperature and containment monitoring (for bolted systems this is usually permanent monitoring of the functionality of the lid system); although studies on how to address this issue have gained some momentum in recent years.

10.5. FUEL INTEGRITY (LEAKING/DAMAGED FUEL)

The general experience for the prolonged wet storage of clad defected spent fuel is that the defect does not deteriorate or propagate with time [2, 4]. The exceptions are water logged or filled canned fuel and MAGNOX fuel. The leaching of activity from a defect in the fuel clad

initially releases the gap inventory, if the defect is greater than a pinhole, followed by a much lower underlying leach rate, which decreases in-line with the half-life of ^{137}Cs.

The dry storage of defected fuel in an inert gas environment at high temperatures remains unaltered [2]. Similarly there has been no defect propagation in fuel clad with a through wall defect stored in dry air at temperatures up to 150°C; i.e. below the temperature where UO_2 converts to U_3O_8.

REFERENCES

[1] INTERNATIONAL ATOMIC ENERGY AGENCY, Storage of Water Reactor Spent Fuel in Water Pools – Survey of World Experience, Technical Report Series No 218, IAEA, Vienna (1982).

[2] INTERNATIONAL ATOMIC ENERGY AGENCY, Spent Fuel Performance Assessment and Research, IAEA-TECDOC-1343, IAEA, Vienna, (2003).

[3] INTERNATIONAL ATOMIC ENERGY AGENCY, Behaviour of Spent Fuel Assemblies During Extended Storage, (BEFAST-I), IAEA-TECDOC-414, IAEA, Vienna (1987).

[4] INTERNATIONAL ATOMIC ENERGY AGENCY, Spent Fuel Performance Assessment and Research: Final Report of a Coordinated Research Project (SPAR-II), IAEA-TECDOC-1680, IAEA, Vienna (2012)

[5] INTERNATIONAL ATOMIC ENERGY AGENCY, Extended Storage of Spent Fuel, (BEFAST-II), IAEA TECDOC-673, IAEA, Vienna (1992).

[6] INTERNATIONAL ATOMIC ENERGY AGENCY, Further analysis of extended storage of spent fuel (BEFAST III), IAEA-TECDOC-944, IAEA, Vienna (1997).

[7] INTERNATIONAL ATOMIC ENERGY AGENCY, Spent Fuel Performance Assessment and Research: Final Report of a Coordinated Research Project on Spent Fuel Performance Assessment and Research (SPAR-III) 2009-2014, IAEA-TECDOC-1771, IAEA, Vienna (2015).

[8] INTERNATIONAL ATOMIC ENERGY AGENCY, Fundamental Safety Principles, Safety Standards Series No. SF–1, IAEA, Vienna (2006).

[9] INTERNATIONAL ATOMIC ENERGY AGENCY, Predisposal Management of Radioactive Waste, Safety Standards Series No. GSR Part 5, IAEA, Vienna (2009).

[10] INTERNATIONAL ATOMIC ENERGY AGENCY, Safety of Nuclear Fuel Cycle Facilities, Safety Standards Series No. SSR–4, IAEA, Vienna (2017).

[11] INTERNATIONAL ATOMIC ENERGY AGENCY, Predisposal Management of Radioactive Waste from Nuclear Fuel Cycle Facilities, Safety Standards Series No. SSG–41, IAEA, Vienna (2016).

[12] INTERNATIONAL ATOMIC ENERGY AGENCY, Safety of Nuclear Fuel Cycle Research and Development Facilities, Safety Standards Series No. SSG–43, IAEA, Vienna (2017).

[13] INTERNATIONAL ATOMIC ENERGY AGENCY, Design of Fuel Handling and Storage Systems in Nuclear Power Plants, Safety Standards Series No. NS-G–1.4, IAEA, Vienna (2003).

[14] INTERNATIONAL ATOMIC ENERGY AGENCY, Storage of Spent Nuclear Fuel, Safety Standards Series No. SSG–15, IAEA, Vienna (2012).

[15] INTERNATIONAL ATOMIC ENERGY AGENCY, The Management System for the Processing, Handling and Storage of Radioactive Waste, Safety Standards Series No. GS-G-3.3, IAEA, Vienna (2008).

[16] INTERNATIONAL ATOMIC ENERGY AGENCY, Radiation Protection and Radioactive Waste Management in the Operation of Nuclear Power Plants, Safety Standards Series No. NS-G-2.7, IAEA, Vienna (2002).

[17] LE BIEZ, V., MACHIELS, A., SOWDER, A., "Advanced Nuclear Fuel Cycles – Main Challenges And Strategic Choices", GLOBAL 2013, Salt Lake City, Utah, September 30–October 3 (2013), paper 7802.

[18] INTERNATIONAL ATOMIC ENERGY AGENCY, Survey of wet and dry spent fuel storage, IAEA-TECDOC-1100, IAEA, Vienna (1999).

[19] INTERNATIONAL ATOMIC ENERGY AGENCY, Spent Fuel Storage Operation – Lessons Learned, IAEA-TECDOC-1725, IAEA, Vienna (2013).
[20] INTERNATIONAL ATOMIC ENERGY AGENCY, Radioactive Waste Management Glossary 2003 Edition, Vienna (2003).
[21] THOMAS, L.E., EINZIGER, R. E., Effect of fission products on air-oxidation of LWR spent fuel, J. Nucl. Mater., 201 (1993) 310-319.
[22] SASAHARA, A., MATSUMURA, T., PAPAIOANNOU, D., "Examinations of Spent Fuels during Interim Storage (5) – Oxidation Behavior of Irradiated UO_2 Fuel in Air", Autumn meeting of the Atomic Energy Society of Japan (2003).
[23] SPILKER, H., PEEHS, M., DYCK, H.P., KASPAR, G., NISSEN, K., Spent LWR Fuel Dry Storage in Large Transport and Storage Casks after Extended Burnup, J. Nucl. Mater. 250 (1997) 63-74.
[24] FERRY, C. et al., Référentiel Scientifique sur l'Evolution à long terme des Combustibles Usés, Commissariat à l'Energie Atomique, RT DPC/SECR 04-032, Gif-sur-Yvette (2005).
[25] QUECEDO M. et al., "Results of thermal creep on highly irradiated ZIRLO™", paper presented at TOP FUEL 2008, Seoul, Republic of Korea, October (2008) Paper 8063.
[26] ELECTRIC POWER RESEARCH INSTITUTE, "Creep Modeling and Analysis Methodology for Spent Fuel in Dry Storage", EPRI 1003135, EPRI, Palo Alto, CA. (2001).
[27] RASHID, J., MACHIELS, A., "Examination of the creep rupture phenomena and the development of an acceptance criterion for spent fuel storage", Storage of Spent Fuel from Power Reactors, IAEA-CSP-20, IAEA, Vienna (2003) 431–441.
[28] GRUSS, K. A., BROWN, C. L., HODGES, M. W., "U.S. Nuclear Regulatory Commission Acceptance Criteria and Cladding Considerations for the Dry Storage of Spent Fuel", paper presented at TOP FUEL 2003, Wurzburg, Germany (2003).
[29] PEEHS, M., GARZAROLLI, F., GOLL, W., "Assessment of Dry Storage Performance of Spent LWR Fuel Assemblies with Increasing Burnup", Storage of Spent Fuel from Power Reactors, IAEA-TECDOC-1089, IAEA, Vienna (1999) 313–324.
[30] ELECTRIC POWER RESEARCH INSTITUTE, "Creep as the Limiting Mechanism for Spent Fuel Dry Storage", EPRI 1001207, EPRI, Palo Alto, CA (2000).
[31] AOMI, M., et al., "Evaluation of hydride reorientation behavior and mechanical property of high burnup fuel cladding tube in interim dry storage", Zirconium in the Nuclear Industry: 15th Int. Symp., STP 1505, ASTM, West Conshohocken (2009) 651.
[32] MCMINN, A., DARBY, E.C., SCHOFIELD, J.S., "The terminal solid solubility of hydrogen in zirconium alloys", Zirconium in the Nuclear Industry: 12th Int. Symp., STP 1354, ASTM, West Conshohocken, PA (2000) 173-195.
[33] KAMMENZIND, B.F., FRANKLIN, D.G., PETERS, H.R. AND DUFFIN, W.J. "Hydrogen pickup and redistribution in alpha-annealed Zry-4," Zirconium in the Nuclear Industry: 11th Int. Symp., STP 1295, ASTM, West Conshohocken, PA (1996) 338–370.
[34] COLAS, K., Fundamental Experiments On Hydride Reorientation In Zircaloy**,** PhD Thesis, The Pennsylvania State University, Department of Mechanical and Nuclear Engineering (2012).
[35] BILLONE, M.C., BURTSEVA, T.A., EINZIGER, R.E., Ductile-to-brittle transition temperature for high burnup cladding alloys exposed to simulated drying–storage conditions, J. Nucl. Mater., **433** (2013) 431–448.
[36] SABOL, G.P., "In-reactor corrosion performance of ZIRLO™ and Zry-4", Zirconium in the Nuclear Industry: 10th Int. Symp., STP 1245, ASTM, West Conshohocken, PA (1994) 724–744.

[37] SAWATZKY, A., Hydrogen in Zircaloy-4: Its Distribution and Heat of Transport, J. Nucl. Mater., **2**, No.4 (1960) 321-328.
[38] HONG, H.S., KIM, S.J., LEE, K.S., Thermotransport of Hydrogen in Zircaloy-4 and Modified Zircaloy-4, J. Nuc. Mat., **257** (1998) 15–20.
[39] FORSBERG, K., MASSIH, A.R. Redistribution of Hydrogen in Zircaloy, J. Nucl. Mater., **172**, (1990) 130–134.
[40] SASAHARA, A., MATSUMURA, T., TSUCHIUHI, Y., "Experiment of Hydrogen Migration under Temperature Gradient in Irradiated Cladding", 2005 Water Reactor Fuel Performance Meeting, Oct. 2–6, 2005, Kyoto, Japan, (2005) Paper #1036.
[41] INTERNATIONAL ATOMIC ENERGY AGENCY, Effects of radiation and environmental factors on the durability of materials in spent fuel storage, IAEA-TECDOC-1316, IAEA, Vienna, (2002).
[42] PARE, F.E., PATTANTYUS, P., HANSON, A.S., "MACSTOR: Dry spent fuel storage for the nuclear industry", Proc. Int. Conf. on Nuclear Waste Management and Environmental Remediation, Prague, Vol 1. ASME New York, NY (1993) 275–279.
[43] SHEK, G.K., WASILUK, B.S., LAMPMAN, T., FREIRE-CANOSA, J., "Testing the susceptibility of CANDU fuel bundle endcap/endplate welds to delayed hydride cracking", paper presented at 10th CNS International Conference on CANDU Fuel, Ottawa, 2008.
[44] KADARMETOV, I.M., BIBILASHVILI, Y.K., MEDVEDEV, A.V., "Evaluation of the maximum allowable temperature of WWER-1000 spent fuel under dry storage conditions", Proc. Int. Symp. on Safety and Engineering Aspects of Spent Fuel Storage, IAEA Proceedings Series STI/PUB/949, IAEA, Vienna (1995) 269–279.
[45] VESELY, J., VALACH, M., FREJTICH, Z., PRIMAN, V., "Creep properties of non-irradiated Zr-1%Nb cladding tubes under normal and abnormal storage conditions", Storage of Spent Fuel from Power Reactors, IAEA-TECDOC-1089, IAEA, Vienna (1999) 305–312.
[46] ZALIOTNYCH, B.A., NOVIKOV, YU.B., TIKHONOV, N.S., MAKARCHUK, T.F., TOKARENKO, A.I., KOZLOV, YU.V., RAZMASHKIN, N.V., "Investigation of the behaviour of WWER spent fuel rods at Novovoronezh NPP", Extended synopses International Symposium on Storage of Spent Fuel from Power Reactors, 9–13 November, 1998, IAEA-SM-352, IAEA, Vienna (1998).
[47] INTERNATIONAL ATOMIC ENERGY AGENCY, WWER-440 fuel rod experiments under simulated dry storage conditions, IAEA-TECDOC-1385, IAEA, Vienna (2004).
[48] UNITED STATES NUCLEAR REGULATORY COMMISSION, "Classifying the Condition of Spent Nuclear for Interim Storage and Transportation Based on Function", ISG-1 Rev. 2, U.S. NRC, Washington, DC (2007).
[49] WOOD, B., "Fuel transfer operations" paper presented at NEI Used Fuel Management Conference, 5–7 May, Orlando, 2015.
[50] RIDDER, R., "Fuel characterization challenges for pool offload at Kewaunee" paper presented at NEI Used Fuel Management Conference, 3–5 May, Orlando, 2016.
[51] DURBIN, S.G., LINGDREN, E.R., "Investigation of zirconium fires during spent fuel pool LOCAs", paper presented at NEI Used Fuel Management Conference, Baltimore, 2011.
[52] ZIGH, G., VELAZQUEZ-LOZADA, E.R., "Zirconium fire on pressurized water reactor (PWR) spent fuel pools (SFP)", paper presented at U.S. NRC Regulatory Information Conference, Washington, DC, 2013.
[53] UNITED STATES NUCLEAR REGULATORY COMMISSION, "Consequence Study of a Beyond - Design Basis Earthquake Affecting the Spent Fuel Pool for a U.S. Mark 1 Boiling Water Reactor", NUREG-2161, U.S. NRC, Washington, DC (2014).

[54] NUCLEAR ENERGY AGENCY, “Status Report on Spent Fuel Pools under Loss-of-Cooling and Loss-of-Coolant Accident Conditions”, NEA/CSNI/R(2015)2, NEA, Paris (2015).
[55] FROST C. R. “Current Interim Used Fuel Storage Practice in Canada”, Ontario Hydro Nuclear Report N-03710-940052, Ontario Hydro (1994).
[56] NUCLEAR DECOMMISSIONING AUTHORITY, MAGNOX Fuel Strategy: Contingency Options (2014), http://www.nda.gov.uk/publication/magnox-fuel-strategy-contingency-options-january-2014
[57] FLEISCH, J., “Analysis of spent fuel behaviour in dry storage cask demonstrations in FRG”, CONF-860417-Volume 1, Proceedings of 3rd International Spent Fuel Storage Technology Symposium/Work Shop, Seattle, PNNL (1986) S-254–262.
[58] MCKINNON, M.A., STEWART, L., “Spent Nuclear Fuel Integrity during Dry Storage”, Storage of spent fuel from power reactors, IAEA-TECDOC-1089, IAEA, Vienna (1999) 297–302.
[59] UNITED STATES NUCLEAR REGULATORY COMMISSION, “Dry Cask Storage Characterization Project – Phase 1: CASTOR V/21 Cask Opening and Examination”, NUREG/CR-6745, U.S. NRC, Washington, DC (2001).
[60] KUMANO, Y., “Integrity inspection of dry storage casks and spent fuels at Fukushima Daiichi nuclear power station”, paper presented at CRIEPI Int. Conf. ISSF 2010, Tokyo, 2010.
[61] TOKYO ELECTRIC POWER COMPANY., “Report of Investigation and Maintenance Results of the Dry Storage Casks at Fukushima Daiichi Nuclear Power Station”, Technical Meeting on Spent Fuel Storage Options, IAEA-TM-45455, Vienna (2013).
[62] BRADLEY, N., BROWN, G.A., “Interim dry storage of irradiated fuel and vitrified high activity level waste”, Nuclear Power Experience – Nuclear Fuel Cycle, Proceedings Series, IAEA-CN-42/142, IAEA, Vienna (1983) 863–874.
[63] GRAVENOR, J.G., BLANCHARD, A., KENDALL, D.S., JACKSON, P.A., “Post-Irradiation testing of AGR element components in support of the Scottish Nuclear Limited dry store project”, Fuel Management and Handling, ISBN 0 7277 2033 3, BNES, London (1995) 128.
[64] INTERNATIONAL ATOMIC ENERGY AGENCY, Durability of spent nuclear fuel and facility components in wet storage, IAEA-TECDOC-1012, IAEA, Vienna (1998).
[65] ISSARD, H., “Anticipating future needs for the transport and storage of spent fuel from evolutionary nuclear power reactors”, Proc. IAEA International Conference on Management of Spent Fuel from Nuclear Power Reactors, 19–23 June 2006, IAEA, Vienna (2007) 341–351.
[66] CENTRAL RESEARCH INSTITUTE OF ELECTRIC POWER INDUSTRY, Basis of Spent Nuclear Fuel Storage, ISBN978-4-900622-55-5, ERC Publishing Co. Ltd., Tokyo (2015) 274–289.
[67] DICKSON, R.M., “Flexibility of the BNFL dry storage systems”, Storage of Spent Fuel from Power Reactors, IAEA-TECDOC-1089, IAEA, Vienna (1999) 195–200.
[68] INTERNATIONAL ATOMIC ENERGY AGENCY, Management of Damaged Spent Fuel, IAEA NE series No. NF-T-3.6, IAEA, Vienna (2009).
[69] INTERNATIONAL ATOMIC ENERGY AGENCY, Review of Fuel Failures in Water Cooled Reactors, Technical Reports Series No. 388, IAEA, Vienna (1998).
[70] PEEHS, M., BANCK, J., BOKELMANN, R., ―Spent fuel storage performance data and storage strategy assessment in nuclear power performance and safety‖, Proc. Int. Conf. Spent Fuel Management, Vienna, 1987, IAEA, Vienna (1988).
[71] PEEHS, M., EINFELD, K., “Effects of long term dry storage of spent fuel”, Proc. of Int. HLRWM Conf., Las Vegas NV (1992).

[72] FORSYTH, R., JONSSON, T., “Experimental Study of Defect Power Reactor Fuel”, Final Report, Studsvik/ NF(P)-82/72 (1982).
[73] JOHNSON, Jr., A.B., et al., Materials Behavior in Interim Storage of Spent Fuel, Trans. Am. Nucl. Soc. 43 (1982) pp. 314-315.
[74] JÉGOU, C., CARABALLO, R., DE BONFILS, J., BROUDIC, V., PEUGET, S., VERCOUTER, T., ROUDIL, D., Oxidizing dissolution of spent MOX47 fuel subjected to water radiolysis: Solution chemistry and surface characterization by Raman spectroscopy, J. Nucl. Mater. **399** (2010) 68–80.
[75] JOHNSON, Jr., A.B., et al., ‘Simulated Dry Storage Test of a Spent PWR Nuclear Fuel Assembly in Air”, Proceedings of Waste Management 85, Tucson, Arizona, USA, March 24-28 (1985).
[76] HASTINGS, I.J., MCCRACKEN, D., “Behavior in Air at 175-400 C of Irradiated UO_2 Fuel”, Proceedings of Int. Workshop -Irradiated Fuel Storage: Operating Experience and Development Programs, Toronto, Canada, October 17-18 (1984), pp. 626-654.
[77] OLSEN, C.S., “Fuel Rod and Crud Behavior Under Long-Term Dry Storage Conditions”, Proceedings of Int. Workshop - Irradiated Fuel Storage: Operating Experience and Development Programs, Toronto, Canada, October 17-18 (1984), pp.432-455.
[78] CUNNINGHAM, M.E., et al., "Status of spent UO_2 oxidation studies supporting on dry storage of spent fuel", Paper presented at INMM Spent Fuel Management Seminar VIII, Washington D.C. (1991).
[79] KOHLI, R., et al., The Behavior of Breached Boiling Water Reactor Fuel Rods on Long-Term Exposure to Air and Argon at 598 K, Nucl. Tech. 69, May (1985), pp.186-197.

LIST OF ABBREVIATIONS

AECL	Atomic Energy Canada Limited
AFR	Away from reactor
AR	At reactor
AGR	Advanced gas cooled reactor
ANL	Argonne National Laboratory (USA)
ASTM	American Society of Testing & Materials
BEFAST	Behaviour of spent fuel assemblies in extended storage
BWR	Boiling water reactor
CANDU	Canadian deuterium uranium reactor
CBB	Crevice bent beam
CC	Concrete canister
CEA	Commissariat à l'Energie Atomique et aux Energies Alternatives (France)
CGR	Crack growth rate
CLAB	Central interim storage facility for spent nuclear fuel (Sweden)
CNEA	Comisión Nacional de Energía Atómica (Argentina)
CRIEPI	Central Research Institute of Electric Power Industry (Japan)
CRL	Chalk River Laboratory (Canada)
CRP	Coordinated research project
CRUD	A deposit on fuel assembly surface (in SPAR context)
CSA	Canadian Standards Association
CSN	Consejo de Seguridad Nuclear (Spain)
CSNI	Committee on Safety of Nuclear Installations (OECD/NEA)
CSSR	Czechoslovak Socialist Republic
CTDT	Cladding tube deformation test
CWSR	Cold worked stress relieved
DBTT	Ductile-to-brittle transition temperature
DHC	Delayed hydride cracking
DLO	Diffusion limited oxidation
DSC	Dry storage container (Canada)
EIS	Electrochemical impedance spectroscopy
EPRI	Electric Power Research Institute (USA)
EN	Electrochemical noise
ENRESA	Empresa Nacional de Residuos Radiactivos (Spain)
ENUSA	Empresa Nacional del Urano, SA (Spain)
EOL	End-of-life
EPR	Ethylene propylene rubber
FA	Fuel assembly
FEM	Finite element modelling
FISPIN	Fission product inventory (UK)
FR	Fast reactor
FRG	Federal Republic of Germany
FSM	Field signature method
GDR	German Democratic Republic
GGBFS	Ground granulated blast furnace slag
HBR	H. B. Robinson (USA)
HCC	Hydride continuity coefficient
HLW	High level waste
HTGR	High temperature gas cooled reactor

HWR	Heavy water reactor
IGA	Intergranular attack
INFCIS	IAEA Nuclear fuel cycle information system
INS	International Nuclear Services (UK)
ISFSI	Independent spent fuel storage installation
JAPC	Japan Atomic Power Company (Japan)
JNES	Japan Nuclear Energy Safety organisation (Japan)
LIBS	Laser induced breakdown spectroscopy
LMP	Larson Miller parameter
LPB	Low plasticity burnishing
LSP	Laser shot peening
LWR	Light water reactor
MAGNOX	Magnesium non oxidizing (magnesium alloy cladding, UK)
MCC	Mining chemical combine
MDA™	Mitsubishi Developed Alloy
MEB	Multi element bottle (UK)
MIC	Microbial induced corrosion
MMC	Metal matrix composites
MOX	Mixed oxide fuel
MPC	Multipurpose canister
MVDS	Modular vault dry storage
NPD	Nuclear power demonstration
NPP	Nuclear power plant
NRC	Nuclear Regulatory Commission (USA)
NRU	National research universal
OECD	Organization for Economic Cooperation and Development
OPC	Ordinary Portland cement
OPG	Ontario Power Generation (Canada)
OS	Off-site
PHWR	Pressurized heavy water reactor
PIE	Post irradiation examination
PURAM	Public limited company for radioactive waste management (Hungary)
PWR	Pressurized water reactor
RBMK	Russian type of graphite modulated water cooled reactor (reaktor bolshoy moshchnosti kanalniy)
RCT	Ring compression test
RH	Relative humidity
RHCF	Radial hydride continuity factor
RHF	Radial hydride fraction
RHT	Hydride reorientation treatment. Also referred to HRT by some experimenters
RIAR	Research Institute of Atomic Reactors (Russia)
RIP	Rod internal pressure
RS	Reactor site
RT	Room temperature
RXA	Recrystalized annealed
SCC	Stress corrosion cracking
SEM	Scanning electron microscope
SF (A)	Spent fuel (assembly)
SKB	Swedish nuclear fuel & waste management company

SNF	Spent nuclear fuel
SP	Shot peening
SPAR	Spent fuel performance assessment and research
SRA	Stress relieved and annealed
SS	Stainless steel
SSC	System, structure, component
TAD	Transportation, ageing and disposal
TC	Thermocouple
t(HM)	Tons of heavy metal
TEM	Transmission electron microscopy
TEPCO	Tokyo Electric Power Company (Japan)
THORP	Thermal oxide fuel reprocessing plant (Sellafield, UK)
TR&S	Thorp receipt and storage (UK)
TSSD	Terminal solid solubility for dissolution
TSSP	Terminal solid solubility for precipitation
UHMW-PE	Ultra high molecular weight polyethylene
UOX	Uranium Oxide
$U_{rep}OX$	Reprocessed uranium oxide
USSR	Union of Soviet Socialist Republics
WWER	Russian type of PWR (wodo-wodyanoi energetichecki reactor)
XRD	X-ray diffraction
ZIRLO™	Zirconium low oxidation
Zr1Nb	Zirconium niobium alloy fuel cladding (WWER)
ZRA	Zero resistance ammeter
Zry	Zircaloy

CONTRIBUTORS TO DRAFTING AND REVIEW

Hanson, B.	Pacific Northwest National Laboratory (PNNL), Washington, United States of America
Hillier, A.	Sellafield Limited, Cumbria, United Kingdom
Issard, H.	TN International, Montigny Le Bretonneux, France
Jussofie, A.	BGZ Gesellschaft für Zwischenlagerung mbH, Essen, Germany
Kyffin, J.	Sellafield Limited, Cumbria, United Kingdom
Machiels, A.	Electric Power Research Institute (EPRI), California, United States of America
McManniman, L.	Sellafield Limited, Cumbria, United Kingdom
Standring, P.	International Atomic Energy Agency
Takáts, F.	TS Enercon, Budapest, Hungary

Consultants Meetings

Vienna, Austria: 11-15 August 2014

IAEA
International Atomic Energy Agency

No. 25

ORDERING LOCALLY

In the following countries, IAEA priced publications may be purchased from the sources listed below or from major local booksellers.

Orders for unpriced publications should be made directly to the IAEA. The contact details are given at the end of this list.

CANADA

Renouf Publishing Co. Ltd

22-1010 Polytek Street, Ottawa, ON K1J 9J1, CANADA
Telephone: +1 613 745 2665 • Fax: +1 643 745 7660
Email: order@renoufbooks.com • Web site: www.renoufbooks.com

Bernan / Rowman & Littlefield

15200 NBN Way, Blue Ridge Summit, PA 17214, USA
Tel: +1 800 462 6420 • Fax: +1 800 338 4550
Email: orders@rowman.com Web site: www.rowman.com/bernan

CZECH REPUBLIC

Suweco CZ, s.r.o.

Sestupná 153/11, 162 00 Prague 6, CZECH REPUBLIC
Telephone: +420 242 459 205 • Fax: +420 284 821 646
Email: nakup@suweco.cz • Web site: www.suweco.cz

FRANCE

Form-Edit

5 rue Janssen, PO Box 25, 75921 Paris CEDEX, FRANCE
Telephone: +33 1 42 01 49 49 • Fax: +33 1 42 01 90 90
Email: formedit@formedit.fr • Web site: www.form-edit.com

GERMANY

Goethe Buchhandlung Teubig GmbH

Schweitzer Fachinformationen
Willstätterstrasse 15, 40549 Düsseldorf, GERMANY
Telephone: +49 (0) 211 49 874 015 • Fax: +49 (0) 211 49 874 28
Email: kundenbetreuung.goethe@schweitzer-online.de • Web site: www.goethebuch.de

INDIA

Allied Publishers

1st Floor, Dubash House, 15, J.N. Heredi Marg, Ballard Estate, Mumbai 400001, INDIA
Telephone: +91 22 4212 6930/31/69 • Fax: +91 22 2261 7928
Email: alliedpl@vsnl.com • Web site: www.alliedpublishers.com

Bookwell

3/79 Nirankari, Delhi 110009, INDIA
Telephone: +91 11 2760 1283/4536
Email: bkwell@nde.vsnl.net.in • Web site: www.bookwellindia.com

ITALY

Libreria Scientifica "AEIOU"

Via Vincenzo Maria Coronelli 6, 20146 Milan, ITALY
Telephone: +39 02 48 95 45 52 • Fax: +39 02 48 95 45 48
Email: info@libreriaaeiou.eu • Web site: www.libreriaaeiou.eu

JAPAN

Maruzen-Yushodo Co., Ltd

10-10 Yotsuyasakamachi, Shinjuku-ku, Tokyo 160-0002, JAPAN
Telephone: +81 3 4335 9312 • Fax: +81 3 4335 9364
Email: bookimport@maruzen.co.jp • Web site: www.maruzen.co.jp

RUSSIAN FEDERATION

Scientific and Engineering Centre for Nuclear and Radiation Safety

107140, Moscow, Malaya Krasnoselskaya st. 2/8, bld. 5, RUSSIAN FEDERATION
Telephone: +7 499 264 00 03 • Fax: +7 499 264 28 59
Email: secnrs@secnrs.ru • Web site: www.secnrs.ru

UNITED STATES OF AMERICA

Bernan / Rowman & Littlefield

15200 NBN Way, Blue Ridge Summit, PA 17214, USA
Tel: +1 800 462 6420 • Fax: +1 800 338 4550
Email: orders@rowman.com • Web site: www.rowman.com/bernan

Renouf Publishing Co. Ltd

812 Proctor Avenue, Ogdensburg, NY 13669-2205, USA
Telephone: +1 888 551 7470 • Fax: +1 888 551 7471
Email: orders@renoufbooks.com • Web site: www.renoufbooks.com

Orders for both priced and unpriced publications may be addressed directly to:

Marketing and Sales Unit
International Atomic Energy Agency
Vienna International Centre, PO Box 100, 1400 Vienna, Austria
Telephone: +43 1 2600 22529 or 22530 • Fax: +43 1 2600 29302 or +43 1 26007 22529
Email: sales.publications@iaea.org • Web site: www.iaea.org/books

19-00021

International Atomic Energy Agency
Vienna
ISBN 978–92–0–100319–5
ISSN 1011–4289